UNIFORMED SERVICES UNIVERSITY OF THE HEALTH SCIENCES
F. EDWARD HÉBERT SCHOOL OF MEDICINE
4301 JONES BRIDGE ROAD
BETHESDA, MARYLAND 20814-4799

May 30, 2006

BIOMEDICAL GRADUATE PROGRAMS

Ph.D. Degrees

Interdisciplinary
-Emerging Infectious Diseases
-Molecular & Cell Biology
-Neuroscience

Departmental
-Clinical Psychology
-Environmental Health Sciences
-Medical Psychology
-Medical Zoology
-Pathology

Doctor of Public Health (Dr.P.H.)

Physician Scientist (MD/Ph.D.)

Master of Science Degrees

-Molecular & Cell Biology
-Public Health

Masters Degrees

-Comparative Medicine
-Military Medical History
-Public Health
-Tropical Medicine & Hygiene

Graduate Education Office
Dr. Eleanor S. Metcalf, Associate Dean
Janet Anastasi, Program Coordinator

Web Site
www.usuhs.mil/geo/gradpgm/index.html

E-mail Address
graduateprogram@usuhs.mil

Phone Numbers
Commercial: 301-295-9474
Toll Free: 800-772-1747
DSN: 295-9474
FAX: 301-295-6772

APPROVAL SHEET

Title of Dissertation: "Spatial-temporal mapping of the T cell receptor NF-κB signaling pathway"

Name of Candidate: Jeremy Rossman
Doctor of Philosophy Degree
20 June 2006

Dissertation and Abstract Approved:

Clifford Snapper, M.D. — 6/20/06
Department of Pathology — Date
Committee Chairperson

Brian Schaefer, Ph.D. — 6/20/06
Department of Microbiology & Immunology — Date
Committee Member

Stephen Davies, Ph.D. — 6/20/06
Department of Microbiology & Immunology — Date
Committee Member

J. Brian McCarthy, Ph.D. — 6/20/06
Department of Pharmacology — Date
Committee Member

Paul Love, M.D., Ph.D. — 6/20/06
National Institute of Child Hlth & Human Dev — Date
Committee Member

Report Documentation Page

Form Approved
OMB No. 0704-0188

1. REPORT DATE	2. REPORT TYPE	3. DATES COVERED
2006		**00-00-2006 to 00-00-2006**

4. TITLE AND SUBTITLE	5a. CONTRACT NUMBER
Spatial-Temporal Mapping of the T Cell Receptor NF-kB Signaling Pathway	5b. GRANT NUMBER
	5c. PROGRAM ELEMENT NUMBER
6. AUTHOR(S)	5d. PROJECT NUMBER
	5e. TASK NUMBER
	5f. WORK UNIT NUMBER
7. PERFORMING ORGANIZATION NAME(S) AND ADDRESS(ES) **Uniformed Services University of the Health Sciences,F. Edward Hebert School of Medicine,4301 Jones Bridge Road,Bethesda,MD,20814-4799**	8. PERFORMING ORGANIZATION REPORT NUMBER
9. SPONSORING/MONITORING AGENCY NAME(S) AND ADDRESS(ES)	10. SPONSOR/MONITOR'S ACRONYM(S)
	11. SPONSOR/MONITOR'S REPORT NUMBER(S)

12. DISTRIBUTION/AVAILABILITY STATEMENT
Approved for public release; distribution unlimited

13. SUPPLEMENTARY NOTES
The original document contains color images.

14. ABSTRACT

15. SUBJECT TERMS

16. SECURITY CLASSIFICATION OF:			17. LIMITATION OF ABSTRACT	18. NUMBER OF PAGES	19a. NAME OF RESPONSIBLE PERSON
a. REPORT	b. ABSTRACT	c. THIS PAGE			
unclassified	**unclassified**	**unclassified**		**130**	

The author hereby certifies that the use of any copyrighted material in the thesis manuscript entitled:

"Spatial-Temporal Mapping of the T Cell Receptor NF-kB Signaling Pathway"

Is appropriately acknowledged and, beyond brief excerpts, is with the permission of the copyright owner.

Jeremy S. Rossman

Emerging Infectious Diseases Program

Uniformed Services University of the Health Sciences

Abstract

Title of Dissertation:

Spatial-Temporal Mapping of the T Cell Receptor NF-κB Signaling Pathway

Jeremy Shai Rossman, Doctor of Philosophy, 2005

Thesis Directed by:

Brian C. Schaefer, Ph.D.

Assistant Professor, Department of Microbiology and Immunology

T lymphocytes are critical mediators of adaptive immunity that recognize antigen through the T cell receptor (TCR). Stimulation of the TCR leads to a complex signal transduction cascade resulting in the activation of the transcription factors NFAT, AP-1 and NF-κB. The activation of these transcription factors is a crucial step in T lymphocyte activation, allowing for proliferation and gain of effector function. TCR stimulation results in the spatial redistribution of several proteins involved in signal transduction to NF-κB. We find that the signaling intermediate Bcl10 forms cytoplasmic oligomers, called POLKADOTS, upon antigen stimulation. The formation of these structures requires the interaction between Bcl10 and MALT1 and is correlated with the activation

of NF-κB. Our research shows that POLKADOTS are foci for functional interactions between signaling intermediates in TCR-mediated activation of NF-κB.

In addition to forming POLKADOTS in the cytoplasm in response to antigen signals, a significant portion of cellular Bcl10 localizes to the nucleus in the steady state. Observations of high enrichment of Bcl10 in the nucleus of MALT lymphoma tumor cells suggest that Bcl10 nuclear localization may be actively regulated by signaling processes. Aberrant redistribution of Bcl10 to the nucleus in MALT lymphomas may contribute to tumorigenesis or pathogenesis. We show that Bcl10 is found in the nucleus of T lymphocytes, that this localization is regulated by PKCθ, and that dose-dependent interactions with MALT1 mediate the nuclear export of Bcl10. We also show that the N-terminus of Bcl10 is essential for NF-κB activation, possibly by functioning as a transcriptional enhancer for NF-κB-responsive genes. These results may further suggest a pathogenic role for nuclear localization of Bcl10 in MALT lymphomas.

In summary, through spatial-temporal analysis of Bcl10 subcellular localization and protein-protein interactions, we have further elucidated the role played by Bcl10 in health and in disease.

SPATIAL-TEMPORAL MAPPING

OF THE T CELL RECEPTOR NF-κB

SIGNALING PATHWAY

by

Jeremy S. Rossman

Thesis submitted to the Faculty of the

Emerging Infectious Diseases Graduate Program

Uniformed Services University of the Health Sciences

in partial fulfillment of the requirements for the degree of

Doctor of Philosophy 2006

Acknowledgements

Clifford M. Snapper, M.D., Ph.D., Thesis Committee Chair

Brian C. Schaefer, Ph.D., Thesis Advisor

Stephen J. Davies, BVSc., Ph.D.

J. Brian McCarthy, Ph.D.

Paul E. Love, M.D., Ph.D.

Members of the Schaefer Lab

Emily Crow

Table of Contents

Table of Tables

Table of Figures

Chapter 1

Introduction

T lymphocytes are a crucial part of the adaptive immune system

The human immune system consists of two branches that are required for protection against a wide range of pathogens, the innate and the adaptive immune systems. The innate immune system responds directly to pathogens through recognition of conserved molecular motifs. Successful activation of innate immune mechanisms enables direct clearance of many infectious agents. However, many pathogens have evolved methods of avoiding the innate immune response, enabling survival within the host. In these cases, a second role for the innate immune system comes into play.

In addition to providing a first line of defense against invading organisms, the innate immune system is also able to activate the adaptive immune system, providing a further means of controlling infectious agents. Adaptive immunity begins when antigen presenting cells (APCs) ingest foreign products. Digestion of these products within the APC results in the production of small peptide antigens. These antigens then bind to major histocompatibility class (MHC) molecules within the APC, and are transported to the cell surface. Once presented on the cell surface, antigen-MHC complexes can be recognized by cells of the adaptive immune system.

The adaptive immune system consists of B and T lymphocytes. Lymphocytes express unique antigen receptors that are generated from genetic recombination of multiple segments of the antigen receptor genes. This recombination creates an extensive library of receptor specificities, with each lymphocyte expressing only one specificity of antigen receptor. T lymphocytes recognize antigen through the T cell receptor (TCR) in conjunction with the coreceptor CD4 or CD8, which specifically recognizes the host's presenting MHC molecule. Full T cell activation also requires signaling through the costimulatory receptor CD28. TCR

stimulation, CD4/8 binding and CD28 costimulation results in the activation of a complex signal transduction cascade, ultimately leading to T lymphocyte activation, proliferation and differentiation. Upon activation, T cells can differentiate into several different types of effector cells. Activated CD8+ T cells differentiate into cytotoxic T cells, which are able to kill infected host cells. Activated CD4+ T cells differentiate into helper T cells, which are crucial for enhancing the activation of a wide range of both innate and adaptive immune cells. Helper T cells act by providing costimulatory signals to antigen presenting cells and by secreting a wide array of cytokines that directly modulate the innate and adaptive immune responses.

T lymphocyte activation requires NFAT, AP-1 and NF-κB

Recognition of antigen through the TCR, activates a complex signal transduction cascade that results in the activation of three transcription factors; nuclear factor of activated T cells (NFAT), AP-1 and nuclear factor κB (NF-κB). These three proteins are crucial for the transcription of genes necessary for T cell activation, proliferation and differentiation [1-3].

The NFAT family consists of five related proteins that are expressed in a wide variety of tissues [3]. Despite its name, NFAT is involved in gene regulation in a diverse range of cell types. NFAT is best known, however, for its role in modulating the expression of many genes that are crucial for the innate and adaptive immune response. NFAT proteins share a conserved structure, containing an N-terminal transactivation domain (TAD-N) and a regulatory region followed by a highly conserved DNA binding domain. Figure 1 is a schematic of the general structure of NFAT proteins [3].

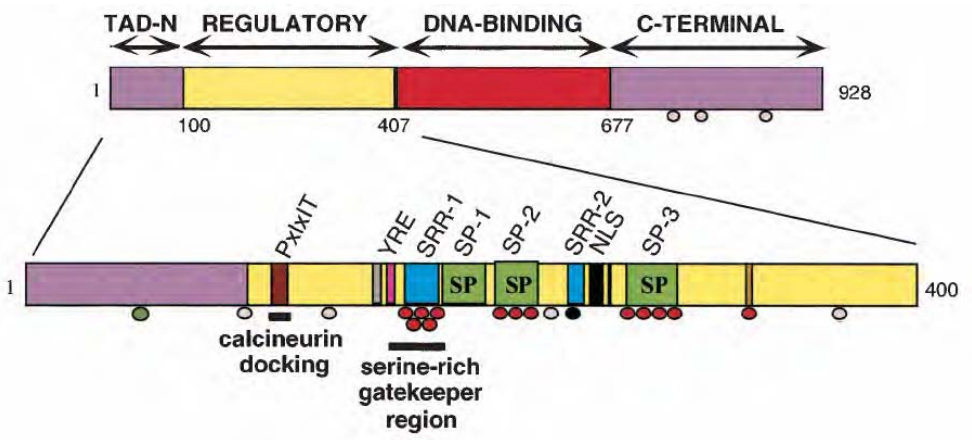

Figure 1. Domains of the NFAT family of proteins.

The regulatory region (depicted in yellow) is normally heavily phosphorylated (filled circles); however, upon T cell activation, the phosphatase calcineurin binds to the regulatory region and dephosphorylates it. Full dephosphorylation exposes a nuclear localization sequence (NLS) and masks a nuclear export signal (NES). Dephosphorylation is also necessary to activate the DNA binding and transcriptional functions of NFAT. Thus, calcineurin binding enables NFAT to enter the nucleus, bind DNA and initiate transcription [3].

AP-1 is a dimeric transcription factor that consists of variable pairings of Fos and Jun proteins. Differential pairing of the seven Fos and Jun proteins results in the creation of eighteen isoforms of the AP-1 transcription factor [3, 4]. The extensive variation in AP-1 dimers allows for a wide range of DNA binding affinities and target genes. This enables the AP-1 transcription factors to elicit a diverse range of responses in a wide range of tissues. Fos and Jun proteins are part of the basic region-leucine zipper (bZIP) protein family. Homo and hetero-dimerization is mediated through a leucine zipper domain, while DNA binding occurs through the basic region motif [4]. The Fos proteins are activated through mitogen activated protein kinase (MAPK) signaling cascades, initiated by a wide range of cellular signals, while the Jun proteins are activated through JNK signaling pathways [4]. Activation of Fos and Jun proteins enables their

dimerization, entry into the nucleus and activation of target gene transcription. NFAT and AP-1 frequently bind cooperatively to composite DNA sequences that contain recognition motifs for both NFAT and AP-1. This composite binding allows for more stable interactions that is possible with single factor binding, resulting in greater levels of transcription [3].

Like NFAT and AP-1, NF-κB has a wide range of actions in multiple tissue types and in response to a variety of cellular signals. The NF-κB family contains five members that are normally bound to IκB molecules as homo- or heterodimers. The IκB family consists of seven members which bind to NF-κB molecules in the cytoplasm, masking their NLS and preventing their nuclear entry. Additionally, IκB molecules contain a NES, enabling nuclear export of NF-κB molecules. [2]. A summary of NF-κB and IκB family members is presented in figure 2 [2].

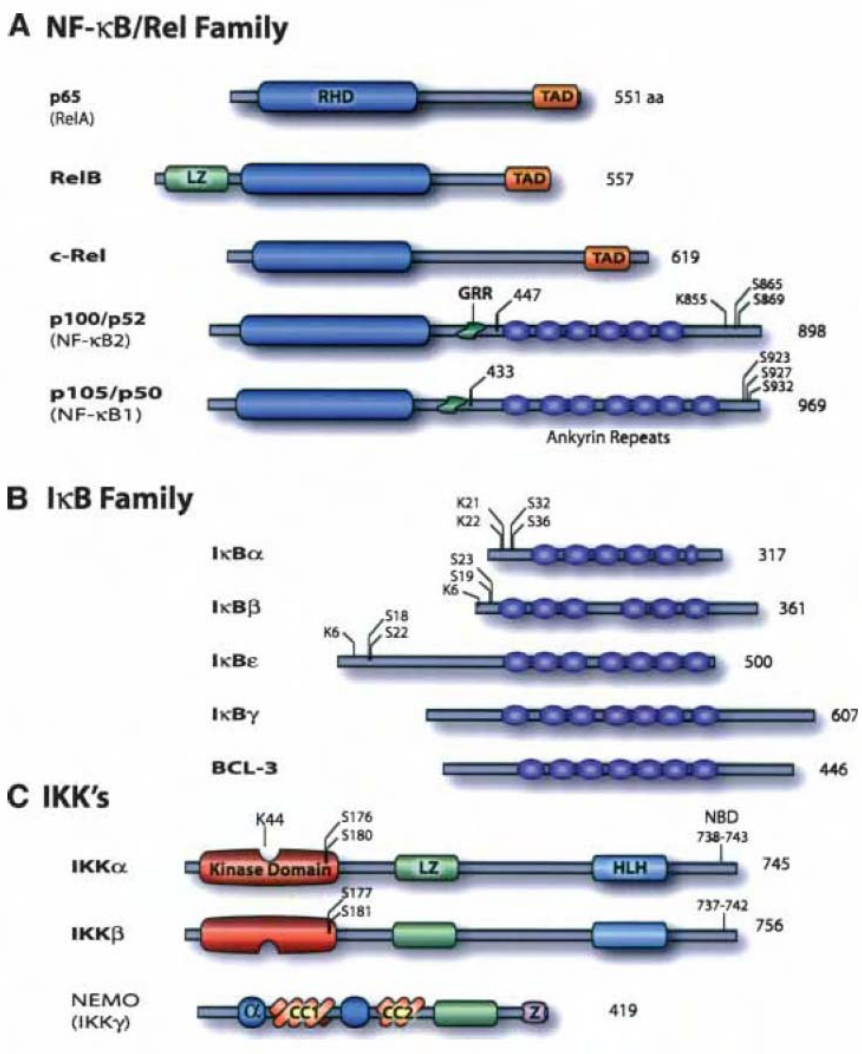

Figure 2. Domains of the NF-κB, IκBα and IKK family members.

NF-κB family members are defined by the presence of an N-terminal Rel homology domain (RHD) that mediates dimerization, binding to IκB proteins and binding to DNA [2]. Activation of NF-κB is mediated by the IκB kinase complex (IKK). In the classical pathway of NF-κB activation, stimulation leads to the phosphorylation and activation of IKKβ. IKKβ then phosphorylates the IκB molecules, mediating their ubiquitination by the SCF-βTrCP ubiquitin-conjugating enzyme complex. Ubiquitination then targets IκB for degradation in the proteosome, freeing NF-κB, allowing for nuclear entry and gene transcription. The alternative pathway

involves the NF-κB family members p100 and p105. These proteins contain internal IκB domains that can be phosphorylated by IKKα and targeted for ubiquitination. Proteosomal cleavage creates the p52 or p50 subunits, allowing for dimerization, nuclear entry and gene transcription [2]. The two main pathways leading to IκB degradation are depicted in figure 3 [2].

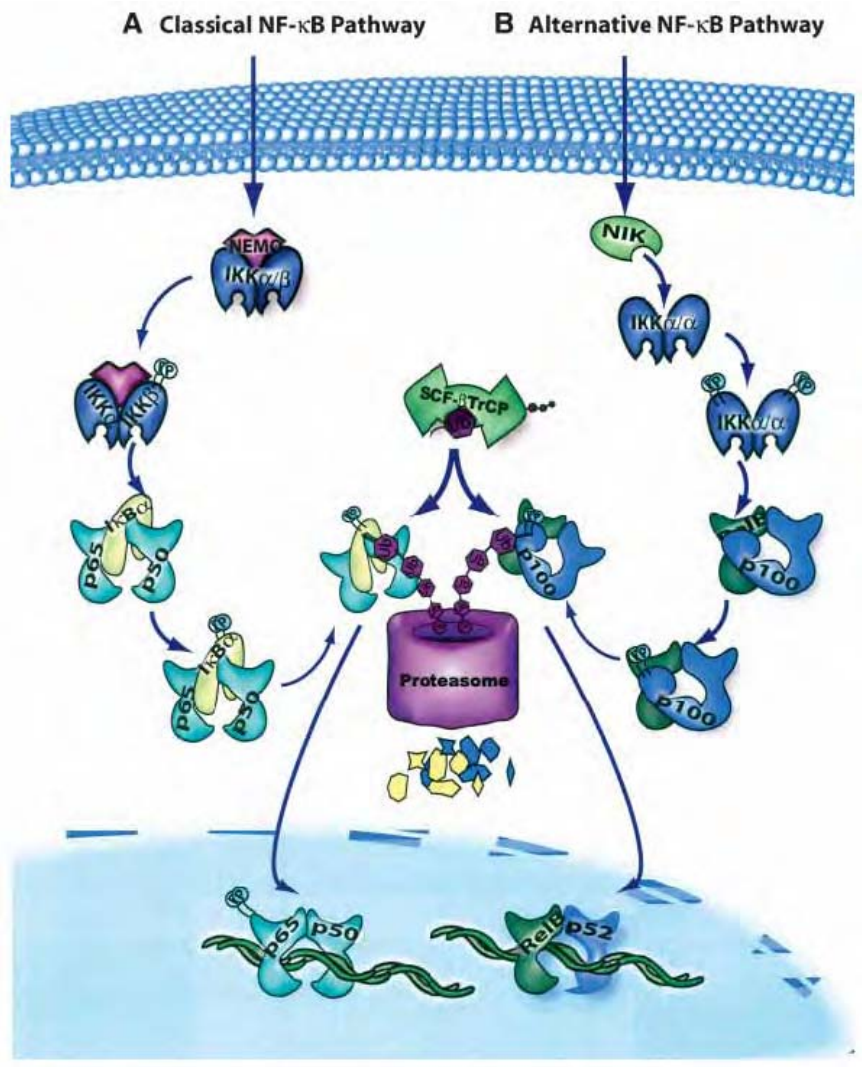

Figure 3. Classical and alternative pathways leading to the activation of NF-κB.

NF-κB, AP-1 and NFAT are all crucial transcription factors for the adaptive immune response. Each of these transcription factors is activated by a different signaling pathway

(Figure 4) [5]. Together, NF-κB, AP-1 and NFAT are able to activate the transcription of a wide variety of genes involved in the immune response, such as: the T cell growth factor IL-2, the cytokines IL-4, 5, 8, 13, INF-γ and TNF-α, the surface receptors CD40L and CD25, and cyclin D1 [1-4]. While many of these factors serve to modulate the immune response, perhaps the most important role is to enable the T cells to pass the G1/S checkpoint [6, 7]. By enabling cell-cycle progression, and by providing growth enhancing cytokines and receptors, NFAT, AP-1 and NF-κB enable T lymphocytes to proliferate and gain effector functions.

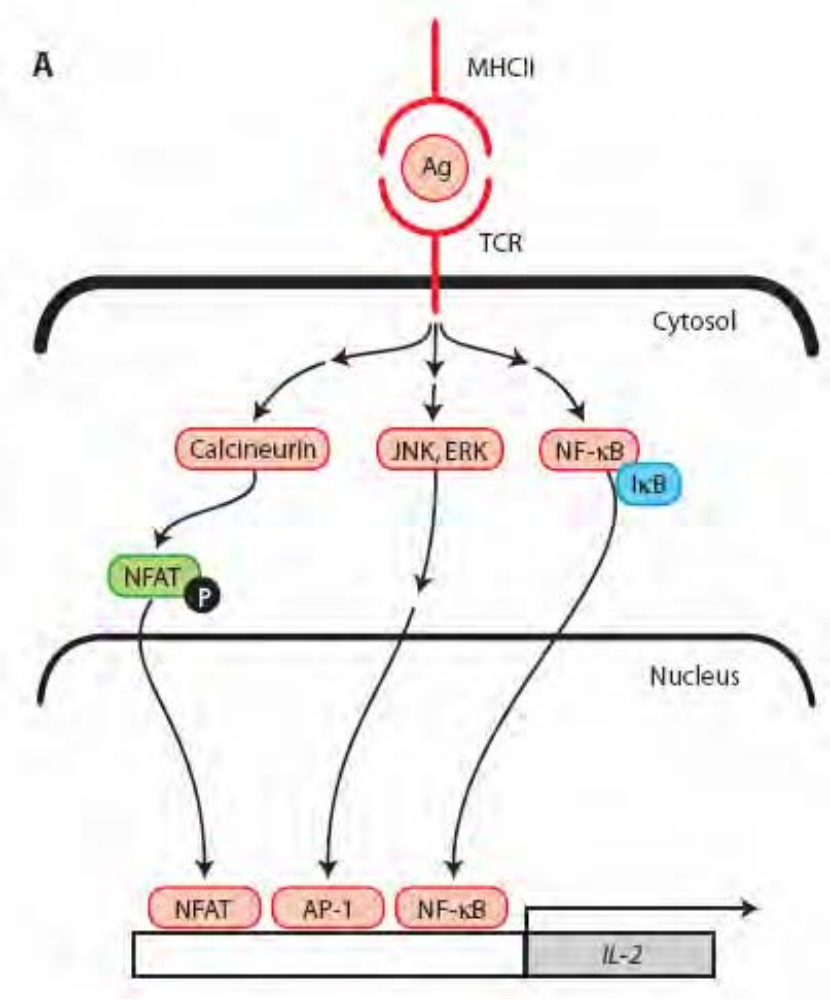

Figure 4. TCR stimulation induces three signaling pathways leading to the activation of NFAT, AP-1 and NF-κB. The cooperative action of these transcription factors is essential for T lymphocyte proliferation and development.

Stimulation of the T cell receptor leads to the activation of multiple signal transduction pathways

The T cell receptor is a heterodimeric transmembrane receptor [8]. The TCR recognizes processed antigen presented by host MHC molecules. The TCR is associated with six transmembrane accessory proteins that are crucial for signal transduction [9, 10]. The four distinct chains of the CD3 complex, in conjunction with a homodimer of ζ chains, are the sites where TCR signal transduction begins [9-11]. Also expressed on the cell surface is the coreceptor CD4, or CD8, and a variety of costimulatory receptors such as CD28.

TCR binding of peptide-MHC complexes induces a dynamic clustering of signal transduction molecules, including the TCR and coreceptors, at the contact point between the T cell and the APC. It is thought that formation of this immunological synapse (IS) brings multiple signaling molecules into close proximity, enhancing signal transduction [12-14].

Upon TCR stimulation, the membrane-bound Src-family kinase, Fyn, is activated [9, 10]. Fyn associates with immunoreceptor tyrosine-based activation motifs (ITAMs) in the cytoplasmic domains of CD3 and ζ chains and mediates their phosphorylation [9, 10]. This allows for the recruitment of the kinase ζ-chain-associated protein 70 (Zap-70) [9, 10]. Zap-70 binds to the phosphorylated ITAMs via its two SH2 domains, but remains in an inactive state until the CD4/8 coreceptor to binds to MHC [15, 16]. The kinase Lck is bound to the cytoplasmic domain of the CD4/8 coreceptor; thus, binding of the coreceptor brings Lck into the proximity of ITAM-bound Zap-70 [11]. Lck phosphorylates Zap-70, which is then able to phosphorylate the linker of activation in T cells (LAT) and the adaptor protein SLP-76 [15, 16]. LAT is associated with lipid rafts, and is able to bind to many proteins through their SH2 domains, mediating signal transduction into the cytoplasm [15, 16]. Phosphorylated LAT is able to bind the adaptor molecule Grb2, which can then bind the guanine-nucleotide exchange factor

Vav [10, 15, 16]. Vav is able to bind to the small G protein Ras, displacing bound GDP and allowing the binding of GTP and the activation of Ras [15-17]. Ras activates the ERK-MAP kinase cascade that results in the activation of Fos [10, 11]. Activation of Jun occurs through CD28 stimulation and JNK-1 signaling, enabling Fos-Jun dimerization and the formation and activation of AP-1 [9-11].

Further upstream, phosphorylated SLP-76 binds to the Tec kinases, mediating their clustering at the TCR, enabling phosphorylation and subsequent activation [9, 15, 16]. The Tec kinases are then able to phosphorylate and activate phospholipase C (PLC)-γ [15, 16]. PLC-γ cleaves inositol phospholipids at the membrane to generate IP_3 and diacylglycerol (DAG) [9, 17]. IP_3 is able to diffuse through the cell, activating the release of intracellular Ca^{2+} stores. Elevated Ca^{2+} levels activate calcineurin to dephosphorylate the transcription factor NFAT, allowing it to enter the nucleus and activate target gene transcription [11]. Generation of DAG at the membrane allows for the recruitment of protein kinase C (PKC)θ to the IS [18-22]. Additionally, CD28 costimulation mediates the recruitment of the phosphoinositide 3-kinase (PI3K) to the IS [23]. PI3K activates the 3-phosphoinositide dependent kinase (PDK-1) and enables its recruitment to the IS [23]. PDK-1 is then able to phosphorylate PKCθ, mediating its activation [23]. Upon activation, PKCθ is able to transduce a signal leading to the activation of NF-κB [20, 21]. A schematic of many of these early signaling events is depicted in Figures 5 [21] and 6 [24].

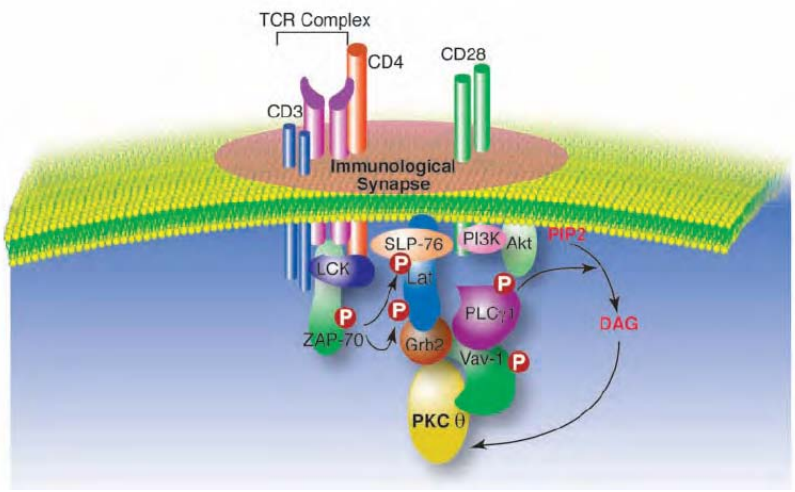

Figure 5. TCR stimulation induces a series of phosphorylation events, resulting in the activation of PKCθ.

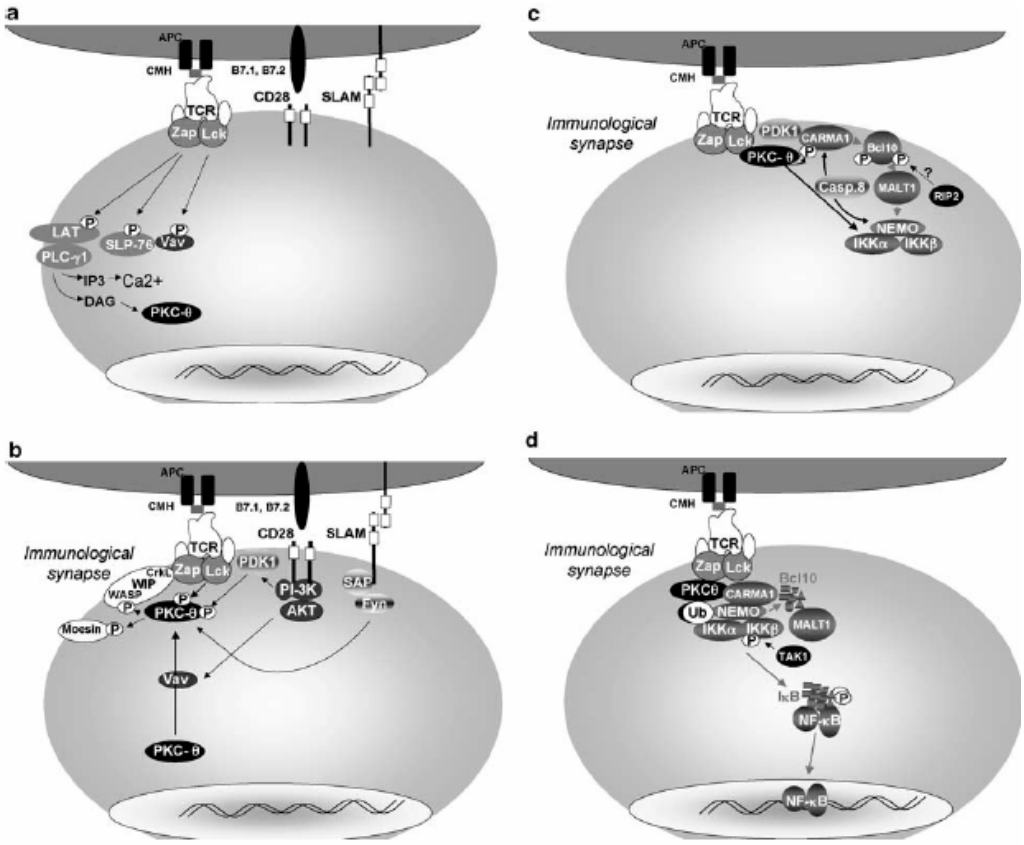

Figure 6. Events following TCR stimulation and leading to the activation of NF-κB. (A) TCR stimulation results in the production of DAG and the recruitment of PKCθ to the IS. (B) CD28 costimulation activates PDK-1, which phosphorylates PKCθ, resulting in its activation. (C) Activated PKCθ then transduces a signal to Bcl10, MALT1 and CARMA1. (D) Bcl10, MALT1 and CARMA1 then activate the ubiquitination of IKKγ, and subsequent activation of NF-κB.

Bcl10, MALT1 and CARMA1 link PKCθ with the activation of NF-κB

The kinase PKCθ is an essential factor for the activation of NF-κB in response to TCR stimulation [18, 20, 25]. Activated PKCθ is able to activate a complex of proteins including Bcl10, MALT1 and CARMA1 [11, 21, 26]. The mechanism of PKCθ-induced activation is unknown; however, it is though that PKCθ, possibly in conjunction with the serine/threonine kinase RIP2, may induce the phosphorylation of Bcl10 and CARMA1 [20, 27, 28]. While the significance of Bcl10 phosphorylation is unknown, the phosphorylation of CARMA1 is thought to mediate its activation and the recruitment of Bcl10 and MALT1 as depicted in figure 7 [27].

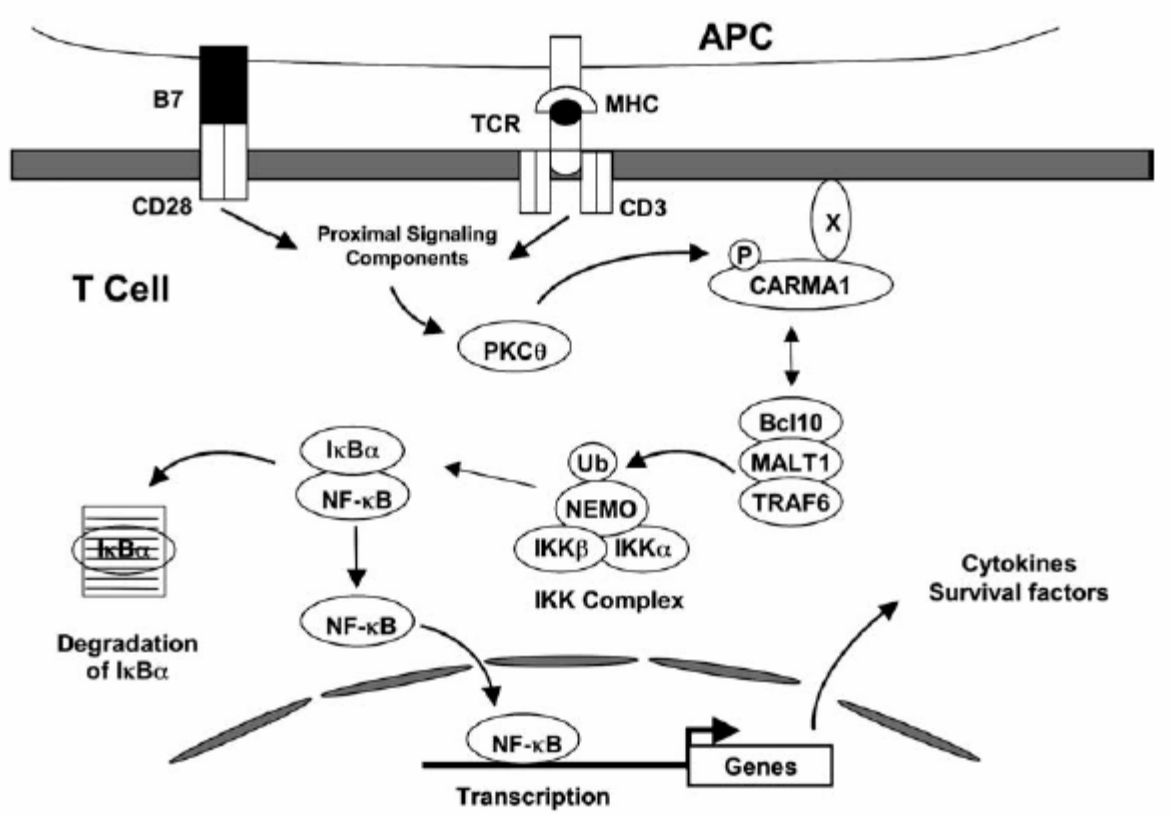

Figure 7. The phosphorylation of CARMA1 may enable the recruitment and activation of Bcl10, MALT1 and TRAF6.

CARMA1 is a membrane-associated guanylate-kinase-like (MAGUK) molecule that contains an N-terminal caspase recruitment domain (CARD) thought to modulate binding to Bcl10 (Figure 8) [11, 29]. Through gene knockout studies, it has been determined that CARMA1 is essential for the activation of NF-κB [30]. It is thought that CARMA1 may enable signal transduction by recruiting PKCθ, Bcl10 and MALT1 to the immunological synapse, thus bringing these crucial signal transducers into close proximity with each other [31].

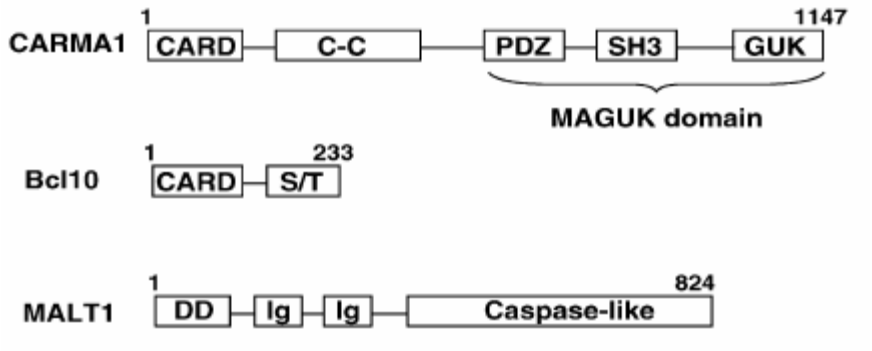

Figure 8. Protein domains of CARMA1, Bcl10 and MALT1.

Bcl10 is an essential adaptor molecule for the TCR-mediated activation of NF-κB (Figure 8) [11]. Bcl10 contains an N-terminal CARD domain that has been shown to mediate binding to other CARD-containing molecules such as CARMA1 and RIP2 [11, 28]. The C-terminus of Bcl10 is serine and threonine rich and has been postulated to be the site of multiple phosphorylation events of unknown function [28, 32-34]. Upon TCR stimulation Bcl10 undergoes a dynamic spatial redistribution into punctate and filamentous structures [35]. Since these filaments resemble death effector filaments involved in apoptosis signaling, they have been called punctate and oligomeric killing or activating domains transducing signals (POLKADOTS; Figure 9) [35].

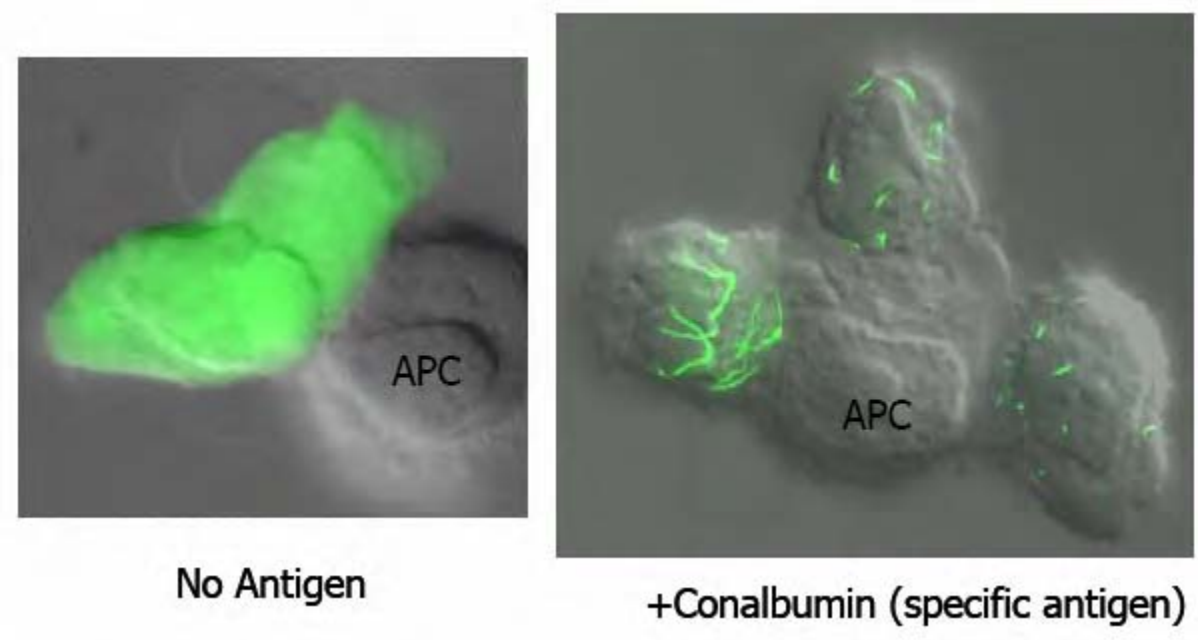

Figure 9. Bcl10-YFP forms POLKADOTS upon antigen stimulation.

Bcl10 also contains a MALT1 binding motif that is crucial for signal transduction [33, 36-38]. It is thought that activation of Bcl10 induces CARD-dependent self-oligomerization [37, 38]. This oligomerization induces the oligomerization of MALT1 [36]. MALT1 is a caspase-like protein that contains an N-terminal death domain, two immunoglobulin-like domains that mediate binding to Bcl10, a caspase-like domain and two TRAF6 binding sites (Figure 8) [33, 36, 39, 40].

Activation-induced oligomerization of MALT1 induces an oligomerization of bound TRAF6 [39]. TRAF6 is an ubiquitin ligase that is activated upon oligomerization. Upon activation, and in conjunction with the ubiquitin-conjugating enzymes Ubc13 and Uev1a, TRAF6 catalyzes the K63-linked ubiquitination of itself and the regulatory IκB Kinase (IKK) IKKγ [39, 41, 42]. K63-ubiquitin chains on IKKγ are recognized by the adaptor protein Tab2, which then mediates activation and recruitment of the kinase Tak1 [43]. Tak1 then phosphorylates the catalytic IKK subunit IKKβ [43]. Phosphorylation activates IKKβ, which

subsequently phosphorylates the inhibitory factor IκB, targeting it for ubiquitin-mediated degradation in the proteosome. IκB normally binds to NF-κB in the cytoplasm, preventing its nuclear entry. Upon degradation of IκB, NF-κB is released, allowing it to enter the nucleus and activate gene transcription [2]. The series of events leading to IKKβ activation is shown in Figure 10 [39].

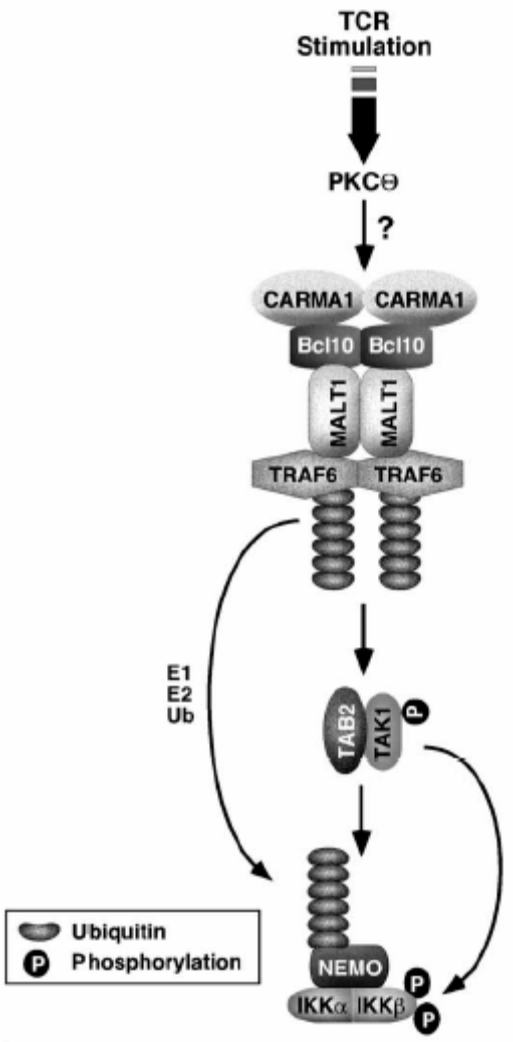

Figure 10. Bcl10, MALT1 and TRAF6 mediate NF-κB activation through the ubiquitination of IKKγ.

Aberrant activation of NF-κB in MALT lymphomas

Bcl10 and MALT1 are both crucial components of the signal transduction pathway linking stimulation of the TCR to activation of NF-κB. Translocations of the Bcl10 and MALT1 genes have been implicated in the pathogenesis of small B-cell lymphomas of the mucosal associated lymphoid tissue (MALT lymphomas) [44, 45]. Two recurrent translocations, t(1;14)(p22;q32) and t(14;18)(q32;q21), put the Bcl10 or MALT1 gene under the control of the immunoglobulin heavy chain gene enhancer, resulting in protein overexpression [45]. It is thought that overexpression of Bcl10 or MALT1 can result in increased activation of NF-κB, though it is not known how these translocation events may mediate pathogenesis in the absence of TCR stimulation.

The most common translocation event, t(11;18)(q21;q21), fuses the cellular inhibitor of apoptosis (cIAP)-2 gene with the MALT1 gene [45, 46]. The translocation fuses the three N-terminal baculoviral IAP repeat (BIR) domains from cIAP2 with the C-terminus of MALT1. The BIR domains are thought to mediate oligomerization, and so may induce an artificial oligomerization of MALT1 [45, 46]. Since this translocation product retains a functional MALT1 C-terminus, aberrant oligomerization of MALT1 results in the oligomerization and activation of TRAF6, allowing for signal transduction and the activation of NF-κB [39, 45, 46]. The mechanisms of aberrant NF-κB activation in these lymphomas is depicted in Figure 11 [21].

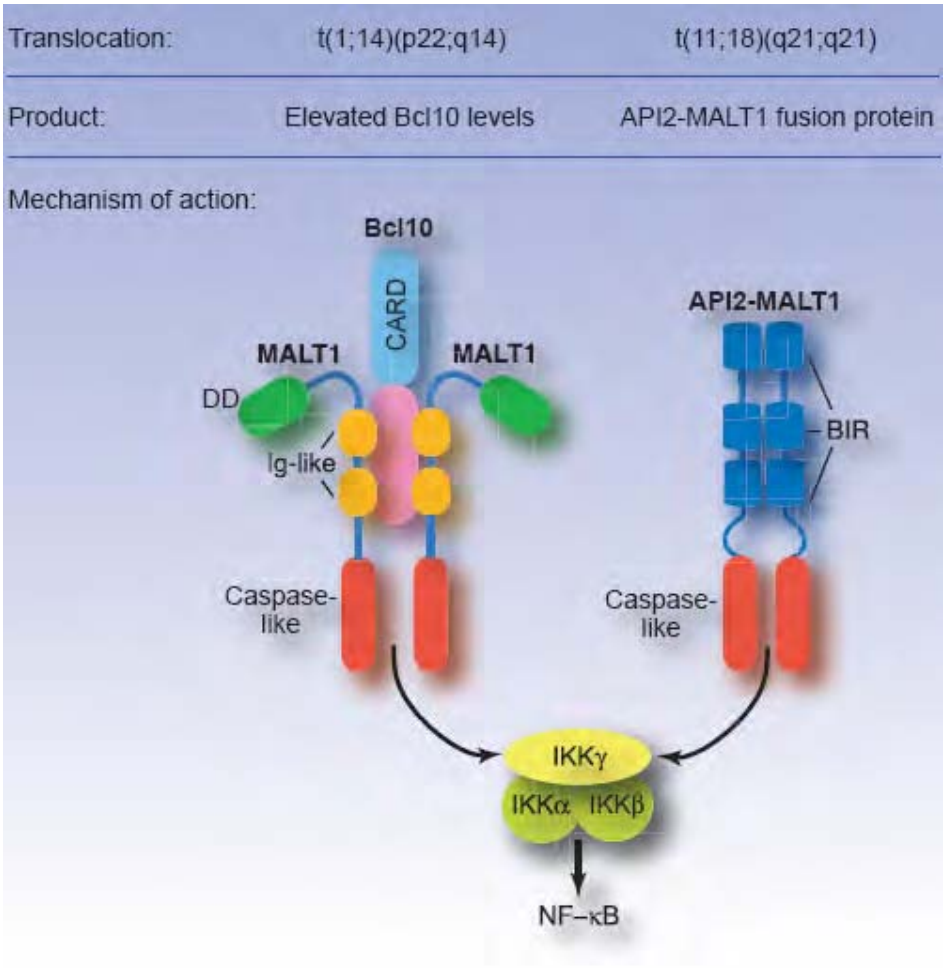

Figure 11. NF-κB activation in MALT lymphomas. Overexpressed Bcl10 can activate NF-κB by binding to MALT1, while the API2-MALT1 fusion protein activates NF-κB through BIR-domain mediated oligomerization.

It is intriguing to note that many of these MALT lymphomas also show a strong pattern of nuclear localization for Bcl10 [45-47]. Recent research has suggested that Bcl10 may have transcriptional activation properties [48]. Thus, aberrant or enhanced nuclear localization of Bcl10 may serve a pathogenic role in these lymphomas [47, 49-51]. Additionally, C-terminal phosphorylation of Bcl10 upon TNFα stimulation has been shown to mediate import into the nucleus via the NF-κB family member Bcl3 [52]. This suggests an additional role for Bcl10 as a, stimulus-induced, transcriptional activator. The implication of Bcl10 and MALT1 translocations

in tumor pathogenesis further illustrates the importance of these proteins in the activation of NF-κB. Additionally, the redistribution of Bcl10 to the nucleus, as well as to POLKADOTS, upon stimulation emphasizes the importance of examining protein localization and redistribution and their impact on normal cellular functions.

Hypothesis and Rationale

Recent research has shown that multiple proteins undergo dramatic spatial redistribution events upon TCR stimulation, and that many of these events are crucial for signal transduction. Furthermore, aberrant localization of the signaling protein Bcl10 is a common finding in MALT lymphoma tumor cells, suggesting a possible role in pathogenesis. Thus, we propose that spatial-temporal mapping of the T cell receptor to NF-κB signaling pathway will help to elucidate the mechanisms of signal transduction and their role in disease pathogenesis. Specifically, we propose to: determine the role for POLKADOTS in the TCR-mediated activation of NF-kB and to elucidate the function and regulation of Bcl10 nuclear localization.

Chapter 2

POLKADOTS Are Foci of Functional Interactions in T-Cell Receptor–mediated Signaling to NF-κB

Published as: Jeremy S. Rossman, Natalia G. Stoicheva, Felicia D. Langel, George H. Patterson, Jennifer Lippincott-Schwartz, and Brian C. Schaefer. 2006. POLKADOTS Are Foci of Functional Interactions in T-Cell Receptor–mediated Signaling to NF-κB. Mol. Bio. Cell **17**(5): 2166-2176.

Abstract

Stimulation of the T-cell receptor (TCR) results in the activation of several transcription factors, including NF-B, that are crucial for T-cell proliferation and gain of effector functions. On TCR engagement, several proteins within the TCR-directed NF-κB signaling pathway undergo dynamic spatial redistribution, but the significance of these redistribution events is largely unknown. We have previously described TCR-induced cytoplasmic structures called POLKADOTS (punctate and oligomeric killing or activating domains transducing signals) that are enriched in the NF-κB signaling intermediate, Bcl10. We now show that these structures are formed only under conditions that promote efficient NF-κB activation. Furthermore, POLKADOTS formation is dependent on functional domains of specific NF-κB signal transducers. Through use of a photoactivatable GFP, we demonstrate that POLKADOTS contain both a highly stable and a rapidly equilibrating protein component. FRET analyses show that POLKADOTS are sites of enriched interactions between Bcl10 and partner signaling proteins. These observations strongly suggest that POLKADOTS are focal sites of dynamic information exchange between cytosolic intermediates in the process of TCR activation of NF-κB.

Introduction

T lymphocytes are critical mediators of the adaptive immune response. The T-cell response to foreign antigen is governed primarily by the T-cell receptor (TCR), a heterodimeric cell surface transmembrane receptor that recognizes processed peptides in the context of the major histocompatibility complex (MHC) [8]. Via its association with a complex of transmembrane molecules called CD3, the TCR activates T-cell cytoplasmic signal transducers, including kinases, phosphatases, and phospholipases [9]. TCR ligation leads to the activation of complex signaling pathways, culminating in the activation of the transcription factors NF-κB, NFAT, and AP-1[53]. Activation of NF-κB is of particular importance in the T-cell response to antigen, because NF-κB activation is required for T-cells to successfully enter S phase [6]. Furthermore, entry into S-phase and subsequent proliferation are required for acquisition of the majority of T-cell effector functions [7].

Recent studies have identified multiple cytosolic mediators that are involved in signal transduction from the TCR to NF-κB. Early TCR-generated signals activate the kinases PDK1 [23] and protein kinase C θ (PKC) [18, 20], which cooperatively transduce a signal [23] to a protein complex containing CARMA1, Bcl10, and MALT1 [26]. Bcl10 is a caspase recruitment domain (CARD)-containing adapter protein that apparently connects the caspase-like protein MALT1 to upstream CARD-containing signaling molecules, including the MAGUK protein, CARMA1 [11], and the kinase, RIP2 [28]. Knockouts of the PKCθ, CARMA1, Bcl10, and MALT1 genes have confirmed that each plays an essential role in TCR activation of NF-κB [11]. Biochemical data suggest that TCR signaling induces the oligomerization of Bcl10 and MALT1, leading to the subsequent oligomerization and activation of the ubiquitin ligase, TRAF6, which

is bound to the C-terminus of MALT1 [39]. Activated TRAF6 mediates the K63-linked ubiquitination of the non-catalytic IκB kinase (IKK) subunit of the IKK complex [54]. K63-ubiquitination of IKK stimulates the recruitment of the kinase TAK1, leading to the phosphorylation of the IKK subunit of the IKK complex [39, 55]. Activated IKK then phosphorylates IκB, resulting in its ubiquitination and subsequent degradation by the proteasome [56]. Degradation of IκB releases cytoplasmic NF-κB, allowing it to enter the nucleus and activate target gene transcription [57].

Previous studies by many groups have shown that several transmembrane and cytoplasmic T-cell signaling proteins undergo dynamic spatial redistribution in response to TCR engagement [58]. In particular, multiple members of the TCR-regulated NF-κB signaling pathway have been shown to redistribute over time to the immunological synapse (IS), the junction between a T-cell and an antigen-presenting cell (APC), where the TCR becomes clustered and transduces signals. Specifically, PKCθ, CARMA1, Bcl10, and the IKK complex have been reported to redistribute to the cytoplasmic face of the stimulated TCR [22, 35, 59, 60]. Interestingly, we have previously reported that a distinct pattern of Bcl10 redistribution precedes its enrichment at the IS. Thus, within the first few minutes after TCR stimulation, Bcl10 initially forms punctate and filamentous structures throughout the T-cell cytosol. Over time, these structures become reorganized, migrating to and clustering at the IS. Because these Bcl10 structures resemble the filamentous structures formed in apoptosis signaling [61], we named them punctate and oligomeric killing or activating domains transducing signals (POLKADOTS; [35].

Our data demonstrated that POLKADOTS formation requires upstream signaling from PKCθ, as well as a functional Bcl10 CARD, whereas cytoskeletal filaments (F-actin,

microtubules, and intermediate filaments) are not required. We also showed that the kinetics of POLKADOTS formation closely mirror the kinetics of biochemical activation of NF-κB. In combination with the biochemical evidence showing that Bcl10 oligomerization is involved in activation of the IKK complex [55], our previous observations [35] suggested that Bcl10 POLKADOTS may be mechanistically involved in transducing TCR-originated signals to NF-κB. In the current study, we sought to further investigate the hypothesis that POLKADOTS are cytoplasmic sites at which oligomerized Bcl10 transmits signals that ultimately result in the activation of NF-κB.

Materials and Methods

Cells and Reagents

D10 T-cells and CH12 B cells were maintained as previously described [35]. Conalbumin was purchased from Sigma (St. Louis, MO). Conalbumin variant peptides [62] were synthesized by the Biomedical Instrumentation Center at the Uniformed Services University, and were used for stimulation experiments at 5 μg/ml. Serine-32 phosphorylated IκBα was detected with a rabbit polyclonal primary antibody (Cell Signaling Technology, Beverly, MA), followed by Alexa555-conjugated goat anti-rabbit IgG (Molecular Probes, Eugene, OR). Anti-LFA-1 antibody I21/7.7 and anti-TCR antibody H57-597 were purified from the hybridomas using protein G and protein A chromatography, respectively. Rat IgG2a isotype control antibody (eBR2a) was purchased from eBioscience (San Diego, CA). Bcl10 was detected with a rabbit polyclonal antibody (H-197; Santa Cruz Biotechnology, Santa Cruz, CA). FLAG-MALT1 was detected with a mouse monoclonal anti-FLAG antibody (M2; Sigma).

Actin was detected with a goat polyclonal antibody (I-19; Santa Cruz Biotechnology). Cellular membranes were stained with CellTrace Bodipy TR methyl ester (Invitrogen, Carlsbad, CA).

Cloning and Retroviral Infections

cDNAs encoding murine Bcl10, PKCθ, MALT1, RIP2, TRAF6, and CARD9 were obtained from IMAGE consortium expressed sequence tag (EST) clones (Invitrogen and ATCC, Rockville, MD). The CARMA1 cDNA was a gift from J. Pomerantz (Johns Hopkins University) and D. Baltimore (Caltech). All cDNAs were of mouse origin, with the exception of the CARD9 cDNA, which was of human origin. cDNAs were fused to the cerulean variant of CFP [63], the citrine variant of YFP [64], mKO (MBL International) or photoactivatable GFP (PA-GFP; [65]. The CFP and YFP genes also contained the A206K mutation, which causes these proteins to behave as monomers, even at high local concentration [66]. Bcl10-ΔMALT1-GFP was constructed from Bcl10-GFP by deleting residues encoding amino acids 107–119, as previously reported [36]. MALT1 constructs were fused with the sequence encoding the FLAG epitope, replacing the starting methionine of MALT1 with the Met-FLAG epitope tag. FLAG-MALT1 deletion constructs were then constructed from the full-length FLAG-MALT1 such that MALT1-ΔC contains amino acids 2–344 of the murine MALT1 protein, MALT1-ΔN contains amino acids 345–832, and MALT1–2EA contains the mutations E661A and E814A in the murine equivalents of the previously reported TRAF6 binding sites [39]. Gene fusions were then cloned into the retroviral expression vectors pEneo or pEhyg [67]. Retroviral infection and selection were as previously described [35]. To confirm that fluorescent protein fusions of signal transduction proteins are fully functional, we compared untagged cDNA constructs to CFP- or YFP-tagged fusion proteins to assess their abilities to activate an NF-κB–responsive luciferase

construct in transient transfection assays. In all tests, there were no statistically significant differences between tagged and untagged constructs in induction of NF-κB activity (Figure 19).

Confocal Microscopy

Conjugates, 2 x 10^5, of D10 T-cells and antigen-loaded CH12 B-cells were fixed with 3% paraformaldehyde for 10 min and mounted in 90:10 glycerol: phosphate-buffered saline, with p-phenylenediamine added to reduce photobleaching. Confocal images were taken at room temperature on a Zeiss Pascal LSM 5 microscope using Zeiss AIM software in multitrack mode (Thornwood, NY). Images were obtained with a 40x Plan-Neofluar 1.3 NA objective or a 100x Plan-Apochromat 1.4 NA objective. CFP was imaged using the 405-nm line of a diode laser (Point-Source, Southampton, United Kingdom) with a 405/488/543-nm excitation filter, a 515-nm dichroic and a 470–500-nm emission filter. YFP was imaged using the 514-nm line of an argon ion laser (Lasos, Jena, Germany) with a 458/514 nm excitation filter, a 515-nm dichroic and a 530–600 nm emission filter. Alexa-555 was imaged using the 543-nm line of a HeNe laser (Lasos) with a 405/488/543-nm excitation filter, a 515-nm dichroic and a 470–500-nm emission filter. CellTrace Bodipy TR methyl ester was imaged using the 543 line of a HeNe laser with a 405/488/543-nm excitation filter, a 515-nm dichroic and a 590-nm long pass emission filter. For live cell imaging, cells were imaged in phenol red–free EMEM (Cellgro, Herndon, VA) with 10% fetal bovine serum and 25 mM HEPES, pH 7.2. Cells were plated in Lab-Tek chamber slides (Naperville, IL) coated with poly-D-lysine, and imaging was performed with stage and objective heaters maintained at a constant temperature of 37°C. POLKADOTS were scored through visual observation of Bcl10 and/or MALT1 clustering. Because both molecules are constitutively enriched in a single cellular focus that colocalizes with the microtubule organizing

center (MTOC; unpublished data), cells were scored as positive for POLKADOTS only if at least two punctate or filamentous structures were observed (the vast majority of cells had more than this) in the cell, which were brighter than the average cytosolic fluorescence by at least a factor of 2.

Fluorescence Energy Resonance Transfer (FRET)

For each pair of proteins examined, three cell lines were prepared: CFP fusion protein only, YFP fusion protein only, and a cell line expressing both fusion proteins. Conjugates from all three cell lines were prepared in tandem, as described above for confocal microscopy. Cells were imaged on a Zeiss Pascal LSM 5 microscope using Zeiss AIM software. Images were obtained with a 40x Plan-Neofluar 1.3 NA objective. Images were collected in multitrack mode with four channels: DIC, CFP, YFP, and fluorescence energy resonance transfer (FRET). CFP was imaged using the 458-nm line of an argon ion laser (Lasos) with a 458/514-nm excitation filter, a 515-nm dichroic and a 470–500-nm emission filter. YFP was imaged as described above. FRET was visualized with the 458-nm line of an argon ion laser (Lasos), a 458/514-nm excitation filter, a 515-nm dichroic and a 530–600-nm emission filter. All filters were from Chroma (Brattleboro, VT). Images were gathered without binning, at 12 bit, with 4 times averaging and with a pixel time of 1.6 µs. N-FRET was calculated as previously described (Xia and Liu, 2001), using the Aim software FRET macro v1.5d (Zeiss) and the default settings. Cross-talk parameters and N-FRET estimates were calculated using 50–100 cells each.

Photo-activation of PA-GFP

D10 T-cells, 1 x 10^5, expressing Bcl10-PA-GFP and MALT1-mKO were conjugated to CH12 B cells for 20 min in poly-D-lysine (Sigma)-coated Lab-Tek chamber slides. Live cell imaging was as described above. Images were obtained on a Zeiss 510 Meta laser scanning confocal microscope with a 63x Plan-Apochromat 1.4 NA objective using Zeiss Aim software. mKO was imaged using the 543-nm line of a HeNe laser (Lasos) with a 700/543-nm excitation filter, a 545-nm dichroic and a 560–615-nm emission filter. Activated PA-GFP was imaged using the 488-nm line of an argon ion laser (Lasos), a 700/488-nm excitation filter and a 500–550-nm emission filter. Multiphoton PA-GFP activation was performed using the Aim software bleach macro (Zeiss) with 800-nm excitation from a TI:Sapphire Chameleon laser (Coherent, Palo Alto, CA) with an activation time of <1 s. One-photon activation of PA-GFP was performed as previously described [65].

Western Blotting

For each time point 2–5 x 10^6 D10 T-cells were stimulated on 100 µg/ml plate-bound anti-TCR antibody. Cells were lysed in 1x Laemmli buffer with sonication, and 1 x 10^6 cell equivalents were run per lane. Samples were subjected to SDS-PAGE gel electrophoreses, transferred to a nitrocellulose membrane, and probed with an anti-P-IκBα antibody (Cell Signaling Technology). Membranes were stripped with Restore Western blot stripping buffer (Pierce, Rockford, IL) and reprobed with additional antibodies, as indicated in Figure 4. Primary antibodies were detected with species-specific HRP-conjugated secondary antibodies (Jackson ImmunoResearch, West Grove, PA). Membranes were developed with SuperSignal Dura

(Pierce), imaged on a Fuji LAS-3000 CCD camera system and quantified using MultiGauge 3.0 software (Fuji, Stamford, CT). p-values were calculated using a Student's t test.

Results

Productive and continuous T cell receptor signaling is required for POLKADOTS formation and maintenance

We have previously shown that T-cell Bcl10 redistributes to POLKADOTS in response to specific antigen stimulation of the TCR, and we showed that POLKADOTS formation is dependent on PKC activity and occurs after PKCθ translocation to the IS [35]. However, these experiments were performed under conditions of optimal antigen stimulation. To determine how suboptimal stimulation of the TCR influences PKCθ translocation and POLKADOTS formation, we performed an antigen titration experiment. D10 T-cells expressing PKCθ-CFP and Bcl10-YFP were stimulated with APCs (CH12 B cells), which had been loaded with increasing doses of stimulatory antigen (conalbumin). Microscopic analyses showed that both PKCθ translocation and Bcl10 POLKADOTS formation occurred with reduced frequency as the concentration of stimulatory antigen was lowered (Figure 12A). Although T-cells with PKCθ translocation almost always also contained Bcl10 POLKADOTS, a large fraction of cells had Bcl10 POLKADOTS in the absence of PKCθ translocation. These results are consistent with our live cell observations showing that PKCθ translocation precedes formation of Bcl10 POLKADOTS ([35]. On initiation of Bcl10 POLKADOTS formation, we observed a reversal of PKCθ enrichment at the IS, with the result that POLKADOTS persisted in an enriched state after detectable PKCθ translocation had terminated [35]. Thus, in cells that contain POLKADOTS,

but no PKCθ translocation (Figure 12A), the enrichment of PKCθ at the IS had presumably already completely reversed.

We also previously observed that POLKADOTS formation commenced 7–10 min after initial (optimal) antigen stimulation, and Bcl10 enrichment in POLKADOTS continued for at least 30 min after initial formation [35]. To assess whether continuous TCR signaling is required for the maintenance of POLKADOTS, D10 T-cells expressing Bcl10-CFP were conjugated with antigen-loaded APC for 20 min. To prematurely terminate TCR signaling, T-cell/APC conjugates were disrupted by addition of anti-LFA-1 antibody, or treated with an isotype control antibody. Microscopic analyses of the cell population after conjugate disruption revealed that continuous cell–cell contact was required for POLKADOTS maintenance. Disruption of T-cell/APC interaction resulted in the decay of cytosolic POLKADOTS over a period of 30 min, to levels comparable to preincubation with anti-LFA-1 (Figure 12B). Together, the data in Figure 12 show that POLKADOTS formation is directly influenced by the efficiency of TCR stimulation, and that continuous TCR signaling is required for the maintenance of POLKADOTS.

We next investigated the effect of a distinct form of suboptimal TCR stimulation on POLKADOTS formation, using single amino acid substitution variants of the stimulatory conalbumin peptide [62]. We stimulated D10 T-cells that express either PKCθ-CFP and Bcl10-YFP or Bcl10-CFP and MALT1-YFP with selected conalbumin peptides having distinct stimulatory efficiencies. Strong agonist peptides (wild-type and I5N) stimulated efficient PKC translocation and POLKADOTS formation. In contrast, modest or weak agonists (W7Y, I5L, I5V, and I5G) stimulated no PKCθ translocation and resulted in minimal POLKADOTS formation (Table 1). Furthermore, stimulation by modest or weak agonist peptides caused no detectable increase in phosphorylation of IκBα, indicating that they induced little to no NF-κB

activation (Table 1). These results show that measurable NF-κB activation occurs only when POLKADOTS formation and PKC translocation are observed, thereby providing further evidence that these translocation events mechanistically participate in TCR activation of NF-κB.

Interaction between Bcl10 and MALT1 is required for POLKADOTS formation

Previous studies have shown that Bcl10 directly interacts with the caspase-like protein, MALT1 [26, 36, 68], and that these proteins cooperatively participate in TCR-mediated activation of NF-κB [39]. On the basis of these observations, we expected that MALT1 would colocalize with Bcl10 in POLKADOTS. We thus performed a time course experiment to determine the degree of colocalization of Bcl10 and MALT1 in POLKADOTS. D10 T-cells expressing Bcl10-CFP and MALT1-YFP were conjugated with antigen-loaded CH12 B cells and imaged via confocal microscopy. Figure 13 shows that small POLKADOTS formed by 20 min after stimulation. Over the next hour, the POLKADOTS coalesced into larger structures, with some moving toward the IS. POLKADOTS formation and coalescence peaked at 90 min and then decayed over the next 90 min. By 180 min, the majority of Bcl10 POLKADOTS had decayed, and the remaining MALT1 POLKADOTS were very small (Figure 13). Thus, over 3 h of TCR stimulation, POLKADOTS form, reach a maximal intensity, and begin to disappear. POLKADOTS contain significant levels of both Bcl10 and MALT1 until the reversal phase. The accelerated disappearance of Bcl10 from POLKADOTS may be related to the reported degradation of Bcl10, post-TCR stimulation [69].

The interaction between Bcl10 and MALT1 has been reported to be functionally important for activation of the IKK complex [39, 55]. To determine whether the interaction between Bcl10 and MALT1 is also necessary for POLKADOTS formation, we constructed a

D10 T-cell line expressing a Bcl10 mutant (Bcl10-ΔMALT1-GFP) that cannot interact with MALT1, and cannot activate NF-κB [36]. The Bcl10-ΔMALT1-GFP cell line was observed to form no POLKADOTS, whereas a control cell line expressing wild-type Bcl10-GFP efficiently formed POLKADOTS upon antigen stimulation (Figure 14). Thus, Bcl10 must interact with MALT1 for Bcl10 POLKADOTS formation to occur.

We next performed experiments to determine the influence of various functional domains of MALT1 on the activation of NF-κB and the formation of POLKADOTS. We constructed mutants of MALT1 lacking the C-terminus (ΔC), lacking the N-terminus (ΔN), or having mutated TRAF6 binding sites (2EA; Figure 15A). The TRAF6 binding sites are required for MALT1-mediated activation of the IKK complex [39]. Because only the N-terminus of MALT1 is required for interaction with Bcl10 [36, 40], we expected that all of the MALT1 constructs except the ΔN mutant would interact with Bcl10. We used FRET to measure interactions between Bcl10-CFP and MALT1-YFP constructs in D10 T-cells. Although there were slight differences in Bcl10 binding efficiency between the wild-type, ΔC, and 2EA mutants, all clearly bound to Bcl10, whereas the ΔN mutant did not bind to Bcl10, either before or after antigen stimulation (Figure 15B).

We next assessed NF-κB activation in these cell lines by quantifying increases in phosphorylation of IκBα. Consistent with previously reported data in the Jurkat T-cell line [40], deletion of the MALT1 C-terminus blocked NF-κB activation. As expected (Sun et al., 2004), mutation of the TRAF6 binding sites (2EA) also blocked NF-κB activation. Moreover, the basal level of NF-κB activation in the 2EA-expressing cell line was also significantly diminished. In contrast, deletion of the MALT1 N-terminus did not inhibit NF-κB activation (Figure 15, C–E), and caused a reproducible enhancement of basal IκBα phosphorylation in unstimulated cells

(albeit statistically insignificant). We also assessed the degree of Bcl10 phosphorylation. Although the significance of Bcl10 phosphorylation has not yet been determined, we previously observed that phosphorylation of Bcl10 is TCR- and PKC-dependent, and occurs with kinetics that closely mimic the kinetics of NF-κB activation [35]. However, as shown in Figure 15C, the occurrence and degree of Bcl10 phosphorylation does not seem to follow a predictable pattern. Although there is some degree of correlation with the level of overexpression of the Bcl10-CFP fusion protein (Figure 21), the lack of correlation with IκBα phosphorylation suggests that phosphorylation of the Bcl10 protein may not participate in NF-κB activation. Indeed, our preliminary data suggest that phosphorylation is confined to the C-terminal third of the Bcl10 protein (F. Langel and B. Schaefer, unpublished data), a region that is not required for Bcl10 activation of NF-κB [36]. Overall, these data show that a MALT1 C-terminal region containing functional TRAF6 binding sites is required for TCR-mediated activation of NF-κB.

We next determined the effects of the MALT1 mutants on POLKADOTS formation, using confocal microscopy to detect Bcl10/MALT1 POLKADOTS after antigen stimulation. We found that only the cell line expressing wild-type MALT1 formed Bcl10/MALT1 POLKADOTS. The ΔC cell line exhibited no POLKADOTS formation, whereas cell lines expressing the ΔN and 2EA mutants formed a few POLKADOTS containing only Bcl10 in a minority population of cells (Figure 15F). We hypothesize that the sporadic Bcl10-only POLKADOTS may reflect the fact that endogenous MALT1 is still being expressed in these cells, allowing for the induction of some POLKADOTS formation. Overall, however, the data in Figure 15 demonstrate that POLKADOTS form only when a fully functional MALT1 interacts with Bcl10. Moreover, the fact that the 2EA mutant fails to form POLKADOTS strongly suggests that TRAF6 must also

interact with this complex in order for Bcl10 and MALT1 to redistribute to the POLKADOTS structures.

POLKADOTS are enriched in both stable and rapidly equilibrating Bcl10

To better understand the physical nature of POLKADOTS, we devised a set of experiments to determine whether POLKADOTS are stable sites of enrichment of cytoplasmic Bcl10, or, alternatively, whether the Bcl10 in POLKADOTS is at rapid equilibrium with the cytosolic pool of Bcl10. For these experiments, Bcl10 was fused to a PA-GFP [65], and MALT1 was fused to the reef coral fluorescent protein, monomeric Kusabira-Orange (mKO) [70]. D10 T-cells expressing Bcl10-PA-GFP and MALT1-mKO were then used in photoactivation experiments. Bcl10-PA-GFP was activated in either the cytoplasm or in POLKADOTS, and then imaged over time. MALT1-mKO was used as a marker for the location of POLKADOTS.

As shown in Figure 16, A and B multiphoton activation of PA-GFP in a single POLKADOT results in stable fluorescence over a period of at least 30 min, with no detectable equilibration of PA-GFP with the cytosolic pool. These results suggested that POLKADOTS are sites of extremely stable enrichment of Bcl10. Next, we activated PA-GFP in the cytosol, to determine equilibration kinetics in the cytoplasm. After cytosol activation, we observed identical PA-GFP fluorescence in the activated cytoplasm region of interest (ROI) and in a distal cytoplasm ROI, from the earliest postactivation time point (8s). Thus, as expected, there is rapid equilibration of PA-GFP in the cytoplasm (Figure 16C). In contrast, we were quite surprised to observe rapid equilibration of photoactivated cytosolic PA-GFP with POLKADOTS (Figure 16D), a result that initially appeared to contradict the results of photoactivation of single POLKADOTS. This experiment was repeated several times to confirm that it was not simply the

result of performing photoactivation during a period in which POLKADOTS were still rapidly forming. In every case, the same phenomenon was observed (four distinct examples are shown in Figure 16E). Importantly, the rapid incorporation of cytosolically activated PA-GFP into POLKADOTS is not followed by any measurable gain in fluorescence over time, further demonstrating that these observations are reflective of a process of rapid equilibration, rather than a continued incorporation of cytosolic Bcl10 into POLKADOTS during their formation. Thus, we conclude that POLKADOTS are also at rapid equilibrium with the cytosolic pool of Bcl10. In sum, these data show that POLKADOTS consist of two distinct pools of Bcl10 protein: a population of Bcl10 protein that is very stably incorporated in POLKADOTS, and a second population of Bcl10 molecules that are in rapid equilibrium with cytosolic Bcl10.

POLKADOTS are Sites of Enrichment of Functional Signaling Interactions

The presence in POLKADOTS of a population of Bcl10 molecules in rapid equilibration with cytosolic Bcl10 suggests that POLKADOTS are sites of dynamic formation and dissociation of protein–protein interactions between Bcl10 and itself, possibly via CARD–CARD homotypic interactions or activation-induced oligomerization of partner proteins such as TRAF6. The close relationship between POLKADOTS and TCR activation of NF-κB further suggests that POLKADOTS may also represent sites of heterotypic interactions between Bcl10 and known partner signaling proteins. Bcl10 has been reported to interact with numerous cytoplasmic signaling molecules including MALT1, the CARD proteins RIP2, CARMA1, and CARD9, and, the ubiquitin ligase TRAF6 (an indirect interaction, via MALT1) [28, 36, 37, 39, 71]. To investigate the interactions between Bcl10 and these partner signaling proteins in T-cells, we made YFP fusions of each of these proteins and introduced them into D10 cells that also

expressed Bcl10-CFP. We then assessed interactions between Bcl10 and each partner signaling protein by performing FRET analyses both in the whole cell and in individual POLKADOTS.

As we showed in Figure 15B, we used FRET to measure the interaction of various MALT1 constructs with Bcl10, confirming that this interaction depends on the N-terminus of the protein, as previously reported [36]. In Figure 17, A and B, we extended these results by performing FRET analysis on both whole cells and POLKADOTS. As is suggested by the strong colocalization of Bcl10 and MALT1 in POLKADOTS, there is also enhanced FRET between Bcl10 and MALT1 in these structures. Bcl10-MALT1 FRET in POLKADOTS peaks at 20 min, and declines significantly by 60 min. This apparent dissociation over time of MALT1-Bcl10 interactions in POLKADOTS is consistent with the distinct kinetics of disappearance of Bcl10 and MALT1 from POLKADOTS at late time points after stimulation (see Figure 13). These FRET kinetics furthermore suggest that dissociation of close Bcl10-MALT1 interactions begins while there is still strong colocalization of Bcl10 and MALT1 in POLKADOTS.

Validity of this FRET assay was confirmed by establishing control cell lines, in which FRET was measured both between nonfused versions of CFP and YFP and between Bcl10-CFP POLKADOTS and nonfused YFP (Figure 22). In both cases, the FRET values were 0.4–0.5%, and the value of 0.5% thus represents the threshold for detection of significant FRET interactions in our studies (dashed red line). Validity of the assay is further supported by our observation that we detected no significant FRET between Bcl10 and MALT1 when the N-terminal domain of MALT1 (required for Bcl10-MALT1 interaction) was not present (Figure 15B).

As anticipated, enhanced Bcl10-Bcl10 FRET was detected in POLKADOTS, and this FRET increased between 20 and 60 min (Figure 17C), suggesting that Bcl10-Bcl10 homotypic interactions increase over time in POLKADOTS. We also measured FRET between Bcl10 and

CARMA1, RIP2, TRAF6, and CARD9 (Figure 17, D–G). With the exception of CARD9, all of these proteins demonstrate measurable interaction with Bcl10 on the whole cell level and enhanced association with Bcl10 in POLKADOTS. It is important to note that the absence of FRET between Bcl10 and CARD9 may have other explanations, such as an orientation or spacing of the CFP and YFP chromophores that does not yield efficient FRET. However, of the above four proteins, only CARD9 has not been reported to participate in TCR activation of NF-κB, and its association with Bcl10 in T lymphocytes has also not been previously investigated. Thus, the observation that CARD9 may not interact with Bcl10 in T-cells, although somewhat surprising, does not contradict previously published data. In contrast, CARMA1, RIP2 and TRAF6 all demonstrate enhanced FRET with Bcl10 in POLKADOTS, suggesting that POLKADOTS are also sites of enrichment of complexes between Bcl10 and these three partner signaling proteins.

The kinetics of FRET between Bcl10 and TRAF6 in POLKADOTS mirrors the kinetics of Bcl10-MALT1 FRET, with the interaction in POLKADOTS maximal at 20 min and declining by 60 min. Because the association of Bcl10 and TRAF6 is mediated by the association of both molecules with MALT1 [39], this observation is consistent with published biochemical data.

The lack of observation of FRET between Bcl10 and CARMA1 in POLKADOTS at the 20-min time point was due to the fact that significant POLKADOTS formation does not occur in this cell line until 60 min. We are unsure of the mechanism that accounts for the delayed kinetics of POLKADOTS formation in the Bcl10-CARMA1 cell line. However, it is notable that this cell line was very difficult to produce, with very few cells surviving the initial retroviral infection with the CARMA1-YFP retrovirus. Thus, it is possible that only cells that are impaired in CARMA1-mediated NF-κB activation survived the initial selection, perhaps causing the

delayed POLKADOTS formation phenotype. Importantly, though, we did observe significantly enhanced Bcl10-CARMA1 FRET in POLKADOTS, once formed.

Finally, as seen with the Bcl10-Bcl10 homotypic CARD–CARD interactions, the heterotypic CARD–CARD interaction between Bcl10 and RIP2 also increased between 20 and 60 min. Because RIP2 has been reported to phosphorylate Bcl10 [28], and because the kinetics of POLKADOTS formation mirror the kinetics of Bcl10 phosphorylation [35], the observation of strong Bcl10-RIP2 FRET in POLKADOTS may suggest that POLKADOTS are a major site of phosphorylation of Bcl10 by RIP2.

In summary, in all cell lines exhibiting FRET, the measured FRET was greatest in the POLKADOTS. The simplest interpretation of these observations is that POLKADOTS are sites of enriched interactions between Bcl10 and partner signaling proteins. However, it is important to note that other phenomena, such as protein conformational changes, can also influence FRET [72]. Given that the data show only increased FRET in POLKADOTS, relative to whole cell FRET, we believe that the data are most consistent with increased protein–protein associations in POLKADOTS. These data thus strongly suggest that POLKADOTS are functional sites of signaling interactions in the TCR-driven NF-κB signaling pathway.

Discussion

Receptor-stimulated assembly of cytoplasmic signal transduction intermediates into macromolecular signaling complexes is poorly understood. For most signaling pathways, there is little or no information regarding whether activated signal transduction intermediates assemble into macromolecular complexes at discrete intracellular sites, or whether assembly of such

protein complexes occurs throughout the cytosol, without obvious spatial organization. In this study, we have performed a series of experiments to address the hypothesis that TCR-induced cytoplasmic structures called POLKADOTS are sites of assembly of macromolecular clusters of signaling intermediates, which actively participate in the transduction of signals to NF-κB.

In support of the above hypothesis, we first showed that antigen dose governs the frequency of PKCθ translocation and Bcl10 POLKADOTS formation in T-cells (Figure 12A). We furthermore showed, via anti-LFA-1 disruption of T-cell/APC conjugates, that maintenance of POLKADOTS requires continuous TCR signaling (Figure 12B). Additionally, using previously characterized substitution mutants of the conalbumin peptide, we showed that efficient PKCθ translocation, formation of Bcl10 POLKADOTS, and measurable activation of NF-κB occur only in response to strong agonist peptides (Table 1). Together, the above data establish that TCR stimulation of PKCθ translocation to the IS, formation of Bcl10 POLKADOTS, and activation of NF-κB are closely linked processes that occur efficiently only under conditions of optimal TCR stimulation.

We next investigated the potential role of functional cooperation between Bcl10 and MALT1 in POLKADOTS formation and activation of NF-κB. In Figure 13, we demonstrated that Bcl10 and MALT1 colocalize in POLKADOTS and are recruited to POLKADOTS with indistinguishable kinetics. The importance of direct interaction between Bcl10 and MALT1 for POLKADOTS formation was demonstrated by showing that either deletion of the MALT1 interaction domain of Bcl10 or deletion of the Bcl10 interaction domain of MALT1 abrogates POLKADOTS formation (Figures 14 and 15). Moreover, interaction of Bcl10 with a signaling-competent form of MALT1 is required for POLKADOTS formation, because deletion or point mutation of the TRAF6 binding sites of MALT1 also blocks POLKADOTS formation (Figure

15). These data suggest that Bcl10, MALT1, and TRAF6 are all required participants in assembly of POLKADOTS.

A potentially complicating observation in these experiments was the fact the cell line expressing the MALT1-ΔN mutant (deletion of the Bcl10-binding domain) was not at all impaired in TCR activation of NF-κB, consistent with previously reported results [40]. These results suggest either that the ΔN mutant is not effective as a dominant negative, or that the ΔN mutant is capable of activating NF-κB by a Bcl10-independent mechanism. The following observations suggest that the second possibility is correct: First, the ΔN mutant blocks the formation of Bcl10 POLKADOTS, strongly suggesting that this construct is indeed a potent dominant negative (note that Bcl10 POLKADOTS form robustly in the absence of ectopically expressed wild-type MALT1) [35]. Second, it has previously been reported that the ΔN mutant can directly interact with CARMA1 [40]. Because CARMA1 is an upstream activator of Bcl10, and because Bcl10-mediated activation of NF-κB appears to be entirely dependent on interaction with MALT1, the direct interaction between CARMA1 and the MALT1 ΔN mutant may bypass the need for Bcl10 in TCR activation of NF-κB. Finally, in some MALT lymphomas that exhibit MALT1 translocations with the IAP-2 gene, the entire Bcl10-interaction domain is deleted, but the translocation product activates NF-κB independently of upstream stimuli, again demonstrating that the MALT1 C-terminus is competent for transducing activating signals. In sum, several lines of evidence strongly suggest that the C-terminus of MALT1 is capable of activating NF-κB independently of interaction with Bcl10 and, consequently, independently of POLKADOTS formation. Further experimentation will be required to determine whether this Bcl10-independent activity of the MALT1 C-terminus occurs only upon substantial overexpression.

In contrast, the presence of the N-terminal Bcl10 interaction domain renders MALT1 completely dependent on Bcl10 for activation of NF-κB, as evidenced by the fact that antigen receptor activation of NF-κB is blocked by deletion of the Bcl10 gene [73]. In the case of MALT1 mutants that contain the Bcl10 interaction domains (ΔC and 2EA mutants), there is a strong correlation between blockade of NF-κB activation and inhibition of formation of POLKADOTS. Thus, the above data both suggest that POLAKDOTS formation is an integral feature of NF-κB activation in the context of a MALT1 protein that is capable of interacting with TRAF6, and they are consistent with our model that POLKADOTS formation plays a mechanistic role in TCR activation of NF-κB.

Previous models of TCR-mediated activation of NF-κB have shown a stepwise signal transduction pathway, whereby oligomerization of Bcl10 leads to the binding and oligomerization of MALT1 and then of TRAF6 [39]. However, our data show that MALT1 and TRAF6 are required for the oligomerization of Bcl10 and the formation of POLKADOTS. Our data furthermore imply that POLKADOTS formation is required for TRAF6-mediated ubiquitination of IKK [39] and subsequent NF-κB activation. Thus, Bcl10, MALT1, and TRAF6 appear to act in concert, transducing TCR signals to NF-κB. In this capacity, these molecules may best be described as a tripartite enzyme.

To better characterize the composition and assembly of POLKADOTS, we performed studies with Bcl10 fused to a photoactivatable variant of GFP [65]. Photoactivation of individual POLKADOTS versus photoactivation of cytoplasmic ROIs led to the surprising observation that there appear to be two distinct pools of Bcl10 in POLKADOTS: a population of molecules that are stable in POLKADOTS over an extended time period, and a population of molecules that are at rapid equilibrium with the cytosolic pool of Bcl10 (Figure 16). These results are consistent

with previous studies that have shown the presence of stable, TCR-signaling induced microdomains that can alter the free diffusion of signaling molecules [74, 75].

We propose a model in which the inner "core" of POLKADOTS would contain oligomerized Bcl10, possibly in association with partner signaling proteins such as MALT1 and TRAF6. Whether such oligomerization is driven by Bcl10 CARD–CARD homotypic interactions, or by the oligomerization of a partner protein (e.g., MALT1 or TRAF6), remains to be established. In this model, molecules in the inner core of the POLKADOTS would not be accessible to the cytosol, and would thus not be at equilibrium with cytosolic Bcl10. In contrast, molecules occupying the outer membrane "shell" of the POLKADOTS would be accessible to the cytosol, and we postulate that this is the population of molecules that is at rapid equilibrium with cytosolic Bcl10 (Figure 18). Alternatively, it is also possible that the interactions between proteins in the stable POLKADOTS-associated pool and the freely diffusible pool may occur throughout a porous POLKADOTS structure, as opposed to our postulated outer shell. However, if the core of the POLKADOTS was found to be separated from the shell by a membrane (Figure 18), this second possibility would be much less likely. Indeed, the existence of a membrane boundary separating the outer shell from the inner core is supported by our preliminary observations that Bcl10 and MALT1 POLKADOTS appear to colocalize with membrane bound structures (Figure 23). However, further work is needed to confirm this observation, and to further establish the characteristics of this putative membrane boundary.

Finally, FRET studies of interactions between Bcl10 and several previously reported partner signaling proteins (Figure 17) confirmed that, in T-cells, Bcl10 interacts to a significant degree with each of these proteins (with the exception of CARD9). Importantly, upon stimulation of the TCR, significantly higher FRET was detected in POLKADOTS than in the

whole cell, demonstrating that POLKADOTS are enriched in interactions between Bcl10 and partner signaling proteins. Similarly, previous reports have shown that TCR-signaling induced microclusters are the sites of early signaling events [76-78]. These data thus strongly support our central hypothesis that POLKADOTS are focal sites of TCR-directed NF-κB signal transduction, because they are sites of enrichment of critical protein–protein interactions in the process of TCR activation of NF-κB.

In the context of our model of the structure of POLKADOTS (Figure 18), we propose that rapid equilibration of the outer shell of Bcl10 with cytosolic Bcl10 allows both temporally controlled recruitment of Bcl10-associated partner signaling proteins and complex interactions between these partner proteins at fixed focal sites (POLKADOTS). We propose that such complex interactions are essential steps in TCR activation of NF-κB. Importantly, our proposed model is consistent with recent single molecule studies of the behavior of cytoplasmic signal transducers in T-cells [75]. These studies showed that, in response to TCR engagement, the T-cell signaling proteins LAT and lck become transiently concentrated in focal, membrane-associated microdomains, which are distinct from lipid rafts. These clusters are static in space, but exchange molecules with the freely diffusible membrane pool of LAT and lck. These LAT-lck membrane aggregates therefore appear to be similar in many respects to POLKADOTS. Thus, further studies may reveal that clustered signaling protein microdomains such as POLKADOTS, which facilitate complex information transfer in discrete focal regions, represent a widely utilized and critically important mechanism for the transduction of receptor-initiated signals in eukaryotic cells.

Acknowledgements

We thank Drs. Joel Pomerantz and David Baltimore for supplying the CARMA1 cDNA clone, Erin Wohl for cloning the N-terminus of the murine MALT1 cDNA, and Drs. Joe Giam and Stephen Davies for critical reading of the manuscript. This research was supported by a Kimmel Scholar Award from the Sidney Kimmel Society for Cancer Research (B.C.S.), a grant from the Dana Foundation Program in Brain and Immuno-imaging (B.C.S.), and an Exploratory Research Award from USUHS (B.C.S.).

Table 1.

Peptide	IL-4 Secretion[1] pg/ml x10^{-2}	POLKADOTS % Cells	PKCθ Translocation % Cells	Relative P-IκBα
Wild-type	20	48.72	24.61	1.83[§]
I5N	20	41.80	23.59	1.82[§]
W7Y	13	9.53*	ND	1.02
I5L	8	9.98*	ND	0.96
I5V	1	4.68	ND	0.99
I5G	1	4.85	ND	1.04
No Antigen	0	2.89	ND	1

[1]Data from Dittel, B.M. & Janeway, C.A. (2000) *Journal of Immunology* **165**, 6334-6340.

[2]Fold increase in phosphorylated IκBα relative to No Antigen

*Smaller POLKADOTS and/or delayed formation

[§]p-value of <0.001 vs No Antigen

ND, None Detected

Figure 12. Formation and maintenance of POLKADOTS is influenced by antigen concentration and duration of TCR signaling. (A) D10 T-cells expressing PKCθ-CFP+Bcl10-YFP were conjugated with CH12 B cells in the presence of the indicated concentrations of conalbumin for 30 min. The percentage of cells having PKCθ translocation, Bcl10 POLKADOTS formation, or both redistributions was quantified. (B) D10 T-cells expressing Bcl10-CFP+MALT1-YFP were conjugated with CH12 B cells in the presence of 250 μg/ml conalbumin. After 20 min, 100 μg/ml anti-LFA-1 antibody, or an isotype control antibody, was added to disrupt T-cell/B-cell conjugates. Data represent 100 cells per time point.

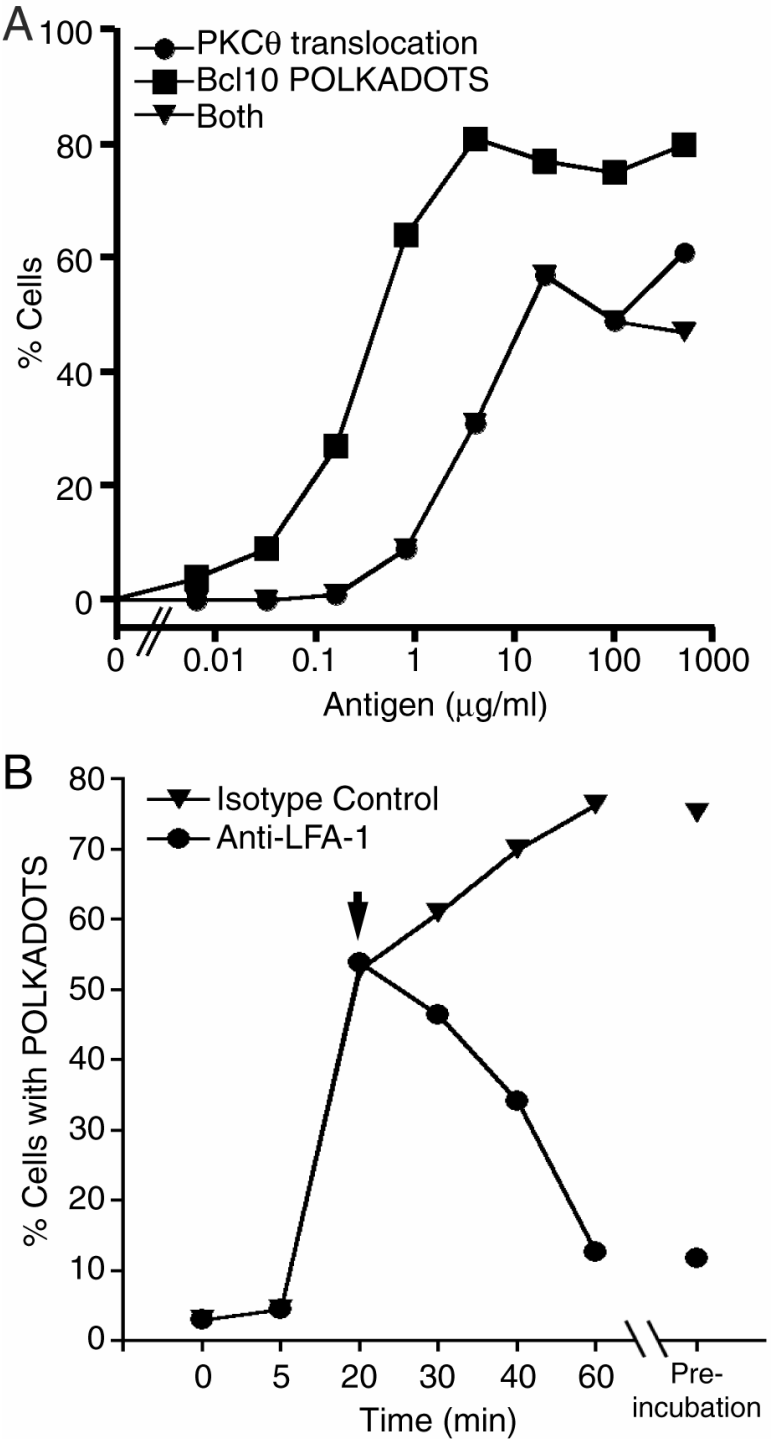
A
PKCθ translocation
Bcl10 POLKADOTS
Both
% Cells
100
80
60
40
20
0
0
0.01
0.1
1
10
100
1000
Antigen (μg/ml)
B
Isotype Control
Anti-LFA-1
% Cells with POLKADOTS
80
70
60
50
40
30
20
10
0
0
5
20
30
40
60
Pre-incubation
Time (min)

Figure 13. Bcl10 and MALT1 colocalize in POLKADOTS. (A) D10 T-cells expressing Bcl10-CFP+MALT1-YFP were conjugated with CH12 B cells in the presence of 250 µg/ml conalbumin. The percentage of cells with Bcl10 or MALT1 POLKADOTS was quantified for 100 cells at various time points. (B) Representative images of Bcl10-CFP (green) and MALT1-YFP (red) POLKADOTS formation and decay at various time points. Bar, 5 µm.

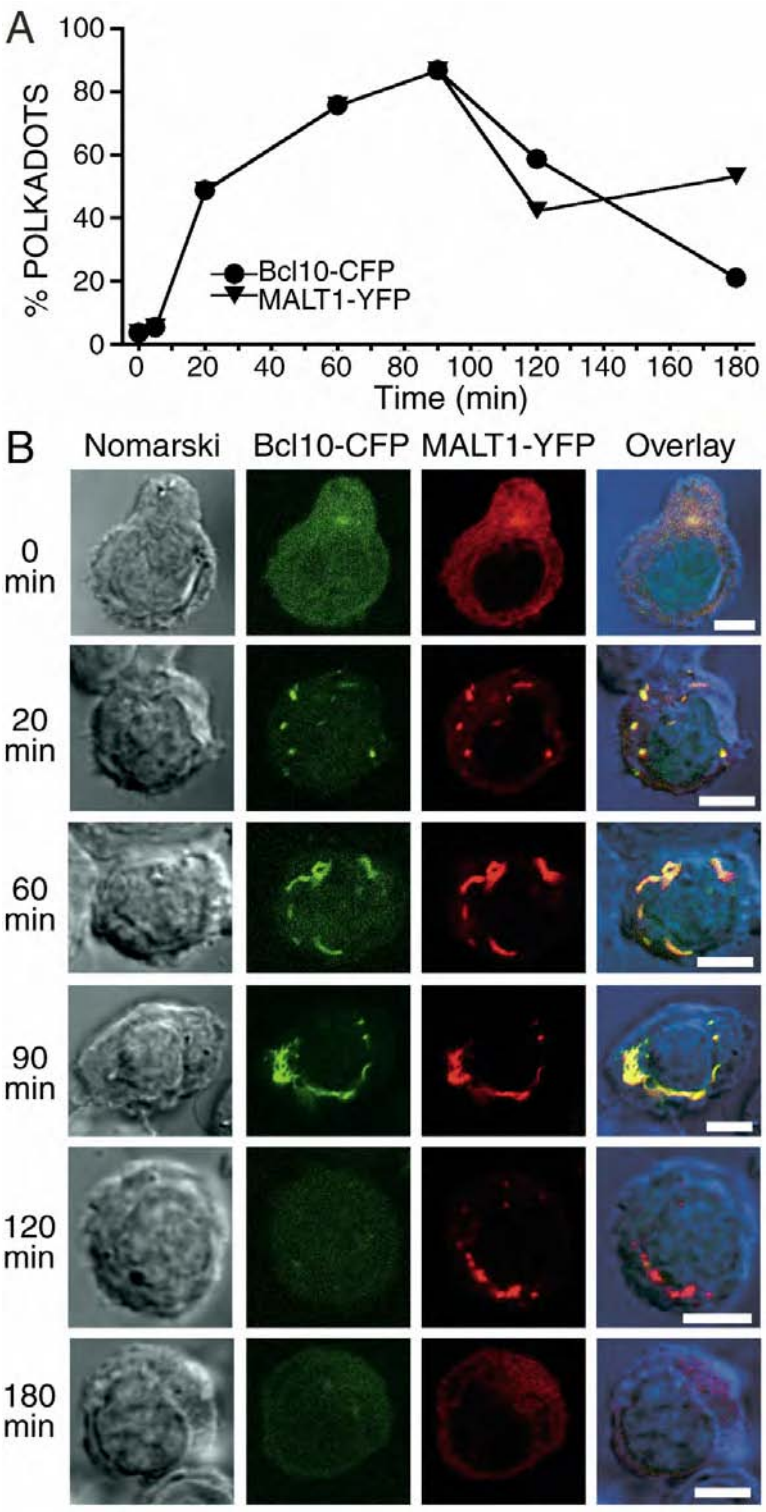
A
% POLKADOTS
100
80
60
40
20
0
Bcl10-CFP
MALT1-YFP
0 20 40 60 80 100 120 140 160 180
Time (min)
B
Nomarski
Bcl10-CFP
MALT1-YFP
Overlay
0 min
20 min
60 min
90 min
120 min
180 min

Figure 14. Interaction between Bcl10 and MALT1 is required for POLKADOTS formation. D10 T-cells expressing Bcl10-GFP or Bcl10-ΔMALT1-GFP (lacking amino acids 107–119) were conjugated with CH12 B cells in the presence or absence of 250 μg/ml conalbumin (Antigen) and imaged via wide-field fluorescence microscopy as previously described [35].

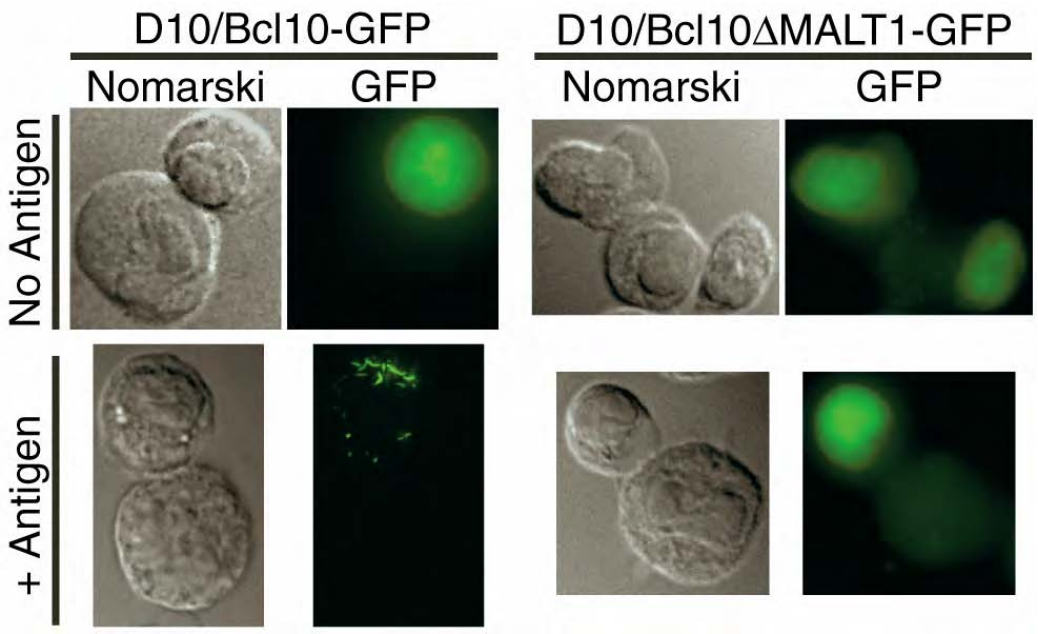
D10/Bcl10-GFP
D10/Bcl10ΔMALT1-GFP
Nomarski
GFP
Nomarski
GFP
No Antigen
+ Antigen

Figure 15. A functional MALT1 C-terminus is required for TCR-mediated NF-κB activation and POLKADOTS formation. (A) Diagram depicting the MALT1 deletions used in this study. (B) %N-FRET between Bcl10-CFP and MALT1-YFP constructs. Red dashed line indicates the threshold for significant FRET detection in this study. Data are means ± SEM. (C) D10 T-cells expressing Bcl10-CFP plus the indicated MALT1-YFP constructs were stimulated with anti-TCR and subjected to Western blot analysis. (D) Relative phosphorylation of IκBα (vs. wild-type, t = 0) was quantified for each cell line. Data are means of three experiments ± SEM. (E) p values for each mutant versus wild-type MALT1 were quantified at each time point, using a Student's t test. (F) POLKADOTS formation was assessed through confocal microscopy. POLKADOTS formation, FRET data and NF-κB activation (as indicated by IκBα phosphorylation) are summarized for each MALT1 construct. Y, yes; N, no. No FRET means FRET was beneath the 0.5% threshold of background, shown in B. Asterisk (*) indicates detection of a small number of cells with POLKADOTS containing only Bcl10-CFP.

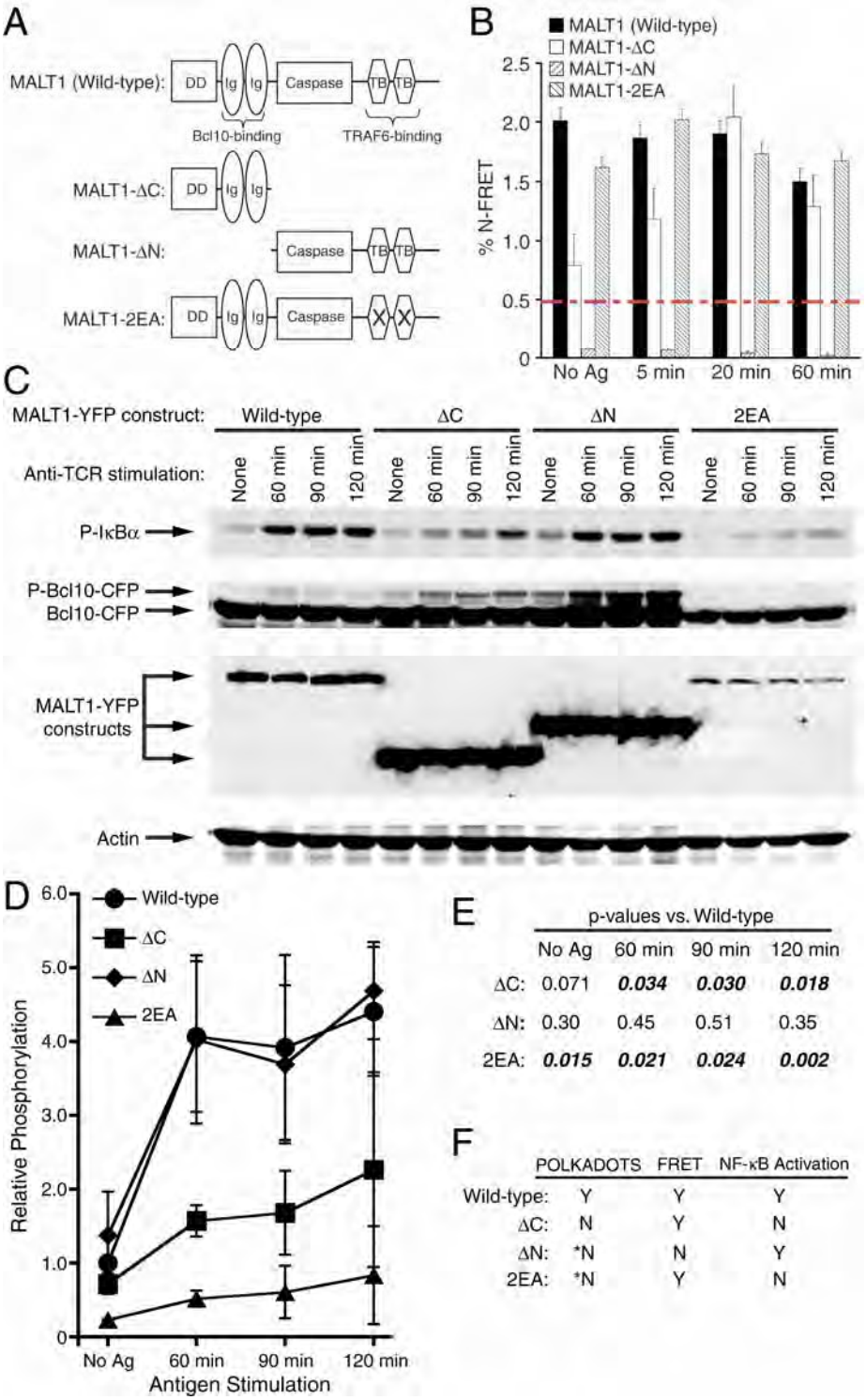

E

	p-values vs. Wild-type			
	No Ag	60 min	90 min	120 min
ΔC:	0.071	***0.034***	***0.030***	***0.018***
ΔN:	0.30	0.45	0.51	0.35
2EA:	***0.015***	***0.021***	***0.024***	***0.002***

F

	POLKADOTS	FRET	NF-κB Activation
Wild-type:	Y	Y	Y
ΔC:	N	Y	N
ΔN:	*N	N	Y
2EA:	*N	Y	N

Figure 16. POLKADOTS contain both stably incorporated Bcl10 and Bcl10 that is at rapid equilibrium with the cytosolic pool. (A) D10 T-cells expressing Bcl10-PA-GFP+MALT1-mKO were conjugated to CH12 B cells in the presence or absence of 250 µg/ml conalbumin. Bcl10-PA-GFP was activated in a single POLKADOT, via 800-nm (multiphoton) excitation. Images were collected for Bcl10-PA-GFP (green), MALT1-mKO (red), and Nomarski (blue). Data are shown immediately before PA-GFP activation (–1 s) and at the indicated time points after activation (see also Figure 20). Arrow is at t = 8 s is site of photoactivation; bar, 5 µm. (B) POLKADOTS fluorescence intensity was quantified after multiphoton activation of a single POLKADOT. (C) Bcl10-PA-GFP was activated via single-photon excitation of a cytoplasmic Region of interest (ROI), using 405-nm excitation. Fluorescence intensity was quantified in the activated cytoplasm ROI and in a distant cytoplasm ROI. (D) Bcl10-PA-GFP was activated in a cytoplasmic ROI as in C, and relative fluorescence intensity was quantified for a distal POLKADOT, as well as for the activated and distal cytoplasm ROIs. (E) Distal POLKADOTS fluorescence intensity data from four cells, with conditions as in D. For all graphs, fluorescence of a cytoplasm ROI in a previously photoactivated cell (Control Cell) was included to show the rate of imaging-induced photobleaching. Results are typical for 5–10 cells per condition.

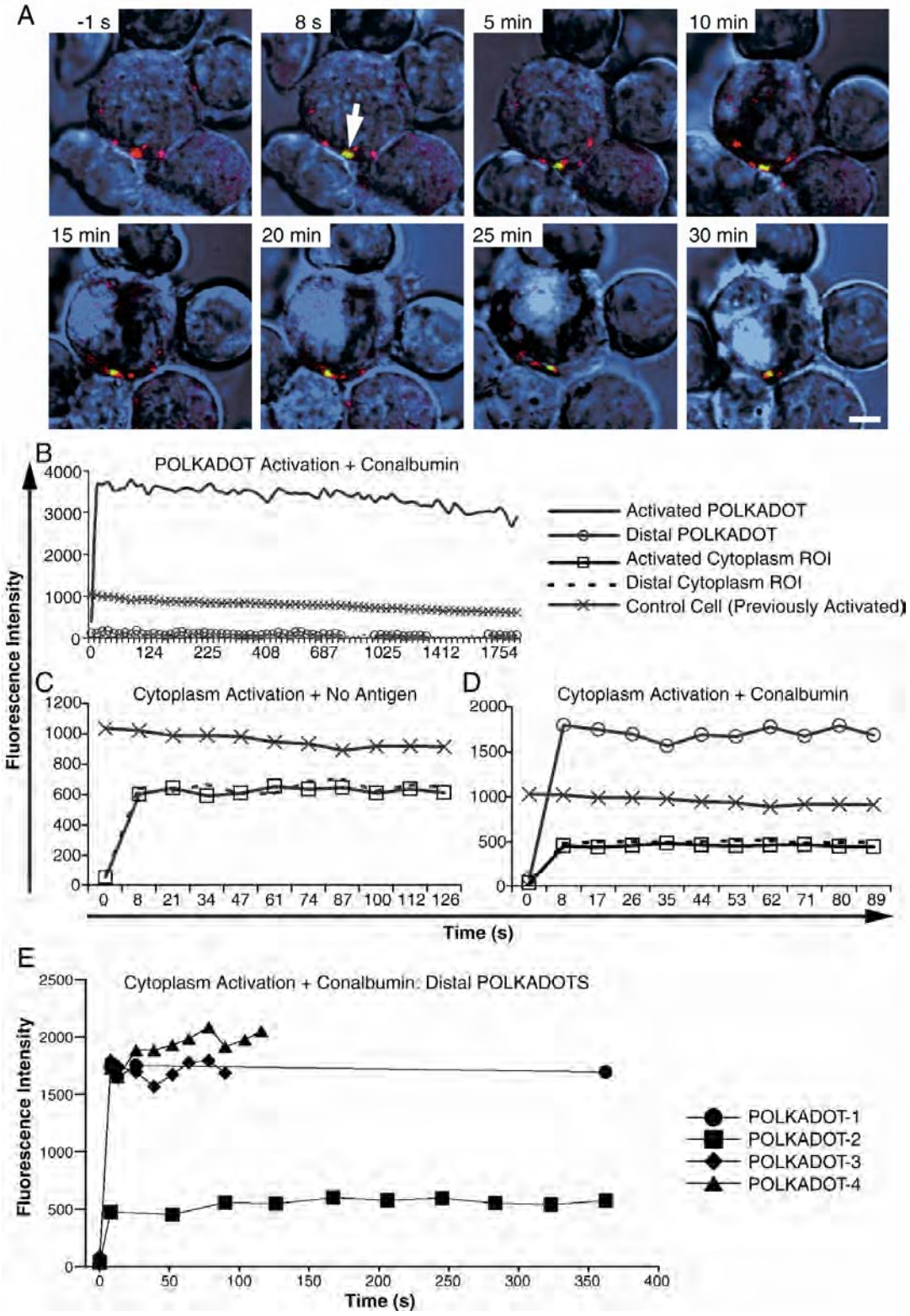
A
-1 s
8 s
5 min
10 min
15 min
20 min
25 min
30 min
B
POLKADOT Activation + Conalbumin
Activated POLKADOT
Distal POLKADOT
Activated Cytoplasm ROI
Distal Cytoplasm ROI
Control Cell (Previously Activated)
Fluorescence Intensity
C
Cytoplasm Activation + No Antigen
D
Cytoplasm Activation + Conalbumin
Time (s)
E
Cytoplasm Activation + Conalbumin: Distal POLKADOTS
POLKADOT-1
POLKADOT-2
POLKADOT-3
POLKADOT-4
Fluorescence Intensity
Time (s)

Figure 17. POLKADOTS are sites of enriched interactions between Bcl10 and partner signaling proteins. (A) Confocal microscopy and FRET analyses were performed on D10 T-cells expressing Bcl10-CFP (blue) and MALT1-YFP (yellow), after 20-min stimulation with CH12 B cells loaded with 250 µg/ml conalbumin. Enhanced FRET (purple) is observed in POLKADOTS. Bar, 5 µm. (B–G) FRET analyses were performed as in A for D10 T-cells expressing both Bcl10-CFP and the indicated YFP-fusions of partner signaling proteins. Cells were stimulated with CH12 B cells loaded with no antigen or with 250 µg/ml conalbumin, for the indicated time periods. Percent N-FRET was calculated for whole cells and for POLKADOTS (when present). The red dashed line indicates the threshold for significant FRET detection (see also Figure 22). *$p < 0.001$ for the indicated time point for whole cell versus POLKADOTS values; #$p < 0.02$ for t = 20 min POLKADOTS versus t = 60 min POLKADOTS values.

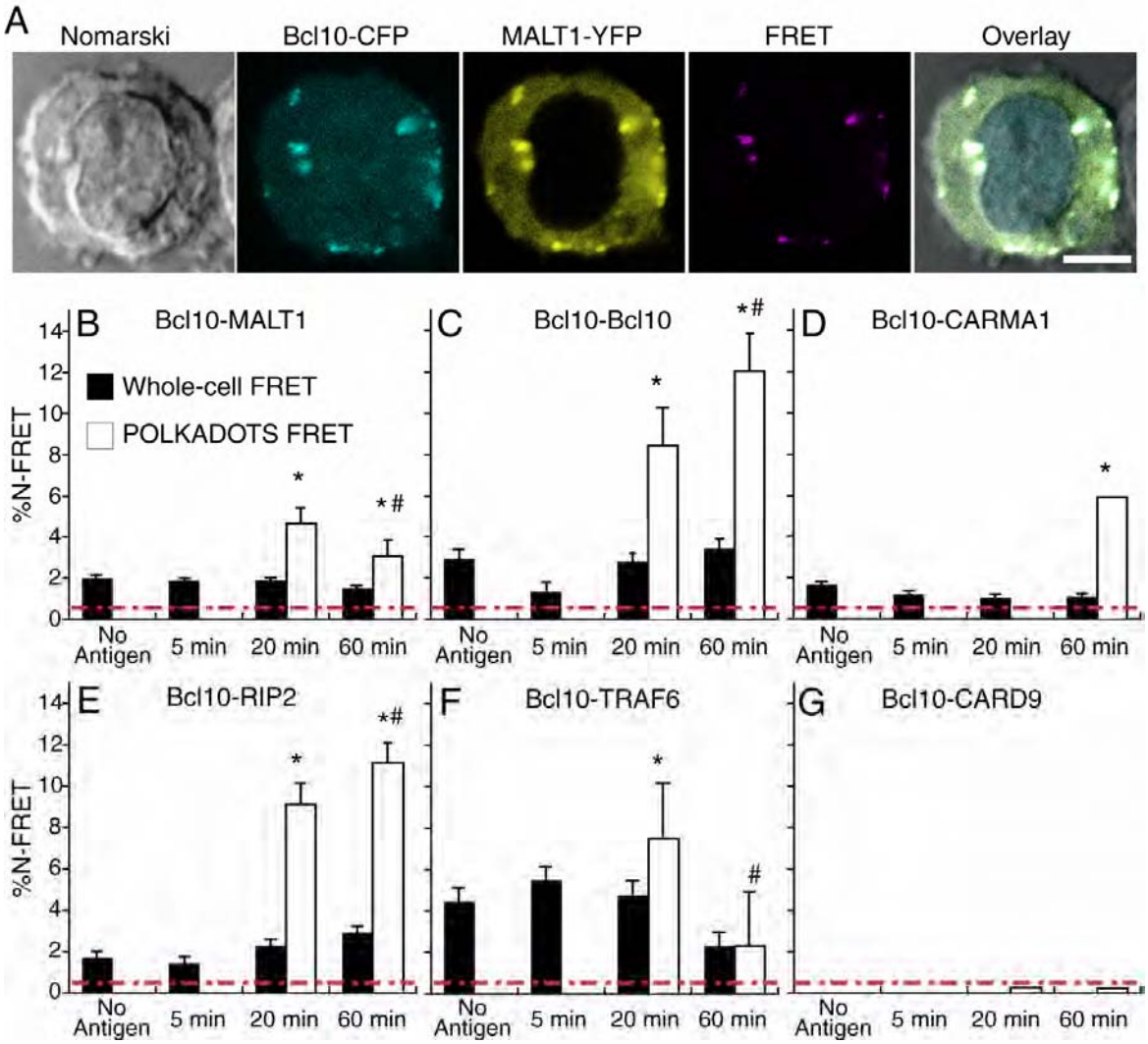
A
Nomarski
Bcl10-CFP
MALT1-YFP
FRET
Overlay
B
Bcl10-MALT1
Whole-cell FRET
POLKADOTS FRET
%N-FRET
C
Bcl10-Bcl10
D
Bcl10-CARMA1
E
Bcl10-RIP2
F
Bcl10-TRAF6
G
Bcl10-CARD9
No Antigen
5 min
20 min
60 min

Figure 18. Model of possible structure and function of POLKADOTS. As suggested by data from photoactivation experiments with Bcl10-PA-GFP (Figure 16), POLKADOTS are depicted as a stable inner core of Bcl10, surrounded by an outer shell of Bcl10 that is at rapid equilibrium with cytoplasmic Bcl10 monomers, and with Bcl10 molecules complexed with partner signaling proteins (note that there are other possible models, in which interactions with partner signaling proteins occur throughout the POLKADOTS structure). A membrane may separate the inner core from the outer shell (see Figure 23). FRET data demonstrate that POLKADOTS are preferential sites of interaction between Bcl10 and partner signal transduction intermediates. Additionally, the high local concentration of these diverse combinations of Bcl10-associated signaling intermediates may facilitate complex interactions and information exchange between signaling intermediates that do not directly interact. Note that the model shows only Bcl10 in the POLKADOTS core, because we have not performed PA-GFP fusions with other partner proteins, to examine their stability in POLKADOTS. It is therefore possible that other Bcl10 partner proteins (e.g., MALT1,TRAF6, etc.) may also reside in this proposed core region.

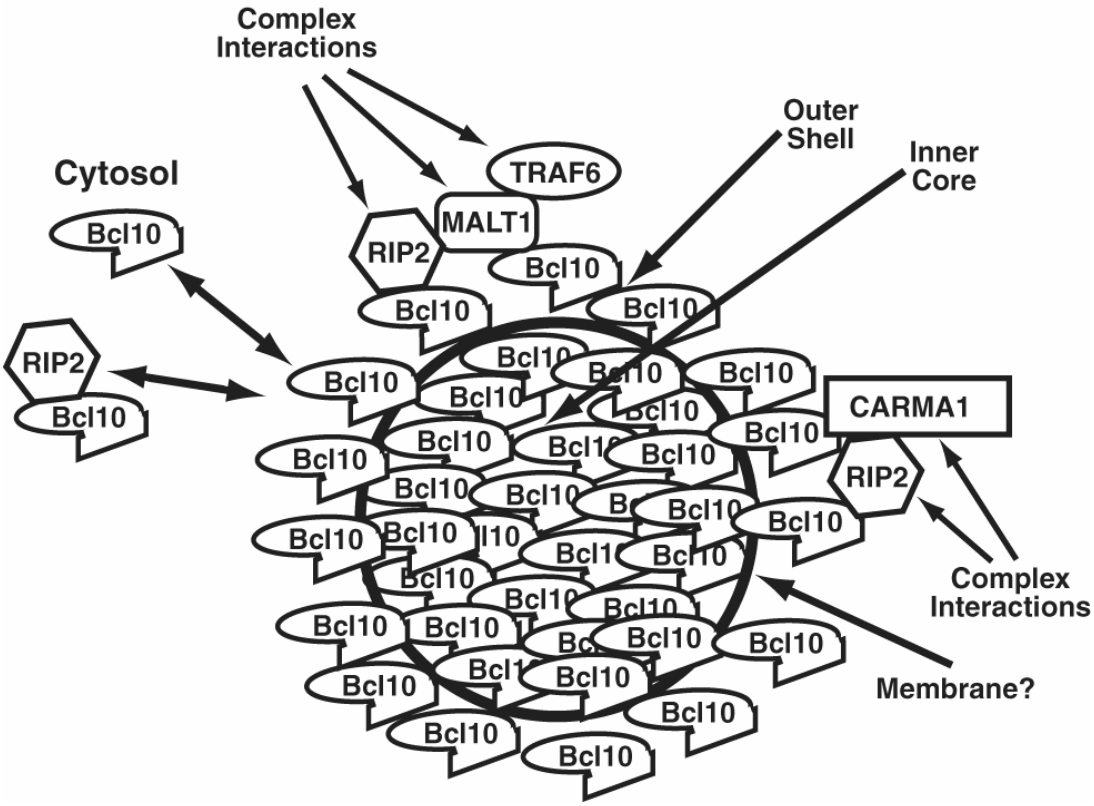
Complex
Interactions
Outer
Shell
Inner
Core
Cytosol
TRAF6
MALT1
RIP2
Bcl10
CARMA1
Complex
Interactions
Membrane?

Figure 19. NF-κB assays of Bcl10, PKCθ, RIP2, CARMA1 and MALT1 constructs. Data show indistinguishable activation of an NF-κB luciferase reporter by unmodified wild-type signaling proteins vs. CFP or YFP fusions, demonstrating that the fluorescent protein tags do not interfere with signaling function (in all cases, t-tests were performed, and p-values indicated no significant difference between unmodified and fluorescent protein tagged signaling proteins). Additionally, the CARD mutant of Bcl10 (G78R), which is known to have severely impaired NF-κB activation, shows minimal enhancement of luciferase activity, as expected. Values are expressed as fold-activation relative to the NF-κB reporter plasmid alone. Error bars are SEM.

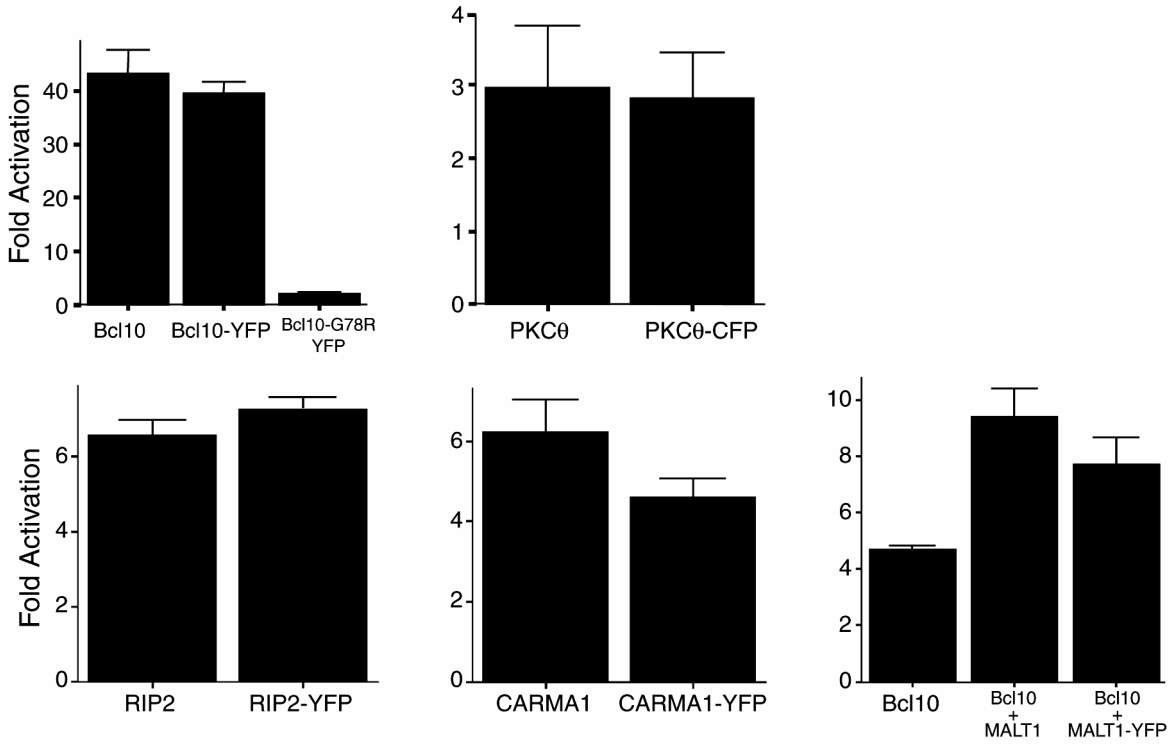
Fold Activation
40
30
20
10
0
Bcl10
Bcl10-YFP
Bcl10-G78R YFP
4
3
2
1
0
PKCθ
PKCθ-CFP
Fold Activation
6
4
2
0
RIP2
RIP2-YFP
6
4
2
0
CARMA1
CARMA1-YFP
10
8
6
4
2
0
Bcl10
Bcl10 + MALT1
Bcl10 + MALT1-YFP

Figure 20. Bcl10-PA-GFP is activated only within the desired ROI. D10 T cells expressing Bcl10-PA-GFP were fixed, and PA-GFP was activated with 405 nm laser excitation. The excitation ROI (red box) encompassed approximately half of the cell. Bar is 5 μM.

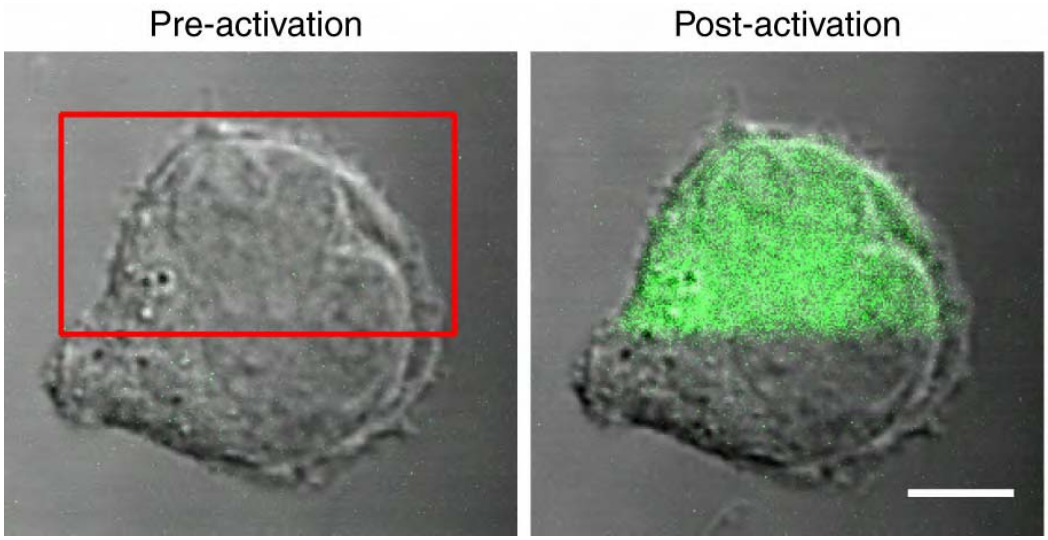
Pre-activation
Post-activation

Figure 21. Bcl10-CFP overexpression levels. The No Antigen samples from Figure 15C were run on an SDS-PAGE gel with an equivalent amount of cell extract from the D10 parental cell line. Labeling of cell lines is as in Fig. 15, except for the parental cell line (D10). Following western blotting with a rabbit anti-Bcl10 antibody, the levels of Bcl10-CFP were compared to the endogenous level of Bcl10 in the parental cell line. The blot was stripped and reprobed with a goat anti-β-actin (Actin) antibody. Note that degradation products of Bcl10-CFP may overlap with the endogenous Bcl10 band in cell lines expressing this fusion protein. Thus, the overexpression levels are relative to the endogenous Bcl10 expression level in the D10 parental cell line (defined as 1.0). Overexpression values were also normalized to relative β-actin expression. N/A, not applicable.

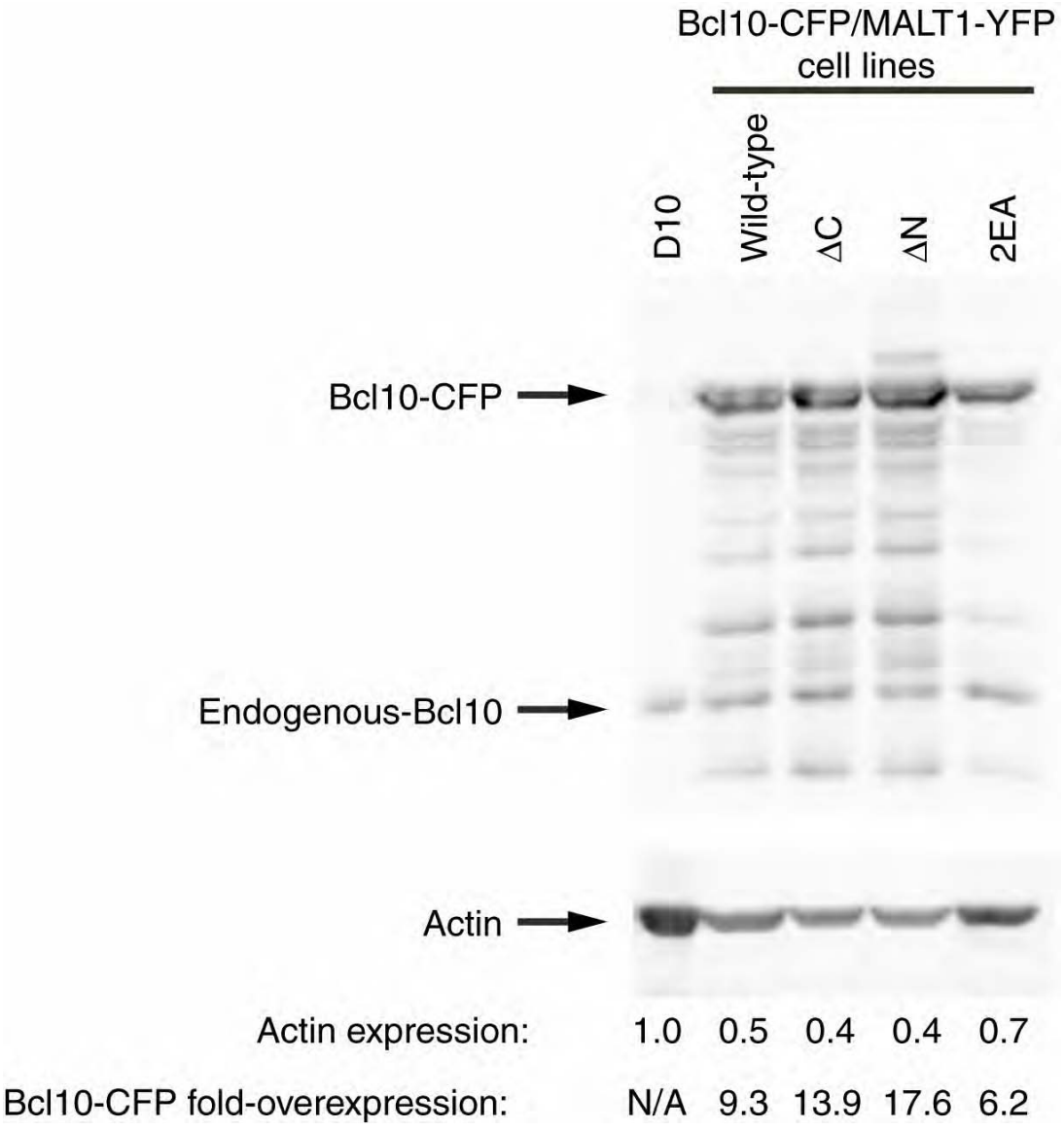
Bcl10-CFP/MALT1-YFP
cell lines
D10
Wild-type
ΔC
ΔN
2EA
Bcl10-CFP
Endogenous-Bcl10
Actin
Actin expression: 1.0 0.5 0.4 0.4 0.7
Bcl10-CFP fold-overexpression: N/A 9.3 13.9 17.6 6.2

Figure 22. Control FRET data. (A) Confocal microscopy and FRET images for D10 T cells expressing Bcl10-CFP+non-fused YFP, 60 min post-conjugation to conalbumin-loaded (250μg/ml) CH12 B cells. Images show minimal FRET. Bar is 5 μM. (B) Calculations of %N-FRET for whole D10 T cells expressing non-fused CFP+non-fused YFP or Bcl10-CFP+non-fused YFP. CH12 B cell stimulation is as in (A). Percent N-FRET was calculated for whole cells or for Bcl10-CFP POLKADOTS, as indicated. The maximal FRET detected in these control experiments (0.5%) was used as the threshold for detection of significant FRET for experiments in Figures 14 and 17. Data are means +/- SEM for 50-100 cells.

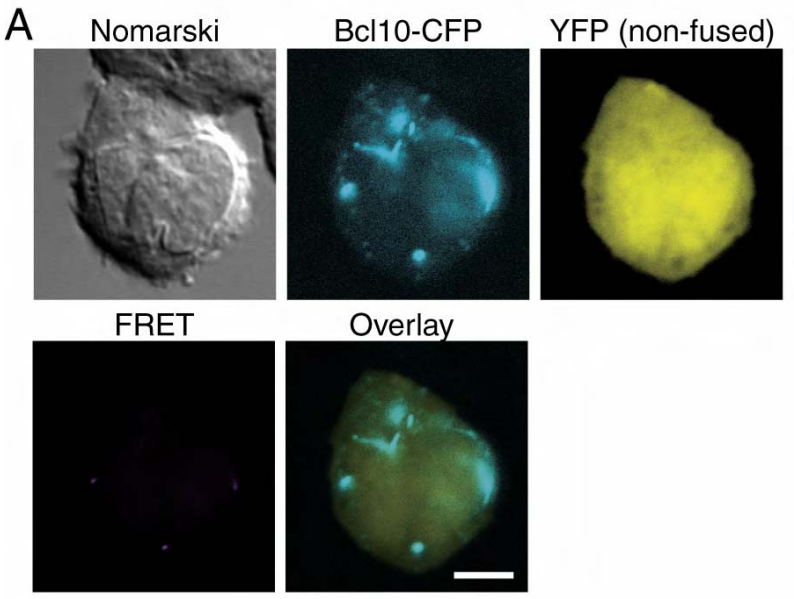
A
Nomarski
Bcl10-CFP
YFP (non-fused)
FRET
Overlay

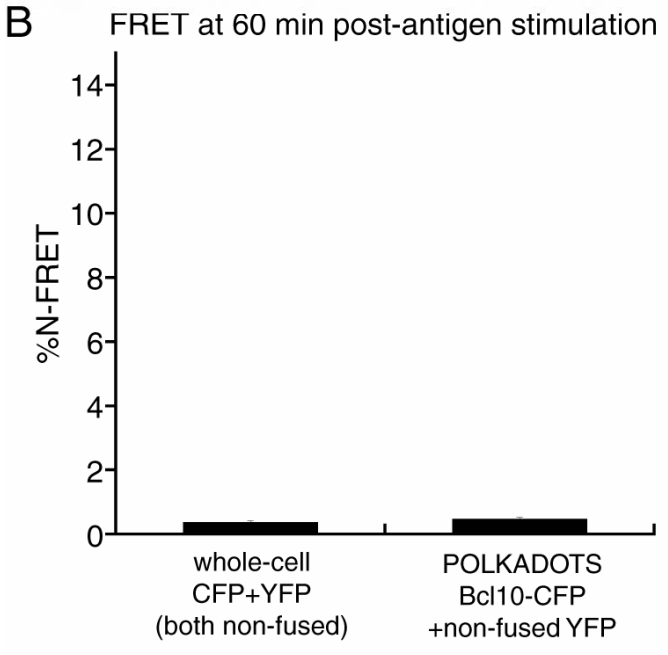
B
FRET at 60 min post-antigen stimulation
%N-FRET
14
12
10
8
6
4
2
0
whole-cell
CFP+YFP
(both non-fused)
POLKADOTS
Bcl10-CFP
+non-fused YFP

Figure 23. POLKADOTS colocalize with membrane-bound structures. D10 T cells expressing Bcl10-CFP (blue) and MALT1-YFP (yellow) were stimulated with antigen-pulsed CH12 B cells for 60min. Cellular membranes were stained with CellTrace Bodipy TR methyl ester (red) for 10 minutes before fixation and confocal imaging.

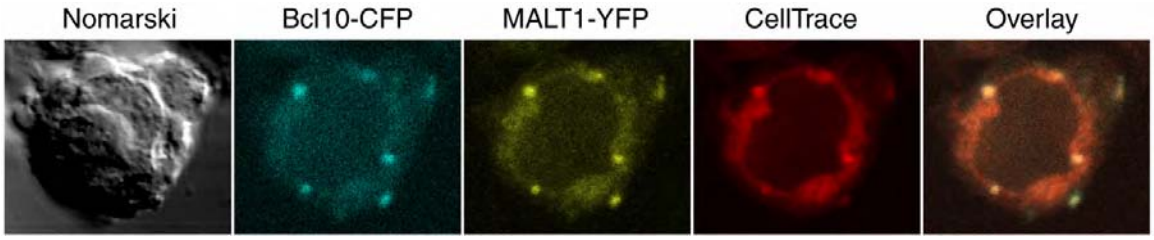
Nomarski
Bcl10-CFP
MALT1-YFP
CellTrace
Overlay

Chapter 3

PKCθ dynamically regulates Bcl10 nuclear localization in T lymphocytes

Abstract

Bcl10 and MALT1 are essential components of the signal transduction pathway linking the T cell receptor to the activation of NF-κB. Translocations of the genes encoding Bcl10 and MALT1 have been implicated in the pathogenesis of MALT lymphomas. In many of these lymphomas, Bcl10 exhibits a strong pattern of nuclear localization, though the significance of this nuclear localization is currently unknown. In this study we examine the regulation of Bcl10 nuclear localization in T lymphocytes. We find that PKCθ directly binds to Bcl10 and is able to modulate the levels of Bcl10 in the nucleus. Bcl10 is phosphorylated in a process requiring PKC signaling. Data indicate that Bcl10 binds to Bcl3 and this interaction likely mediates imported into the nucleus. Nuclear export occurs through binding to MALT1 in a dose-dependent manner. In the nucleus, Bcl10 is able to enhance NF-κB-dependent gene transcription, possibly through binding to TFIIB. These results demonstrate a functional role for Bcl10 within the nucleus of healthy T lymphocytes, and suggest a mechanism for nuclear enrichment of Bcl10 and Bcl10-mediated pathogenicity in MALT lymphomas.

Introduction

Bcl10 is a crucial adaptor molecule in T cell receptor (TCR) mediated activation of NF-κB. Bcl10 contains an N-terminal caspase recruitment domain (CARD) that is responsible for protein-protein interactions with other CARD-containing molecules such as CARMA1 [11] and RIP2 [28]. Distal to the CARD domain (amino acids 107-119) is a minimal MALT1 interaction motif [36]. Both the CARD and the MALT1 interaction motif are required for signal transduction [33, 36-38]. The distal C-terminal domain of Bcl10 (amino acids 120-233) is the site of numerous phosphorylation events of unknown significance [28, 32-34]. However, Bcl10 phosphorylation is known to be induced following stimulation of the TCR [28, 35, 69].

Recent studies have identified several cytosolic mediators of signal transduction from the TCR to NF-κB. A series of events immediately following stimulation of the TCR results in the activation of protein kinase C (PKC)-θ [18, 20]. Activated PKCθ transmits the activation signal to a complex of proteins including Bcl10, MALT1 and CARMA1 [23, 26] and recent evidence suggests that CARMA1 is a direct target of PKCθ phosphorylation [27, 79]. Stimulation of this complex leads to the oligomerization of Bcl10 and MALT1, which consequently induces the oligomerization and activation of TRAF6 [39]. Activation of TRAF6 leads to a well-defined signaling pathway, resulting in the activation of NF-κB [39, 54-57] [2, 57].

Knockout studies of PKCθ, Bcl10, CARMA1 and MALT1 have confirmed their crucial role in TCR-mediated activation of NF-κB [11]. Furthermore, translocations of the Bcl10 and MALT1 genes have been implicated in the development of high-grade, H. pylori-independent MALT lymphomas [45]. Mucosal associated lymphoid tissue (MALT) lymphomas are B cell neoplasms that represent the largest class of non-Hodgkin-type lymphomas [44].

Three different translocation events have been correlated with MALT lymphoma pathogenesis: t(11;18)(q21;q21) which fuses MALT1 with the cellular inhibitor of apoptosis gene 2 (cIAP2), t(1;14)(p22;q32) which puts the Bcl10 gene under the control of the immunoglobulin (Ig) heavy chain gene enhancer, and t(14;18)(q32;q21) which puts the MALT1 gene under the control of the Ig heavy chain gene enhancer [45]. t(1;14)(p22;q32) and t(14;18)(q32;q21) appear to mediate pathogenesis through overexpression of Bcl10 and MALT1 respectively [45]. The most common translocation, t(11;18)(q21;q21), creates a novel cIAP2-MALT1 fusion protein [45, 46]. This translocation fuses the N-terminal BIR domains of cIAP2 with the C-terminus of MALT1 [45, 46]. Evidence suggests that the BIR domains enable oligomerization of the fusion protein, resulting in the activation of TRAF6 and the mis-regulated activation of NF-κB [45, 46].

Histological analysis of t(11;18)(q21;q21)- and t(1;14)(p22;q32)-positive lymphomas has shown the presence of Bcl10 within the nucleus, though the significance of this nuclear localization is unknown [45-47, 49, 51]. Aberrant nuclear localization of Bcl10 has also been detected in translocation-negative nasal NK/T-cell lymphomas [80]. Furthermore, there is some indication that enhanced nuclear localization of Bcl10 is an indicator for more pathogenic lymphomas [47, 49, 51, 80]. Thus, enhanced nuclear localization of Bcl10 may be a common feature of certain lymphomas and a marker for pathogenicity.

Recent studies have identified several mechanisms that may potentially regulate nuclear localization of Bcl10, but these observations were primarily made in non-lymphoid cell lines, and the relevance of these observations to lymphocytes is therefore unclear. The studies of Yeh et. al. suggest that Bcl10 may be specifically imported into the nucleus through binding to Bcl3 [52]. Bcl3 is an NF-κB family member that is known to shuttle between the cytoplasm and the

nucleus [81]. Bcl3 is able to bind other NF-κB family members and has been shown to act as a transactivator and to promote lymphocyte survival [81, 82]. These authors reported that in the breast cancer carcinoma cell line MCF7, Bcl10 is phosphorylated at S218/S231 by Akt1 upon tumor necrosis factor (TNF)α signaling [52]. There is also evidence that in T lymphocytes, Akt may integrate signals from the CD28 coreceptor and enhance phosphorylation of Bcl10 [83]. The phosphorylation of Bcl10 has been shown to mediate binding to Bcl3 and the subsequent import of Bcl10 into the nucleus [52]. Deletion of the C-terminal 27 amino acids of Bcl10, containing the two Akt1 phosphorylation sites, allowed for increased binding to Bcl3 in the absence of Akt1 signaling, suggesting that the phosphorylation events enable binding to Bcl3 [52]. Nakagawa et. al. recently identified two nuclear export signals (NES) in the C-terminus of MALT1 [84]. They showed that in COS7 cells, deletion of the NES led to increased levels of nuclear Bcl10, suggesting that MALT1 is a nuclear export factor for Bcl10 [84].

Although the function of nuclear Bcl10 has not been definitively established, some interesting data relating to a possible role of Bcl10 as a transcriptional enhancer have recently been reported. In 2003, Chen et. al. provided the first evidence for a possible role of nuclear Bcl10 as a transcriptional activator [85]. Using Gal4 DNA binding domain fusions with Bcl10, they later showed that the first 13 amino acids of Bcl10 are sufficient and necessary to activate gene transcription in HeLa cells, and that this activation likely occurs through binding to TFIIB, which is a necessary component of the RNA polymerase machinery [48].

Despite numerous observations of nuclear Bcl10 in MALT lymphoma tumor cells and biopsies, the significance and regulation of Bcl10 nuclear localization remains poorly understood. Furthermore, the applicability of many previous studies to Bcl10 nuclear regulation in lymphocytes is unclear. Given the possibility that increased Bcl10 nuclear localization may

contribute to MALT lymphoma pathogenesis [51, 86, 87], a complete understanding of the factors that influence Bcl10 nuclear localization in lymphocytes and the elucidation of the function of nuclear Bcl10 is essential. The aim of this present study is to investigate, in lymphocytes, the factors that influence Bcl10 nuclear localization and the potential role of nuclear Bcl10 in NF-κB signal transduction.

Methods

Cells and Reagents

D10 T cells, CH12 B cells and 293T cells were maintained as previously described [35]. Conalbumin was purchased from Sigma (St. Louis, MO). The following proteins were detected with monoclonal antibodies: Bcl10 (331.3; Santa Cruz Biotechnology, Santa Cruz, CA), TFIIB (24; BD Transduction Laboratories, San Diego, CA), 14-3-3 (3B9; Sigma) or polyclonal antibodies: Bcl10 (H197; Santa Cruz Biotechnology), Bcl3 (C14; Santa Cruz Biotechnology) and histones (053; Chemicon, Temecula, CA). HRP-conjugated secondary antibodies were purchased from Jackson ImmunoResearch (West Grove, PA). Bisindolylmaleimide, the Akt inhibitor Akti1/2 and the PI3 kinase inhibitor LY294002 were purchased from CalBioChem (San Diego, CA).

Cloning and Retroviral Infections

The cloning of Bcl10, MALT1, MALT1-ΔN (MALT1-Δ1-344), PKCθ, RIP2 and CARMA1 was previously described [88]. Fusions with the cerulean variant of CFP [63], the citrine variant of YFP [64] or EGFP were also previously described [88]. Bcl10-Δ217-233 was

constructed from Bcl10-GFP by PCR using forward primer 5'-GGGCCATGGAGGCTCCCGCACCGTCCCTCA-3' and reverse anti-sense Bcl10 truncation oligomer ending at amino acid 216. Bcl10-Δ1-13 was constructed from Bcl10-CFP by PCR using forward primer 5'-AAGATCTATGACTGAAGTGAAGAAGGAC GCTTTAG-3' and reverse anti-sense primer 5'-TTGAAGTTGGCCTTGATGCCGTTC-3'. Cloned PCR products were verified by sequencing. 3xHA-Bcl10-GFP was cloned from Bcl10-GFP by inserting the Met-3xHA tag directly before the starting methionine of the Bcl10 cDNA. Gene fusions were introduced into the pE retroviral expression vectors and used for retroviral infection and selection as previously described [35]. The HTLV-luciferase reporter vector was provided by Dr. Joe Giam (Uniformed Services University, Bethesda, MD). Luciferase reporter assays were performed as previously described [88].

Immunoprecipitations

293T cells were either transfected with 3xHA-Bcl10-GFP or co-transfected with 3xHA-Bcl10-GFP and Bcl3-pMiT [81]. 48 hours after transfection cells were lysed as previously described [89]. Cell lysates were pre-cleared by incubating with protein G sepharose beads for 1 hour, beads isolated by centrifugation and supernatants isolated. Pre-cleared lysates were then incubated with 3μg of anti-Bcl10 antibody (331.3) overnight followed by incubation with protein G sepharose beads for 1 hour. Captured proteins were then washed with lysis buffer, denatured and subjected to SDS-PAGE and immunoblotting.

Nuclear Extraction and Western Blotting

Nuclear extractions were performed using the CellLytic NuClear Extraction kit (Sigma). Briefly, $1x10^7$ cells were lysed in 100µl of isotonic lysis buffer supplemented with DTT and protease inhibitors for 30 minutes on ice. Cells were then lysed with 0.6% Igepal, vortexed briefly and then centrifuged for 5 minutes at 500x*g*. Supernatant containing the cytoplasmic fraction was then removed and the nuclei were washed with isotonic lysis buffer. Nuclei were lysed in 100µl extraction buffer supplemented with DTT and protease inhibitors on ice for 30 minutes with vortexing. The insoluble fraction was then separated by centrifugation at 14,000x*g* for 5 minutes. The supernatant containing the nuclear fraction was isolated. Fractions were then combined with 2x Laemmli buffer and $5x10^6$ cell equivalents were loaded per lane. SDS-PAGE gel electrophoreses, nitrocellulose membrane transfer, antibody probing and chemiluminescent imaging were performed as previously described [88].

Confocal Microscopy and Fluorescent Resonance Energy Transfer

Conjugate formation and confocal imaging was performed as previously described [88]. Bcl10-CFP and MALT1-YFP intensities were quantitated using Zeiss AIM software (Thornwood, NY). For nuclear concentration analysis, cells were viewed using the bright-field channel and regions of interest (ROI) within the nucleus and around the whole cell were defined. Bcl10 nuclear enrichment was the calculated by dividing the average Bcl10 fluorescence intensity within the nuclear ROI by the average Bcl10 fluorescence intensity within the whole-cell ROI, for each individual cell. FRET experiments were performed as previously described [88]. Statistics were calculated using the Student's t-test.

Results

Bcl10 is present in the nucleus of T lymphocytes

We previously described the spatial redistribution of Bcl10 in response to TCR stimulation [35, 88]. Because of the potential importance of nuclear Bcl10 in the pathogenesis of MALT lymphoma and in normal lymphocyte biology, we performed a series of experiments to identify the mechanisms that control Bcl10 nuclear localization in lymphocytes. We first performed cellular fractionation studies to biochemically confirm the presence of Bcl10 within the cytoplasm and the nucleus. We found that Bcl10 is present in both the cytoplasm and the nucleus of unstimulated D10 T cells (Figure 24a). Additionally, although the higher molecular weight phosphorylated form of Bcl10 is present as a minority species in the cytosol, this was the only form detected in the nucleus (Figure 24a). To verify efficient separation of cytoplasmic and nuclear compartments, we probed our fractionated cells for the cytoplasmic protein 14-3-3 and for histones. We show that there is minimal cross-contamination between the isolated cellular compartments (Figure 24b). This confirms our observation that Bcl10 is present in the nucleus of unstimulated lymphocytes, and suggests that phosphorylated Bcl10 is preferentially localized to the nucleus, as have been previously reported in TNFα-stimulated MCF-7 cells [52].

Bcl10 nuclear import is mediated by phosphorylation and binding to Bcl3

Previous reports have suggested that C-terminal phosphorylation of Bcl10 enables binding to Bcl3 and subsequent nuclear entry [52], and the data in Figure 24 suggest that the nucleus of T lymphocytes contains only a phosphorylated form of Bcl10. Utilizing cellular fractionation and a D10 T cell line over-expressing a Bcl10-CFP fusion protein, we show that

the nucleus contains only phosphorylated forms of Bcl10, while the cytoplasm contains various phosphorylated and unphosphorylated forms (Figure 25a). We next constructed a deletion mutant of the Bcl10 molecule which lacks the C-terminal 17 amino acids (Bcl10-Δ217-233). This deletion encompasses residues S218 and S231 which are postulated to mediate phosphorylation and repression of Bcl3 binding [52]. We observed that this deletion mutant was enriched in the nucleus as compared to wild-type Bcl10 (Figure 25b). Additionally, using co-immunoprecipitation we demonstrated that Bcl10 can be co-immunoprecipitated with Bcl3 (Figure 25c), as has been previously reported [52]. Taken together these data suggest that Bcl10 is phosphorylated on it C-terminus. C-terminal phosphorylation enables binding to Bcl3, which is then able to mediate Bcl10 import into the nucleus. These data suggest that modulation of Bcl10 phosphorylation is a key event in Bcl10 nuclear localization. However, it is important to note that Bcl10 may be phosphorylated on multiple residues and that these different phosphorylation events may modulate other functions of Bcl10, outside of nuclear localization.

Maximal Bcl10 nuclear localization requires PKC but not Akt signaling

Since Bcl10 has been reported to be phosphorylated on the C-terminus by the kinase Akt1 [52], we examined the nuclear localization of Bcl10 in T lymphocytes, when treated with various kinase inhibitors. Surprisingly, we found that the Akt1 and Akt2 specific inhibitor, Akti1/2, did not alter the levels of Bcl10 within the nucleus (Figure 26a). Additionally, the PI3 kinase inhibitor LY294002 did not appear to alter nuclear localization of Bcl10 (data not shown). Since PI3-kinase is an upstream activator of Akt, this observation further suggests that the PI3-kinase-Akt pathway does not significantly influence the subcellular localization of Bcl10 in lymphocytes. Interestingly, while testing the effects of other protein kinase inhibitors on Bcl10

nuclear localization, we found that treatment with the protein kinase C inhibitor, bisindolylmaleimide (BIM), significantly reduced the amount of Bcl10 in the nucleus (Figure 26a). Our previous results have shown that BIM significantly reduces Bcl10 phosphorylation [35], providing further evidence for a link between Bcl10 phosphorylation and nuclear localization.

In order to investigate the possible role of the PKC isoform, PKCθ, on Bcl10 nuclear localization we utilized Fluorescence Resonance Energy Transfer (FRET) to examine interactions between Bcl10 and PKCθ. FRET analysis showed that there is a specific interaction between Bcl10 and PKCθ, and that the strength of this interaction decreases upon antigen stimulation (Figure 26b). Interestingly, we also observed a significant FRET interaction between Bcl10 and PKCθ in the nucleus (Figure 26b). Collectively, these data suggest that subcellular localization of Bcl10 may also be determined, in part, by this previously unknown direct interaction with PKCθ.

We then assessed the impact of PKCθ expression on the levels of nuclear Bcl10. We found that the presence of PKCθ significantly increased the amount of Bcl10 in the nucleus. Additionally, the presence of RIP2 and CARMA1 also slightly increased levels of nuclear Bcl10 (Figure 26c). Additionally, we found that antigen stimulation of D10 T cells co-expressing Bcl10 and PKCθ significantly lowers the levels of Bcl10 in the nucleus (Figure 26d). Taken together, these results suggest that PKCθ is able to dynamically regulate the levels of Bcl10 in the nucleus, further emphasizing the importance of PKC signaling in Bcl10 nuclear localization.

MALT1 is a dose-dependent nuclear export factor for Bcl10

Recent reports have shown that MALT1 can act as a nuclear export factor for Bcl10 in the African Green Monkey kidney cell line COS-7 [84]. We have previously shown that Bcl10 is able to interact with MALT1 in the cytoplasm of T lymphocytes [88]. To examine the possible role for MALT1 in mediating the nuclear export of Bcl10 in T cells, we performed FRET between Bcl10 and MALT1. FRET analysis of the interaction between Bcl10 and MALT1 shows that the two molecules specifically interact within the nucleus of T lymphocytes (Figure 27a), as well as in the cytosol.

To further confirm the role of Bcl10-MALT1 association in the nucleus, we utilized a previously described MALT1 deletion mutant (MALT1-Δ1-344), which has an N-terminal deletion that prevents interaction with Bcl10 [36, 88]. FRET analysis confirmed that the N-terminus of MALT1 is required for interaction with Bcl10, in the cytoplasm as well as the nucleus (Figure 27a). In examining the levels of nuclear Bcl10, we observed that when Bcl10 and MALT1 are unable to interact there is a significant increase in the level of nuclear Bcl10 (Figure 27b). These data provide strongly suggest that MALT1 acts as a nuclear export factor for Bcl10 in T cells.

In performing our analyses, we observed an apparent correlation between the amount of Bcl10 in the nucleus and the total amount of MALT1 in the cell. To verify our observations, we quantitatively correlated the nuclear levels of Bcl10 with the relative concentrations of Bcl10 and MALT1 in the cell. As seen in Figure 27c, nuclear Bcl10 levels exhibit a direct correlation with the ratio of Bcl10:MALT1. Furthermore, we found that cells expressing MALT1-Δ1-344 do not demonstrate this correlation (Figure 27c), demonstrating that this correlation only exists when MALT1 and Bcl10 can directly interact. These data provide strong evidence that MALT1-

mediated export of Bcl10 from the nucleus occurs with a defined stoichiometric relationship. Thus, conditions that alter the levels of Bcl10 or MALT1 within the cell will also influence the amount of Bcl10 in the nucleus. Taken together, these data demonstrate that the amount of Bcl10 in the nucleus is regulated via binding to, and export by, MALT1, in a dose-dependent manner.

Bcl10 is a transcriptional activator

We next examined the potential functional role of Bcl10 within the nucleus. Recent reports have shown that the first 13 amino acids of Bcl10 can bind to the transcriptional machinery component TFIIB, up-regulating gene transcription [48]. However, the above transcriptional studies employed fusions of Bcl10 sequences to the Gal4 DNA binding domain, which transactivated a Gal4-responsibe luciferase reporter construct. Thus, it remains unclear whether the first 13 amino acids of Bcl10 normally have a function in Bcl10-mediated signaling. We first confirmed the interaction between Bcl10 and TFIIB by co-immunoprecipitation analysis in 293T cells (Figure 28a). In order to assess the possible role of the first 13 amino acids of Bcl10 in Bcl10-dicrected NF-κB activation, we constructed a deletion mutant of Bcl10 that lacks the first 13 amino acids (Bcl10-Δ1-13). We then assessed the ability of this mutant to activate an NF-κB-dependent luciferase reporter construct, in comparison to full-length Bcl10. Figure 28b shows that Bcl10-Δ1-13 is significantly impaired in its ability to induce NF-κB-dependent gene transcription. However, neither Bcl10 protein had an effect on the activation of a control HTLV-luciferase reporter construct, which does not contain NF-κB binding sites (Figure 28c). The above data establish an essential function for amino acids 1-13 in Bcl10-mediated activation of NF-κB, and suggest that the nuclear complex of Bcl10 and TFIIB does not act as a general, non-

specific, transcriptional enhancer. Thus, although the functional significance of the interaction between the N-terminus of Bcl10 and TFIIB remains uncertain, these data clearly establish that Bcl10 amino acids 1-13 are critical for NF-κB-dependent gene transcription.

Discussion

The role of Bcl10 in antigen-receptor signal transduction has been the source of extensive research in recent years. Many studies have helped define the crucial roles for Bcl10 and MALT1 in signal transduction from the TCR to NF-κB. Additionally, translocations of the Bcl10 and MALT1 genes have been implicated in the pathogenesis of MALT lymphomas. Recent studies have noted the presence of Bcl10 in the nuclei of various tumor cell lines and enrichment of Bcl10 in the nuclei of MALT lymphoma tumor samples. However, little is known about the specific role of nuclear Bcl10 in pathogenesis. The aim of this study was to establish which cellular proteins and signals control Bcl10 nuclear localization in lymphocytes, and to identify a potential role for nuclear Bcl10.

We detected Bcl10 in the nucleus of unstimulated D10 T lymphocytes (Figure 24a). We also showed that only phosphorylated forms of Bcl10 are present in the nucleus (Figure 24a and 25a). It has been postulated that upon C-terminal phosphorylation, Bcl10 is able to bind Bcl3, and that this interaction is crucial for nuclear import of Bcl10 [52]. We show here that Bcl10 is able to bind Bcl3, and that deletion of the C-terminus of Bcl10 enhances nuclear localization (Figure 25b and 25c). It is important to note that Bcl10 is not proposed to bind to Bcl3 through its distal C-terminus [52]. Rather the C-terminus of Bcl10 normally prevents binding to Bcl3. Phosphorylation, or deletion, of the C-terminus modifies Bcl10 in such a way that it can now

bind to Bcl3. These results are consistent with the model proposed by Yeh, et. al. in which C-terminal phosphorylation of Bcl10 mediates its binding to Bcl3 and subsequent imported into the nucleus [52].

Previous studies have showed that in TNFα-stimulated MCF7 cells, C-terminal phosphorylation of Bcl10, and its subsequent nuclear localization, is mediated by the kinase Akt1 [52]. Interestingly, we see no impact of Akt inhibitors on Bcl10 nuclear localization (Figure 26a). It is important to note that the study by Yeh, et. al. was performed in a non-lymphoid cell line following TNFα stimulation. It is possible that different kinases mediate the phosphorylation of Bcl10 through different pathways. Early studies with Bcl10 suggested that it was able to mediate TNFα signaling by binding to TRAF6 in 293T cells [34]. This raises the interesting possibility that Bcl10 may also be involved in signal transduction from the TNF receptor to NF-κB. However, further research is needed to determine the role of Bcl10 in other signaling pathways and in non-lymphoid cells.

Our data suggest that Akt is not be the primary phosphorylating agent for Bcl10 in T cells. It is important to note that Yeh, et. al. saw Bcl10 phosphorylation even in the presence of the Akt inhibitor Akti1/2 [52], suggesting that other kinases are likely to play a role in Bcl10 phosphorylation in non-lymphoid cell types, as well. Thus, the collective evidence suggests that phosphorylation of Bcl10 is the result of multiple kinases and the functional role of phosphorylation is likely to vary with cell type and with the residue(s) that become phosphorylated. Furthermore, the kinase(s) that are responsible for Bcl10 phosphorylation may differ from cell type to cell type. Thus, the combined data suggest that the regulation of Bcl10 phosphorylation is complex, and that findings in one cell type are not likely to be generalizable to other cell types.

Although we observed no role for Akt1 signaling, we did see strong evidence of a role for PKCθ in Bcl10 nuclear localization. Blocking PKC activity impairs the phosphorylation of Bcl10 [35], and significantly reduces the amount of Bcl10 in the nucleus (Figure 26a). Here we show a specific interaction between PKCθ and Bcl10 within the cell, rasing the possibility that PKCθ may directly phosphorylate Bcl10 (Figure 26b). It is important to note that the actual phosphorylation of Bcl10 may be mediated by an intermediate protein between PKCθ and Bcl10. One possible candidate is the serine/threonine kinase RIP2. T lymphocytes from RIP2 knock-out mice show a deficiency in Bcl10 phosphorylation [28]. However, expression of PKCθ had a greater impact on the levels of nuclear Bcl10 than did expression of RIP2 (Figure 26c). Further research is needed to assess the role of RIP2 on Bcl10 phosphorylation and nuclear localization.

While the presence of PKCθ increases steady-state nuclear Bcl10 levels (Figure 26c), TCR stimulation of these cells leads to a dramatic loss of Bcl10 from the nucleus (Figure 26d). The reason for this loss is not clear; however, it is intriguing to note that stimulation induces the loss of Bcl10 from the nucleus and a reduction of the interaction between Bcl10 and PKCθ in the nucleus (Figure 26b and 26d). Thus, binding to PKCθ may directly mediate the levels of Bcl10 in the nucleus. These results suggest that PKCθ might be able to modulate Bcl10 nuclear localization in two distinct ways: through its kinase activity, and through a direction interaction with Bcl10. Further research is needed to directly assess the mechanism of PKCθ regulation of Bcl10 nuclear localization. However, these results clearly demonstrate the importance of PKC signaling on the nuclear localization of Bcl10 in T lymphocytes. Since PKCθ is largely a T cell-specific isoform, we would expect that other isoforms, such as PKCβ, may play this role in B lymphocytes and MALT lymphoma cells. Indeed, recent evidence suggests that PKCθ and PKCβ are responsible for phosphorylating CARMA1 in T cells and B cells, respectively [27, 79].

It has been previously demonstrated that MALT1 is also able to regulate the levels of Bcl10 in the nucleus, though this regulation has not been addressed in lymphocytes [84]. Here we confirm the role of MALT1 as a nuclear export factor, showing that Bcl10 and MALT1 can interact within the nucleus of T cells (Figure 27a). Furthermore, we define a dose-response relationship between Bcl10 nuclear localization and the ratio of Bcl10 to MALT1 in the cell (Figure 27c). Given the fact that Bcl10 is targeted for degradation upon TCR stimulation [69], it is possible that stimulation may alter levels of nuclear Bcl10 by modulating the ratio of Bcl10 to MALT1 in the cell. A reduction in the amount of cellular Bcl10 could allow for enhanced MALT1-mediated export of Bcl10 from the nucleus. This could provide a means of regulating putative functional activity of Bcl10 in the nucleus.

The discovery of a dose-dependent relationship between Bcl10 nuclear localization and the concentration of Bcl10 to MALT1 in the cells provides a plausible explanation for the observation of enhanced Bcl10 nuclear localization in some MALT lymphomas. t(11;18)(q21;q21) translocations fuse the C-terminus of MALT1 with the N-terminus of cIAP2. This translocation deletes the N-terminus of MALT, which should eliminate its ability to bind Bcl10, as with our MALT1-Δ1-344 construct (Figure 27a). This may effectively lower the concentration of MALT1 that is available to bind to Bcl10, resulting in increased levels of Bcl10 in the nucleus.

Similarly, the t(1;14)(p22;q32) translocation, which leads to Bcl10 overexpression, raises the Bcl10:MALT1 ratio in the cell and would be expected to lead to enhanced Bcl10 nuclear localization. Conversely, the t(14;18)(q32;q21) translocation, resulting in MALT1 overexpression, lowers the Bcl10:MALT1 ratio in the cell and our data suggest that this scenario would result in lowered levels of nuclear Bcl10. These explanations are consistent with the

histological findings that t(11;18)(q21;q21)- and t(1;14)(p22;q32)-positive lymphomas show strong patterns of Bcl10 nuclear localization, while t(14;18)(q32;q21)-positive lymphomas show cytoplasmic localization of Bcl10 [45]. Thus our data show that the ratio of Bcl10 to MALT1 directly modulates the levels of Bcl10 found in the nucleus of T lymphocytes, and this mechanism is consistent with observations in MALT lymphomas.

Previous studies using fusions of Bcl10 with the Gal4 DNA binding domain have shown that Bcl10 can act as a transcriptional activator [48]. Our study confirms that the first 13 amino acids of Bcl10 can interact with TFIIB, and demonstrates for the first time that these same amino acids are critical for Bcl10 mediated activation of an NF-κB-responsive promoter. Although we present evidence that Bcl10 does not have activity as a general transcriptional enhancer (Figure 28c), our data do not discriminate between an effect of the first 13 amino acids of Bcl10 on Bcl10-mediated cytosolic signaling, or on potential enhancement of transcription of NF-κB responsive promoters. Without a mechanism specifically directing an activated form of Bcl10 to NF-κB binding sites in the nucleus, a transcriptional effect is still extremely speculative.

However, the complete loss of Bcl10-mediated NF-κB activation upon deletion of the same domain that mediates association with TFIIB is intriguing (Figure 28a and 28b). It is also intriguing to note that polymorphisms at Bcl10 amino acids 5 and 8 have been associated with increased metastasis in certain germ cell tumors [90]. Further research will show if these polymorphisms are able to enhance Bcl10-mediated activation of NF-κB responsive promoters.

Taken together, these results allow us to propose a model for Bcl10 nuclear localization. We propose that PKCθ signaling directly or indirectly induces the phosphorylation of Bcl10. Phosphorylated Bcl10 then binds to Bcl3, which facilitates import into the nucleus. Once in the nucleus, Bcl10 may enhance NF-κB-dependent gene transcription by binding to TFIIB and being

targeted to NF-κB responsive promoters by an unknown mechanism. However, we emphasize that this possible functional role of nuclear Bcl10 is extremely speculative, with little direct data to support it. Bcl10 is also able to bind to MALT1 in the nucleus, allowing for nuclear export in a dose-dependent manner. TCR stimulation induces the degradation of Bcl10, terminating the signal transduction cascade that leads to NF-κB activation. Additionally, degradation of Bcl10, upon stimulation, alters the ratio of Bcl10 to MALT1 in the cell, enabling MALT1 to export more Bcl10 from the nucleus. Bcl10 export during T cell activation may also be mediated by association with PKCθ, which is directly associated with some portion of cytosolic and nuclear Bcl10. Lower levels of nuclear Bcl10 could further modulate signal transduction by reducing NF-κB-dependent gene transcription, provided that Bcl10 indeed has such an activity in the nucleus.

This study also suggests a plausible explanation for the increased pathogenesis that is frequently observed in MALT1 lymphomas with strong Bcl10 nuclear localization. In these tumor cells, nuclear Bcl10 may enhance NF-κB-dependent transcription that is already aberrantly activated. In the case of the t(11;18)(q21;q21), cIAP2-MALT1 translocation, NF-κB can be aberrantly activated through BIR-domain dependent oligomerization of MALT1 [45]. Activated NF-κB transcription is then enhanced by high levels of nuclear Bcl10. Since this activation occurs even in the absence of stimulation, Bcl10 is not degraded, and therefore there is no termination signal for NF-κB activation or NF-κB-dependent transcription.

It is important to note that further research is needed in order to define the precise steps required for Bcl10 nuclear import and to verify whether or not Bcl10 plays any role as a transcriptional enhancer of NF-κB responsive genes. Furthermore, multiple kinases have been proposed to mediate Bcl10 phosphorylation in response to a variety of cellular stimuli. The

effects of these different phosphorylation events remain to be addressed. The data presented here clearly demonstrate that Bcl10 nuclear localization is dynamically regulated in response to T cell signaling events. Our data further suggest that nuclear Bcl10 is of functional importance for the regulation of NF-κB-dependent gene transcription. Finally, these data provide a likely mechanism to explain the presence of high levels of Bcl10 in a subset of MALT lymphoma tumors, and they also may suggest the functional significance of enriched nuclear Bcl10 in the pathogenesis of MALT lymphoma.

Acknowledgements

We would like to thank Dr. Thomas Mitchell for supplying the Bcl3-pMiT plasmid and Dr. Joe Giam for the HTLV-Luciferase reporter plasmid.

Figure 24. Bcl10 is present in the nucleus of T lymphocytes. Nuclear and cytoplasmic compartments were separated from D10 T cells, subjected to SDS-PAGE and probed for (A) Bcl10 (H197), (B) histones or the cytoplasmic protein 14-3-3.

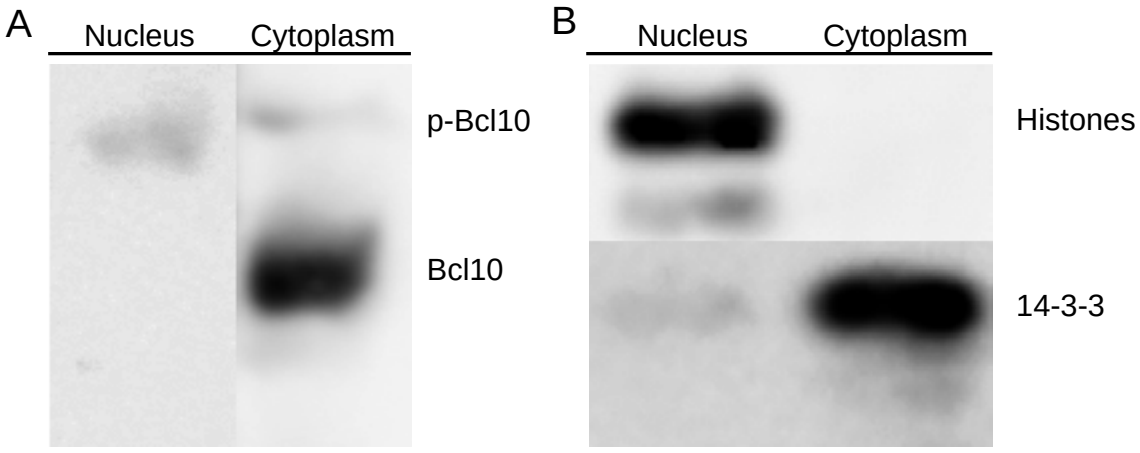
A
Nucleus
Cytoplasm
p-Bcl10
Bcl10
B
Nucleus
Cytoplasm
Histones
14-3-3

Figure 25. C-terminal phosphorylation of Bcl10 mediates nuclear localization and binding to Bcl3. (A) Nuclear and cytoplasmic compartments were separated from D10 T cells expressing Bcl10-CFP, subjected to SDS-PAGE and probed for Bcl10. (B) D10 T cells expressing Bcl10-CFP or Bcl10-Δ217-233-GFP were conjugated with CH12 B cells and nuclear enrichment was quantified. Data are means +/- SEM for 50-100 cells. Asterisk (*) indicates $p<0.0001$ compared to full-length Bcl10 as calculated by the Student's t-test. (C) 293T cells were co-transfected with 3xHA-Bcl10+Bcl3-pMiT and immunoprecipitated in the presence or absence of anti-Bcl10 (331.3) antibody. Immunoprecipitations were subjected to SDS-PAGE and probed for Bcl3 and Bcl10 (H197).

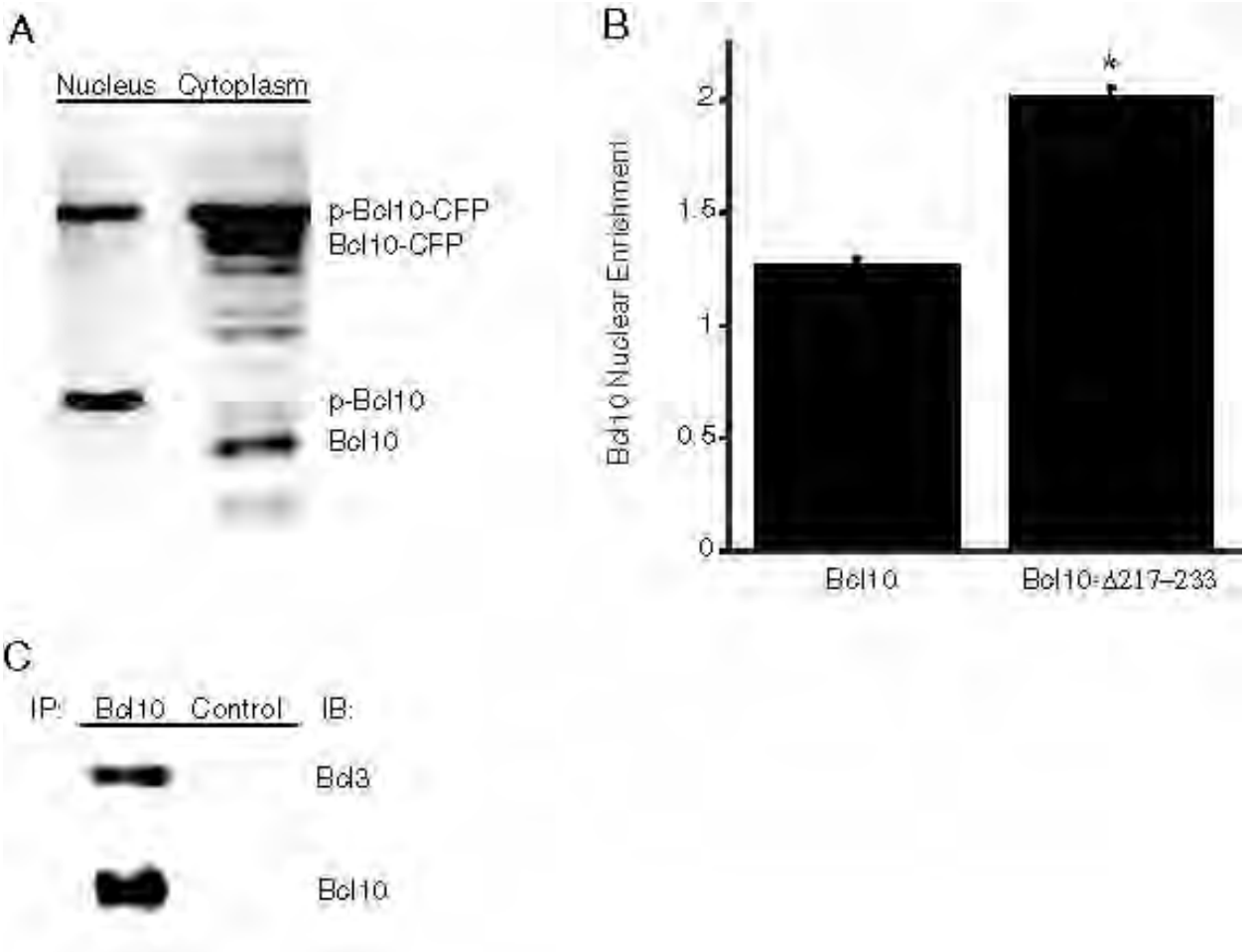
A
Nucleus
Cytoplasm
p-Bcl10-CFP
Bcl10-CFP
p-Bcl10
Bcl10
B
Bcl10 Nuclear Enrichment
2
1.5
1
0.5
0
*
Bcl10
Bcl10-Δ217–233
C
IP:
Bcl10
Control
IB:
Bcl3
Bcl10

Figure 26. PKC but not Akt signaling is required for maximal Bcl10 nuclear localization. (A) D10 T cells expressing Bcl10-CFP+MALT1-YFP were incubated in 20uM Akti1/2 or 20uM bisindolylmaleimide for 1 hour and conjugated with CH12 B cells. Fold change in Bcl10 nuclear enrichment was quantified compared to DMSO-treated cells. Asterisk (*) indicates $p<0.0001$ compared to untreated cells, as calculated by the Student's t-test (B) D10 T cells expressing Bcl10-YFP+PKCθ-CFP were conjugated to CH12 B cells in the presence of 250μg/ml conalbumin for the indicated time and %N-FRET was calculated for the whole-cell or the nucleus. White dashed line indicates the threshold for significant FRET detection in this study, which was determined as previously described [88]. (C) D10 T cells expressing Bcl10-CFP and either PKCθ, RIP2 or CARMA1 were conjugated with CH12 B cells and Bcl10 nuclear enrichment was quantified. Asterisk (*) indicates $p<0.0001$, pound (#) indicates $p<0.05$ compared Bcl10 only cells, as calculated by the Student's t-test. (D) D10 T cells expressing Bcl10-YFP+PKCθ-CFP were conjugated with CH12 B cells in the presence or absence of 250μg/ml conalbumin for various lengths of time and nuclear enrichment of Bcl10 was quantified. Data are means +/- SEM for 50-100 cells.

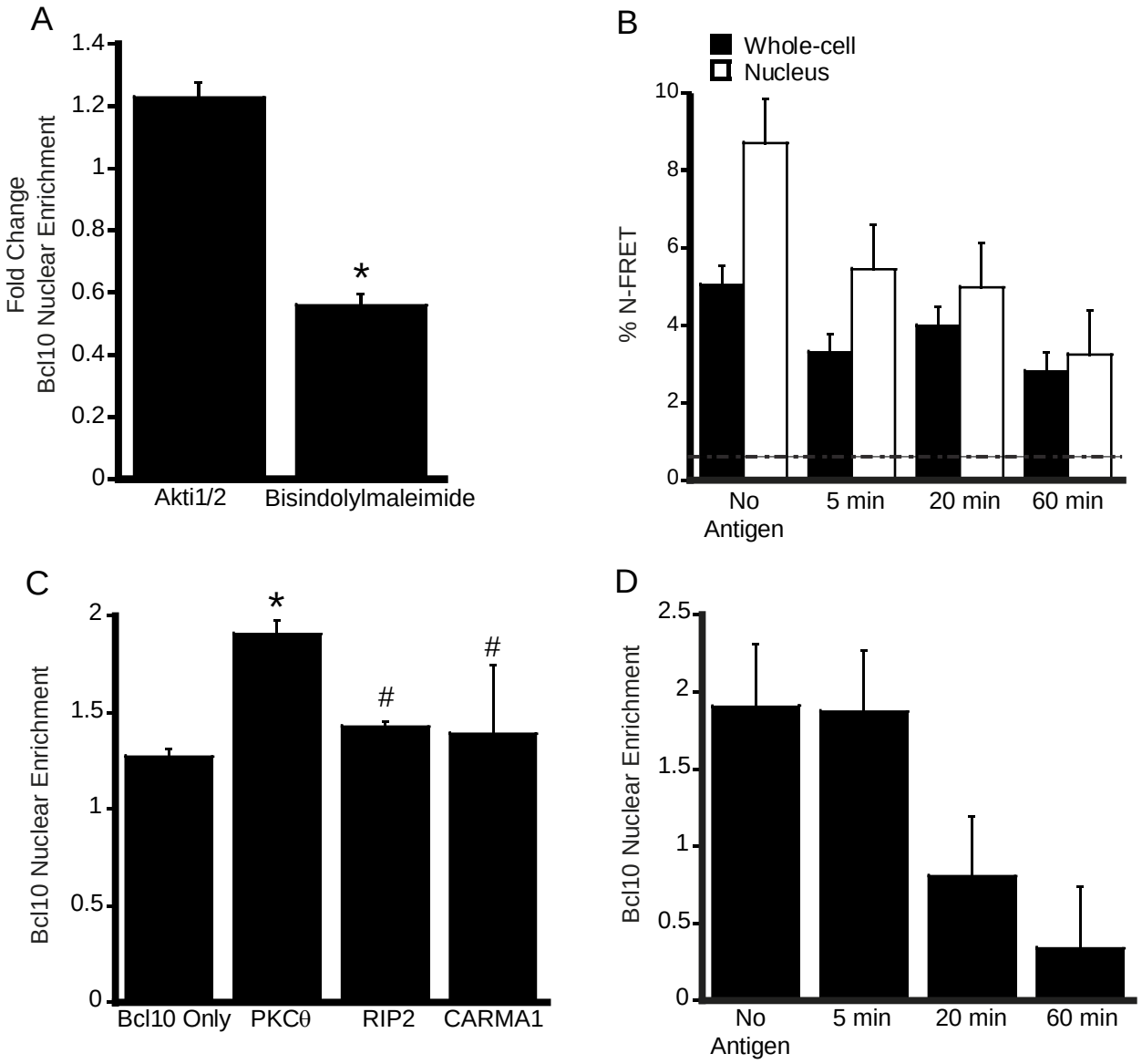
A
Fold Change
Bcl10 Nuclear Enrichment
1.4
1.2
1
0.8
0.6
0.4
0.2
0
*
Akti1/2
Bisindolylmaleimide
B
Whole-cell
Nucleus
% N-FRET
10
8
6
4
2
0
No
Antigen
5 min
20 min
60 min
C
Bcl10 Nuclear Enrichment
2
1.5
1
0.5
0
*
#
#
Bcl10 Only
PKCθ
RIP2
CARMA1
D
Bcl10 Nuclear Enrichment
2.5
2
1.5
1
0.5
0
No
Antigen
5 min
20 min
60 min

Figure 27. MALT1 is a dose-dependent nuclear export factor for Bcl10. D10 T cells expressing Bcl10-CFP and MALT1-YFP or MALT1-Δ1-344-YFP were conjugated to CH12 B cells and (A) %N-FRET was calculated for the whole-cell and the nucleus. White dashed line indicates the threshold for significant FRET detection in this study. Asterisk (*) indicates $p<0.002$ compared to whole-cells with full-length MALT1. Pound (#) indicates $p<0.0001$ compared to full-length MALT1 in the whole-cell or nucleus respectively. (B) Bcl10 nuclear enrichment was quantified. Asterisk (*) indicates $p<0.05$ compared to with full-length MALT1. (C) Bcl10 nuclear enrichment was quantified and plotted against the whole-cell intensity of Bcl10/MALT1. Data are means +/- SEM for 50-100 cells. Significance was calculated by the Student's t-test.

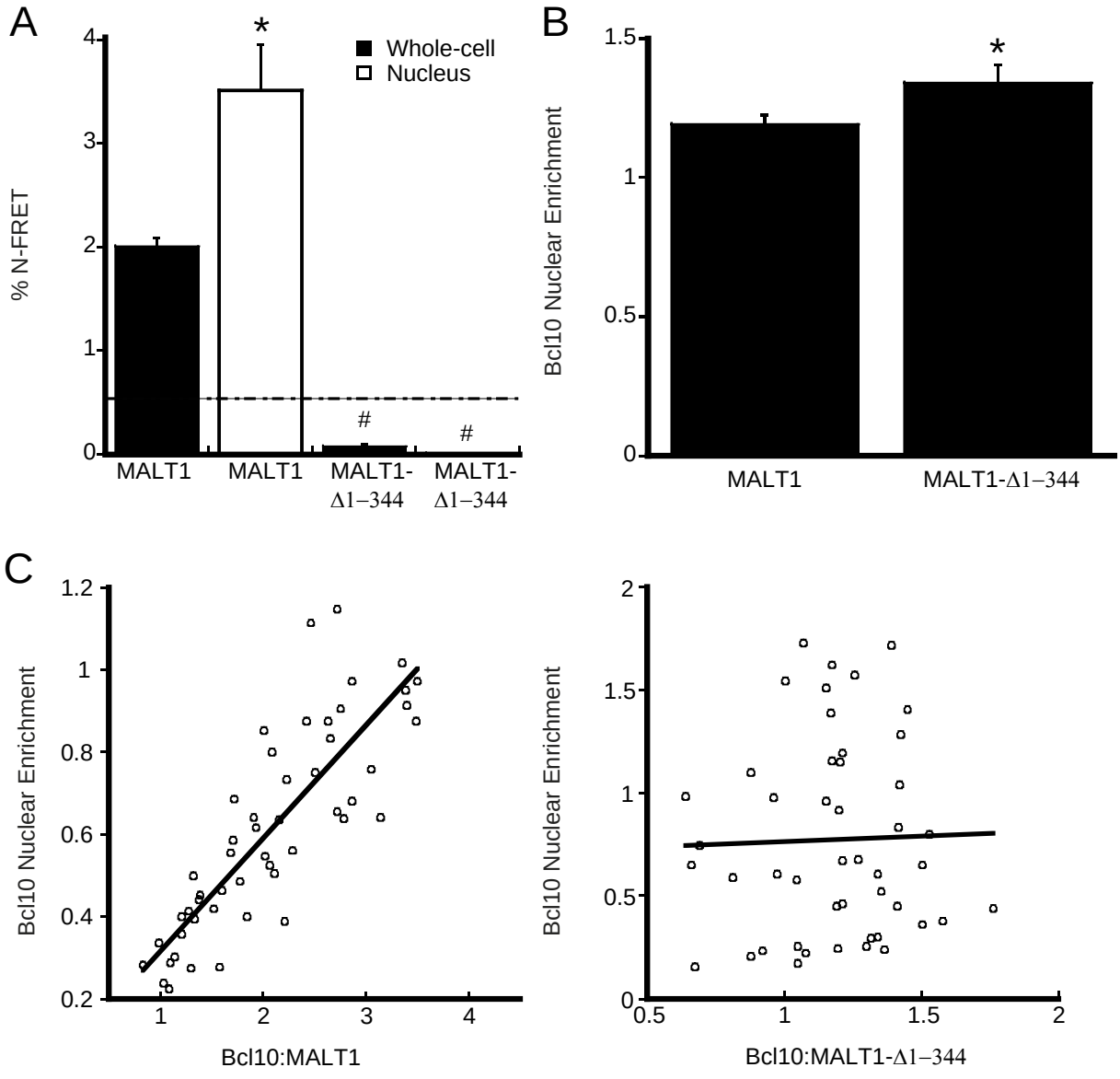
A
% N-FRET
Whole-cell
Nucleus
*
#
#
MALT1
MALT1
MALT1-Δ1–344
MALT1-Δ1–344
B
Bcl10 Nuclear Enrichment
*
MALT1
MALT1-Δ1–344
C
Bcl10 Nuclear Enrichment
Bcl10:MALT1
Bcl10 Nuclear Enrichment
Bcl10:MALT1-Δ1–344

Figure 28. Bcl10 is a transcriptional activator. 293T cells were transfected with Bcl10-CFP or Bcl10-Δ1-13-CFP and (A) NF-κB dependent luciferase production or (B) HTLV-dependent luciferase production was assessed. Data is means +/- SEM for 12 wells. Asterisk (*) indicates $p<0.0001$ compared to full-length Bcl10. Significance was calculated by the Student's t-test. (C) 293T cells were transfected with 3xHA-Bcl10 or Bcl10-Δ1-13 and immunoprecipitated in the presence or absence of anti-Bcl10 (331.3) antibody. Immunoprecipitations were subjected to SDS-PAGE and probed for TFIIB and Bcl10 (H157).

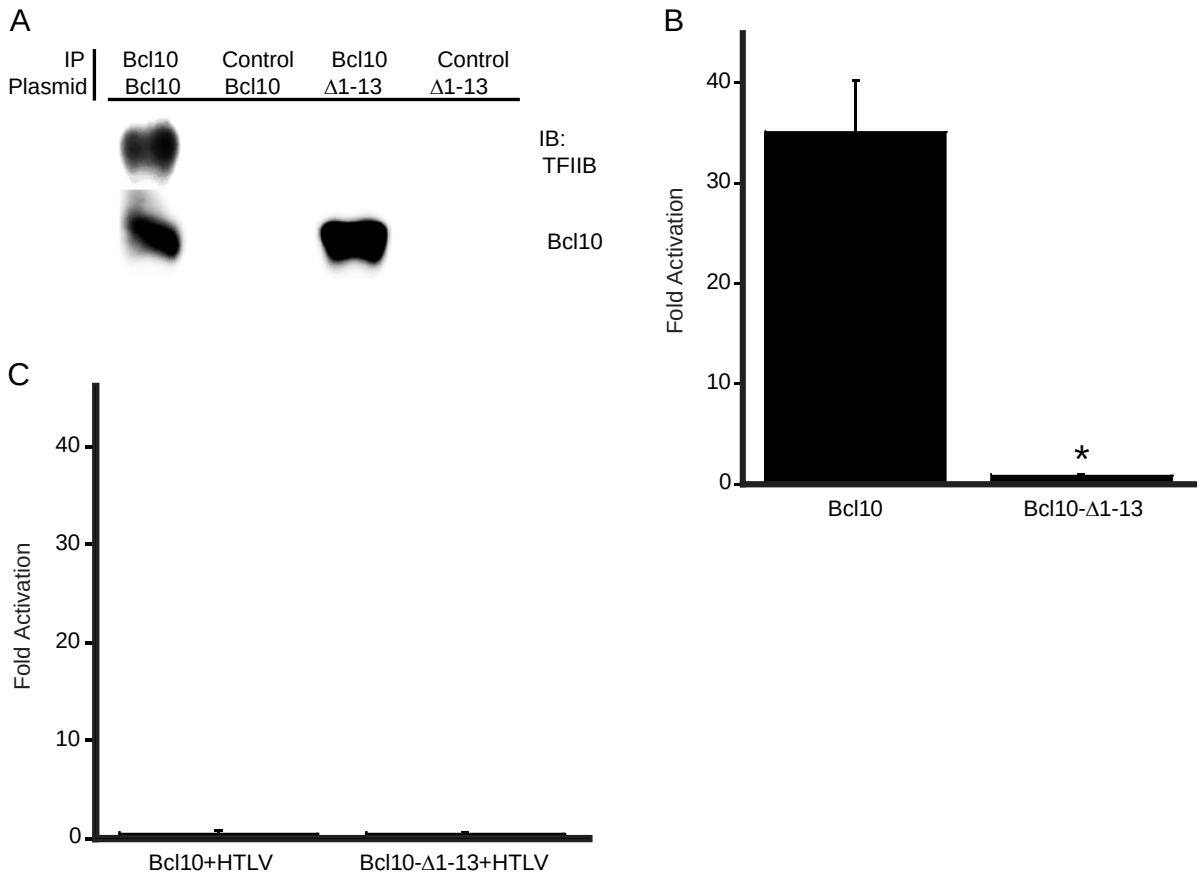
A
IP
Plasmid
Bcl10
Bcl10
Control
Bcl10
Bcl10
Δ1-13
Control
Δ1-13
IB:
TFIIB
Bcl10
B
Fold Activation
40
30
20
10
0
*
Bcl10
Bcl10-Δ1-13
C
Fold Activation
40
30
20
10
0
Bcl10+HTLV
Bcl10-Δ1-13+HTLV

Chapter 4

Discussion and Future Directions

We have proposed that spatial-temporal mapping of the T cell receptor to NF-κB signaling pathway will help to elucidate the mechanisms of signal transduction and their aberrations in disease. To address our hypothesis, we have directed our research towards two specific aims: to determine the role of POLKADOTS in the TCR-mediated activation of NF-kB, and to elucidate the function and regulation of nuclear Bcl10.

Specific Aim 1

POLKADOTS Are Foci of Functional Interactions in T-Cell Receptor–Mediated Signaling to NF-κB

We have previously described dynamic redistribution events that occur upon TCR stimulation [35]. Upon stimulation, PKCθ is recruited to the immunological synapse. When PKCθ reaches its maximum enrichment at the synapse, Bcl10 begins to redistribute to punctate structures throughout the cell. These structures move toward the IS, eventually coalescing into larger, filamentous structures. Despite their dynamic nature, and their dependence on TCR-induced PKC signaling, [35] no direct role for these POLKADOTS has been determined. In this study, we have examined the dynamics and functions of POLKADOTS in the TCR-mediated activation of NF-κB.

We first sought to examine the conditions required for POLKADOTS formation. To address this, we conjugated Bcl10-YFP+PKCθ-CFP expressing D10 T cells with CH12 B cells in the presence of varying concentrations of the specific antigen conalbumin. We find that there is a clear dose-dependence and relationship between Bcl10 POLKADOTS formation and the concentration of antigen (Figure 12a). To further examine the conditions required for

POLKADOTS formation, we assessed Bcl10 POLKADOTS formation upon stimulation with antigens of varying strengths. Table 1 shows that efficient POLKADOTS formation requires strong agonist stimulation. We also looked at the duration of TCR stimulation that is required for POLKADOTS formation. By adding an antibody to the adhesin LFA-1 we were able to disrupt T cell – B cell conjugation, terminating TCR signaling. We find that addition of anti-LFA-1 anytime before POLKADOTS begin to form effectively prohibits subsequent POLKADOTS formation. Terminating TCR signaling after POLKADOTS formation blocks the further formation of POLKADOTS and induces a decay of currently formed POLKADOTS (Figure 12b). This indicates that continuous TCR signaling is required for the maintenance, and continued development, of POLKADOTS. These results show that POLKADOTS formation requires a specific signaling threshold, in terms of antigen concentration, antigenic strength and TCR signaling duration.

The question remains, however, what the relationship is between the antigenic conditions required for POKADOTS formation and the antigenic conditions required for NF-κB activation. To address this question we examined the induction of IκBα phosphorylation, as a marker for the subsequent activation of NF-κB. Table 1 shows that only strong antigenic conditions, leading to robust POLKADOTS formation, also result in a significant increase in IκBα phosphorylation. This indicates that POLKADOTS formation is correlated with the subsequent activation of NF-κB.

Since there is a strong correlation between POLKADOTS formation and the activation of NF-κB, we next investigated the dynamics of POLKADOTS formation in D10 T cells. We find that Bcl10 forms POLKADOTS by 20 minutes post-antigen stimulation (Figure 13). The development of POLKADOTS continues until 90 minutes post-stimulation, with many

POLKADOTS coalescing into larger, filamentous structures. Over the next 90 minutes, the POLKADOTS begin to decay, resulting in a complete loss of POLKADOTS by 3 hours post-stimulation. Additionally, Bcl10 within these cells is significantly degradation by 3 hours post-stimulation, which is consistent with a recent study showing that Bcl10 is targeted for degradation upon TCR stimulation [69]. The degradation of Bcl10 may thus provide a mechanistic explanation for the loss of Bcl10 POLKADOTS, raising the interesting possibility that Bcl10 degradation may serve to terminate signal transduction to NF-κB.

Previous studies of Bcl10 have shown that the binding of Bcl10 to MALT1 is crucial for the TCR-mediated activation of NF-κB [36]. We thus examined a cell line expressing Bcl10-CFP and MALT1-YFP for the formation of MALT1-containing POLKADOTS upon TCR stimulation. We observed that MALT1 co-localizes with Bcl10 in POLKADOTS and that the two molecules have identical rates of POLKADOTS formation (Figure 13). However, the decay of MALT1 POLKADOTS is slower than that of Bcl10. This is consistent with the model of TCR-induced Bcl10 degradation, which would leave only MALT1 remaining in POLKADOTS. It is intriguing that although MALT1 is not degraded upon stimulation, MALT1-containing POLKADOTS undergo a similar reversal to Bcl10-containing POLKADOTS. This suggests that the interaction between Bcl10 and MALT1 is required for POLKADOTS formation and maintenance.

To investigate the importance of Bcl10-MALT1 interactions in POLKADOTS formation, we constructed a previously described mutant of Bcl10 that is missing the MALT1 interaction motif (amino acids 107-119) [36]. We find that when Bcl10 cannot interact with MALT1 POLKADOTS formation is prohibited (Figure 14). Lucas et. al. have also shown that this mutant Bcl10 molecule is completely deficient in its ability to activate NF-κB [36], providing a

further correlation between POLKADOTS formation and NF-κB activation. We also created several deletion mutants of MALT1 (shown in Figure 15a) in order to further assess the importance of MALT1 interaction with Bcl10 on POLKADOTS formation and NF-κB activation. We find that when MALT1 cannot interact with Bcl10 POLKADOTS formation does not occur (Figure 15). However, POLKADOTS formation also required the C-terminus of MALT1 and the TRAF6 binding sites within MALT1. It is possible that these mutations alter the confirmation of MALT1 in such a way that it is no longer able to bind to Bcl10 and form POLKADOTS. However this is unlikely, as these constructs were still able to interact with Bcl10 in a FRET assay (Figure 15b). Alternatively, the C-terminus of MALT1 may bind to other proteins, which play some crucial role in POLKADOTS formation. Considering that the 2EA mutation of MALT1 prohibits POLKADOTS formation, it is possible that binding to TRAF6 is required for POLKADOTS formation. It will be intriguing to further examine the role of TRAF6 in POLKADOTS formation and signal transduction.

We also assessed the ability of the various MALT1 deletions to activate NF-κB, upon TCR stimulation. We find that deletion of the MALT1 C-terminus, or mutation of the TRAF6 binding sites, prohibits POLKADOTS formation and significantly attenuates the phosphorylation of IκBα (Figure 15). However, we were surprised to discover that deletion of the N-terminus of MALT1 has no detectable effect on the activation of NF-κB. This construct does not show spontaneous activation of NF-κB; rather, it seems to allow for TCR-induced activation of NF-κB in the absence of binding to Bcl10 and POLKADOTS formation. It is important to note that this MALT1 mutant is missing the immunoglobulin-like domains and the death domain. While the Ig domains have been reported to mediate binding to Bcl10 [36], the role of the death domain has not been established. It is possible that the death domain mediates an inhibitory binding

interaction, possibly with an as yet undefined interaction partner. Bcl10-MALT1 binding, possibly within POLKADOTS, may induce a conformational change in MALT1, enabling activation and signal transduction. In the absence of its N-terminus, MALT1 may be able to mediate signal transduction without requiring this conformational change. It is intriguing to note that this mutant still requires TCR signaling for activation. It has been thought that MALT1 is activated by binding to Bcl10 and by Bcl10-mediated oligomerization [36]. Since this construct can no longer bind to Bcl10, another input signal appears to be required for the activation of MALT1, though the nature of this signal is unknown.

We next sought to define a functional role for POLKADOTS in TCR signal transduction to NF-κB. Since Bcl10 has been shown to be a crucial adaptor molecule that interacts with many other signaling proteins [28, 29, 36, 39, 91, 92], we examined interactions between Bcl10 and other signaling molecules. We find that Bcl10 is able to specifically interact with itself, MALT1, TRAF6, CARMA1 and RIP2 (Figure 17). Furthermore, we find that these interactions are the strongest within the POLKADOTS. This indicates that POLKADOTS are enriched in interactions between multiple TCR-induced signaling intermediates. Oligomerization of Bcl10 has been proposed to mediate signal transduction to MALT1 and subsequently to TRAF6 [36-39, 92]. We see strong Bcl10-Bcl10 interactions within POLKADOTS upon TCR stimulation. Additionally, we see Bcl10-MALT1 and Bcl10-TRAF6 interactions within the POLKADOTS. This strongly suggests that POLKADOTS are the cytoplasmic sites of signal transduction to NF-κB. Interestingly, CARMA1 and RIP2 do not appear to colocalize with Bcl10-containing POLKADOTS, despite the fact that we see a significant FRET interaction within the POLKADOTS. In order to assess the dynamics of Bcl10 that may allow for these interactions to occur, we utilized a photoactivatable-GFP to allow for tracking of Bcl10 molecules. We find

that POLKADOTS contain two distinct populations of Bcl10: a stably incorporated pool, and a pool that is at rapid equilibrium with the cytoplasmic pool (Figure 16). The presence of these two populations of POLKADOTS-associated Bcl10 allows us to propose a model accounting for the different types of interactions seen in POLKADOTS.

We propose that POLKADOTS contain a core of stably-associated, possibly oligomerized, Bcl10 molecules. Other proteins that are recruited to POLKADOTS, such as MALT1 and TRAF6, may also be incorporated into this core structure, and are perhaps even required for its formation. It is possible that this core provides the scaffold on which other signaling interactions can be assembled. We also propose that POLKADOTS possess an outer shell that contains a freely diffusible population of Bcl10. This pool of Bcl10 is able to interact with the POLKADOTS but is also highly mobile. It is possible that this outer shell is the site of signaling interactions between many highly diffusible cytoplasmic signaling intermediates, such as CARMA1 and RIP2. This inner core–outer shell structure of POLKADOTS may provide a basis for the integration of signaling interactions between upstream, freely diffusible molecules, and downstream, oligomerization-induced, signaling events. This model of POLKADOTS structure and function is depicted in figure 18.

Our results raise many interesting questions about the structure and function of POLKADOTS. Future studies utilizing fusions with PA-GFP could allow for precise determination of which proteins are incorporated into the core structure vs. shell-associated proteins. Additionally, the two populations of molecules, core and shell-associated, may be separated by membrane. Preliminary results indicate that POLKADOTS colocalize with a marker for cytoplasmic membrane structures (Figure 23). It is an intriguing possibility that POLKADOTS may be membrane-bound organelles. Further studies are needed to assess the

exact structure of POLKADOTS and any possible relationship with other cellular organelles. It is also intriguing to note that early signaling intermediates from TCR stimulation, such as Lck and Zap-70, have been shown to form small microclusters near the IS [13, 77, 78]. The relationship between microclusters and POLKADOTS is unclear; however, it is possible that microclusters are early foci of signaling components which eventually develop into fully-formed POLKADOTS. Thus, spatial organization of signaling molecules may prove to be an important mechanism of regulating signal transduction.

We have shown that POLKADOTS are dynamic structures that are foci for interactions involved in signal transduction from the TCR to NF-κB. Our data suggest that the redistribution of cytoplasmic Bcl10 into POLKADOTS represents a crucial step in signal transduction. Thus, stimulation-induced spatial regulation of Bcl10 may mediate signal transduction in health T lymphocytes. However, there is also evidence that aberrant spatial regulation of Bcl10 may mediate pathogenesis in MALT lymphomas [51, 86, 87]. To examine this further, we have investigated the regulation of the nuclear localization of Bcl10 in unstimulated lymphocytes in an attempt to ascertain the functional significance of this localization and the possible mechanism of pathogenesis in MALT lymphomas.

Specific Aim 2

PKCθ dynamically regulates Bcl10 nuclear localization in T lymphocytes

We first examined unstimulated D10 T cells for the presence of Bcl10 in the nucleus. We find that D10 T cells do contain Bcl10 in the nucleus and that this pool of Bcl10 is phosphorylated (Figure 24a and 25a). Yeh et. al. have previously shown that C-terminal

phosphorylation of Bcl10 by the kinase Akt, mediates binding to Bcl3 and import into the nucleus [52]. We confirm these results by showing that Bcl10 co-immunoprecipitates with Bcl3, suggesting that the two molecules can associate (Figure 25c). Furthermore, we constructed a mutant of Bcl10 that is lacking the C-terminal 17 amino acids. We find that this mutant is enriched in the nucleus as compared to full-length Bcl10 (Figure 25b). Previous results have suggested that deletion of the C-terminus of Bcl10 enables binding to Bcl3 in a similar manner as C-terminal phosphorylation [52]. This suggests that the C-terminus of Bcl10 normally blocks binding to Bcl3. Phosphorylation or deletion of the C-terminus removes this blockade, allowing for binding to Bcl3 through some, as yet undefined, motif within the Bcl10 molecule.

Since the study by Yeh et. al. showed that the C-terminal phosphorylation of Bcl10 is mediated by Akt, we examined the consequences of kinase inhibition on Bcl10 nuclear localization. We find that inhibition of Akt has no detectable effect on Bcl10 nuclear localization in T lymphocytes (Figure 26a). However, it is important to note that the previous study was preformed in a breast cancer carcinoma cell line, upon TNFα stimulation [52]. Thus, the phosphorylation events leading to Bcl10 nuclear localization may be mediated by different kinases in different cell lines and in response to different stimuli.

In contrast to Akt inhibition, blockade of PKC activity significantly reduces the amount of Bcl10 in the nucleus of D10 T cells (Figure 26a). Since PKCθ has been shown to be the main isoform in T lymphocytes [20], we looked for interactions between PKCθ and Bcl10 within D10 T cells. We see a strong interaction between PKCθ and Bcl10 within both the cytoplasm and the nucleus (Figure 26b). This interaction suggests a direct role for PKCθ in Bcl10 nuclear localization, although we have no evidence that PKCθ is the kinase responsible for Bcl10 C-terminal phosphorylation. However, it is intriguing to note that there is an interaction between

Bcl10 and PKCθ within the nucleus, and that this interaction decays upon TCR stimulation, correlating with the loss of Bcl10 from the nucleus (Figure 26b and 26d). This suggests that the interaction with PKCθ in the nucleus may enable the maintenance of high levels of nuclear Bcl10. Upon stimulation, the nuclear interaction between Bcl10 and PKCθ decays resulting in lowered levels of Bcl10 in the nucleus (Figure 26d). PKCθ is known to redistribute to the IS upon TCR stimulation [18, 20]; thus, by virtue of its interaction with Bcl10, movement of PKCθ to the IS could mediate export of Bcl10 out of the nucleus. It should be noted that there is no direct evidence for PKCθ-mediated nuclear export of Bcl10. Further research is needed to assess the nature of PKCθ's role on Bcl10 nuclear localization. Additionally, it will be important to determine the kinases that are responsible for Bcl10 C-terminal phosphorylation and subsequent nuclear localization.

One possible candidate for a Bcl10-phosphorylating kinase is RIP2. Previous reports have suggested that RIP2 is responsible for Bcl10 phosphorylation upon TCR stimulation [28]. We examined the consequences of overexpression of PKCθ, RIP2 and CARMA1 on Bcl10 nuclear localization. We find that in unstimulated D10 T cells, all three proteins increase the level of Bcl10 in the nucleus, although, overexpression of PKCθ leads to a far greater increase in nuclear Bcl10 levels (Figure 26c). This reaffirms the significant role PKCθ is playing in the nuclear localization of Bcl10. The observation that RIP2 and CARMA1 increased nuclear Bcl10 levels also suggests that other kinases or signaling proteins may be involved in regulating the nuclear localization of Bcl10.

MALT1 has also been shown to be directly involved in the regulation of Bcl10 nuclear localization [84]. Nakagawa et. al. showed that MALT1 contains a NES and can modulate the levels of Bcl10 in the nucleus of COS-7 cells. In examining the role of MALT1 in Bcl10 nuclear

localization, we find that Bcl10 and MALT1 specifically interact in both the cytoplasm and nucleus of T lymphocytes (Figure 27a). This interaction is dependent on specific domains within Bcl10 and MALT1, as has been previously shown [36, 88]. Furthermore, inhibition of Bcl10-MALT1 binding leads to significantly elevated levels of Bcl10 in the nucleus, demonstrating the ability of MALT1 to mediate the nuclear export of Bcl10 in T lymphocytes (Figure 27b).

Intriguingly, while examining the role of MALT1 in the nuclear export of Bcl10, we noticed a relationship between the levels of nuclear Bcl10 and the relative concentrations of Bcl10 and MALT1 in the cell. In examining this relationship further, we found that the levels of Bcl10 in the nucleus are directly correlated with the ratio of Bcl10 to MALT1 in the cell (Figure 27c). This shows that MALT1 is able to export Bcl10 from the nucleus in a dose-dependent manner. The observation of this dose-dependent relationship provides a plausible explanation for the patterns of Bcl10 nuclear localization seen in many MALT lymphomas. t(11;18)(q21;q21)- and t(1;14)(p22;q32)- positive lymphomas show strong nuclear localization of Bcl10. It is possible that these lymphomas have elevated levels of Bcl10 in their nucleus due to an increase in the ratio of Bcl10 to MALT1 in the cell, either by overexpression of Bcl10 or by a loss of MALT1's ability to bind to Bcl10, respectively. Conversely, t(14;18)(q32;q21)-positive lymphomas may show lower levels of Bcl10 in the nucleus due to an overexpression of MALT1, resulting in enhanced nuclear export of Bcl10. Thus, aberrant expression of Bcl10 or MALT1 may directly modulate the levels of Bcl10 in the nucleus of MALT lymphomas.

Recent research has suggested that the first 13 amino acids of Bcl10 may act as a transcriptional activator by binding to TFIIB [48]. In an attempt to assess the potential role for Bcl10 in transcriptional activation, we examined the ability of Bcl10 to bind to TFIIB. We saw that Bcl10 is able to co-imunoprecipitate with TFIIB and that this interaction is dependant on the

presence of the first 13 amino acids of Bcl10 (Figure 28a). This confirms that Bcl10 is able to associate with a component of the transcriptional machinery.

We next examined the ability of Bcl10 to activate an NF-κB-dependent luciferase reporter construct. We saw that Bcl10 is able to activate NF-κB-dependent transcription and that this activation is dependent on the presence of the first 13 amino acids of Bcl10 (Figure 28b). We also found that this activation is specific for activation of NF-κB-dependent transcription (Figure 28c). While these results do not conclusively prove that Bcl10 is a transcriptional activator in T lymphocytes, they do suggest that Bcl10 may enhance transcription in an NF-κB-dependent manner. Further experiments are needed to assess whether or not this activation is directly regulates transcription, and to define the mechanism by which Bcl10 may associate with TFIIB and activate the transcriptional machinery. However, if Bcl10 is able to enhance NF-κB-dependent transcription, then the strong nuclear localization of Bcl10 seen in MALT lymphomas may be pathogenic. Since NF-κB is known to mediate the transcription of many genes involved in lymphocyte growth and development, this transcriptional enhancement could provide a growth advantage for these tumors, thus explaining the correlation seen between Bcl10 nuclear localization and increased pathogenesis of MALT lymphomas [51, 86, 87].

We have shown that Bcl10 is present in the nucleus of unstimulated T lymphocytes, and that this localization is correlated with the phosphorylation of Bcl10. C-terminal phosphorylation of Bcl10 may mediate binding to, and nuclear import by, Bcl3. Steady state signaling through PKC, possibly through nuclear binding to PKCθ, mediates maximal nuclear localization of Bcl10. In the nucleus, Bcl10 may enhance NF-κB-dependent transcription, possibly by binding to TFIIB and associating with the transcriptional machinery. Export of Bcl10 from the nucleus is regulated by MALT1 in a dose-dependent fashion. A schematic of

these events is depicted in figure 29. Our results suggest the nuclear Bcl10 may play a functional role in healthy T lymphocytes. Increased levels of nuclear Bcl10 in MALT lymphomas may disrupt the normal regulation of Bcl10 nuclear localization, resulting in enhanced tumor pathogenesis.

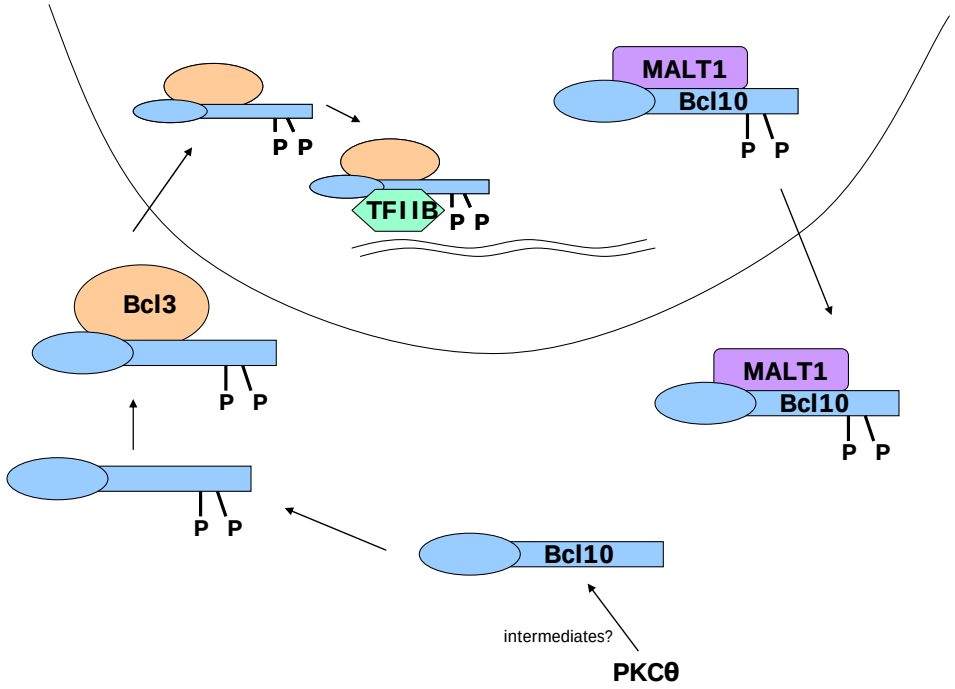

Figure 29. Regulation of Bcl10 nuclear localization. Bcl10 is phosphorylated on the C-terminus in an event that involves PKCθ. Phosphorylated Bcl10 may then bind Bcl3 and be imported into the nucleus. In the nucleus, Bcl10 can bind to TFIIB, possibly enhancing NF-κB-dependent gene transcription. Binding to MALT1 then mediates the export of Bcl10 from the nucleus.

Our research has also shown that, in addition to nuclear localization, Bcl10 also undergoes another, very different, spatial redistribution event, the formation of POLKADOTS. We have shown that Bcl10 and MALT1 form punctate structures upon TCR signaling. The formation of these POLKADOTS is dependent on specific antigenic conditions and requires continual TCR signaling. Bcl10 and MALT1 interact within the POLKADOTS, and this interaction is crucial for POLKADOTS formation and signal transduction. Other signaling

molecules also interact with Bcl10 in the POLKADOTS, though their interactions may occur with a highly-diffusible population of POLKADOTS-associated Bcl10 molecules (shown in Figure 18). These results show that POLKADOTS are foci for signal transduction and that the redistribution of Bcl10 to POLKADOTS is a crucial step in the TCR-mediated activation of NF-κB.

It is intriguing that Bcl10 has two distinct roles in response to TCR stimulation, and that these two activities are regulated by the same set of signaling proteins. We have shown that the nuclear localization of Bcl10 is dependent on, and regulated by, interactions with PKCθ and MALT1. We have also shown that the redistribution of Bcl10 to POLKADOTS requires PKC signaling and interaction with MALT1 [35, 88]. It would be interesting to see if these two redistribution events are connected and if the presence of nuclear Bcl10 serves to enhance TCR-induced NF-κB-dependent gene transcription. It is likely that these two signaling pathways work together, integrating signal transduction and regulating the activation of NF-κB.

Ongoing research into the TCR-regulated NF-κB signaling pathway may help to illuminate the role of, and interactions between, these two signaling activities of Bcl10. We demonstrate here that observation of spatial redistribution events can greatly enhance our understanding of crucial signaling pathways, as well as suggest mechanisms by which aberrant signaling can cause pathogenesis. We have already shown how understanding spatial redistribution events can lead to a better understanding of signal transduction and can provide explanations for its pathogenesis in disease. Further spatial-temporal mapping studies of known and novel signaling molecules should provide even more insight into the function and regulation of normal cellular events and how they too may be implicated in pathogenesis, ultimately leading to development of new therapeutic agents and possibly disease prevention.

References

1. Shaulian, E. and M. Karin, *AP-1 in cell proliferation and survival.* Oncogene, 2001. **20**(19): p. 2390-400.
2. Hayden, M.S. and S. Ghosh, *Signaling to NF-kappaB.* Genes Dev, 2004. **18**(18): p. 2195-224.
3. Macian, F., C. Lopez-Rodriguez, and A. Rao, *Partners in transcription: NFAT and AP-1.* Oncogene, 2001. **20**(19): p. 2476-89.
4. Chinenov, Y. and T.K. Kerppola, *Close encounters of many kinds: Fos-Jun interactions that mediate transcription regulatory specificity.* Oncogene, 2001. **20**(19): p. 2438-52.
5. Liu, J.O., *The yins of T cell activation.* Sci STKE, 2005. **2005**(265): p. re1.
6. Boothby, M.R., et al., *Perturbation of the T lymphocyte lineage in transgenic mice expressing a constitutive repressor of nuclear factor (NF)-kappaB.* J Exp Med, 1997. **185**(11): p. 1897-907.
7. Lanzavecchia, A. and F. Sallusto, *Progressive differentiation and selection of the fittest in the immune response.* Nat Rev Immunol, 2002. **2**(12): p. 982-7.
8. Davis, M.M., et al., *Ligand recognition by alpha beta T cell receptors.* Annu Rev Immunol, 1998. **16**: p. 523-44.
9. Nel, A.E., *T-cell activation through the antigen receptor. Part 1: signaling components, signaling pathways, and signal integration at the T-cell antigen receptor synapse.* J Allergy Clin Immunol, 2002. **109**(5): p. 758-70.
10. Nel, A.E. and N. Slaughter, *T-cell activation through the antigen receptor. Part 2: role of signaling cascades in T-cell differentiation, anergy, immune senescence, and development of immunotherapy.* J Allergy Clin Immunol, 2002. **109**(6): p. 901-15.
11. Lin, X. and D. Wang, *The roles of CARMA1, Bcl10, and MALT1 in antigen receptor signaling.* Semin Immunol, 2004. **16**(6): p. 429-35.
12. Freiberg, B.A., et al., *Staging and resetting T cell activation in SMACs.* Nat Immunol, 2002. **3**(10): p. 911-7.
13. Mossman, K.D., et al., *Altered TCR signaling from geometrically repatterned immunological synapses.* Science, 2005. **310**(5751): p. 1191-3.
14. Purtic, B., et al., *T cell receptor (TCR) clustering in the immunological synapse integrates TCR and costimulatory signaling in selected T cells.* Proc Natl Acad Sci U S A, 2005. **102**(8): p. 2904-9.
15. Clements, J.L., et al., *Integration of T cell receptor-dependent signaling pathways by adapter proteins.* Annu Rev Immunol, 1999. **17**: p. 89-108.
16. Rudd, C.E., *Adaptors and molecular scaffolds in immune cell signaling.* Cell, 1999. **96**(1): p. 5-8.
17. Kane, L.P. and A. Weiss, *The PI-3 kinase/Akt pathway and T cell activation: pleiotropic pathways downstream of PIP3.* Immunol Rev, 2003. **192**: p. 7-20.
18. Villalba, M., et al., *A novel functional interaction between Vav and PKCtheta is required for TCR-induced T cell activation.* Immunity, 2000. **12**(2): p. 151-60.
19. Khoshnan, A., et al., *The physical association of protein kinase C theta with a lipid raft-associated inhibitor of kappa B factor kinase (IKK) complex plays a role in the activation of the NF-kappa B cascade by TCR and CD28.* J Immunol, 2000. **165**(12): p. 6933-40.

20. Sedwick, C.E. and A. Altman, *Perspectives on PKCtheta in T cell activation.* Mol Immunol, 2004. **41**(6-7): p. 675-86.
21. Lucas, P.C., L.M. McAllister-Lucas, and G. Nunez, *NF-kappaB signaling in lymphocytes: a new cast of characters.* J Cell Sci, 2004. **117**(Pt 1): p. 31-9.
22. Monks, C.R., et al., *Selective modulation of protein kinase C-theta during T-cell activation.* Nature, 1997. **385**(6611): p. 83-6.
23. Lee, K.Y., et al., *PDK1 nucleates T cell receptor-induced signaling complex for NF-kappaB activation.* Science, 2005. **308**(5718): p. 114-8.
24. Weil, R. and A. Israel, *Deciphering the pathway from the TCR to NF-kappaB.* Cell Death Differ, 2006. **13**(5): p. 826-33.
25. Sun, Z., et al., *PKC-theta is required for TCR-induced NF-kappaB activation in mature but not immature T lymphocytes.* Nature, 2000. **404**(6776): p. 402-7.
26. McAllister-Lucas, L.M., et al., *Bimp1, a MAGUK family member linking protein kinase C activation to Bcl10-mediated NF-kappaB induction.* J Biol Chem, 2001. **276**(33): p. 30589-97.
27. Matsumoto, R., et al., *Phosphorylation of CARMA1 plays a critical role in T Cell receptor-mediated NF-kappaB activation.* Immunity, 2005. **23**(6): p. 575-85.
28. Ruefli-Brasse, A.A., et al., *Rip2 participates in Bcl10 signaling and T-cell receptor-mediated NF-kappaB activation.* J Biol Chem, 2004. **279**(2): p. 1570-4.
29. Bertin, J., et al., *CARD11 and CARD14 are novel caspase recruitment domain (CARD)/membrane-associated guanylate kinase (MAGUK) family members that interact with BCL10 and activate NF-kappa B.* J Biol Chem, 2001. **276**(15): p. 11877-82.
30. Wang, D., et al., *A requirement for CARMA1 in TCR-induced NF-kappa B activation.* Nat Immunol, 2002. **3**(9): p. 830-5.
31. Wang, D., et al., *CD3/CD28 costimulation-induced NF-kappaB activation is mediated by recruitment of protein kinase C-theta, Bcl10, and IkappaB kinase beta to the immunological synapse through CARMA1.* Mol Cell Biol, 2004. **24**(1): p. 164-71.
32. Gaide, O., et al., *Carma1, a CARD-containing binding partner of Bcl10, induces Bcl10 phosphorylation and NF-kappaB activation.* FEBS Lett, 2001. **496**(2-3): p. 121-7.
33. Yan, M., et al., *mE10, a novel caspase recruitment domain-containing proapoptotic molecule.* J Biol Chem, 1999. **274**(15): p. 10287-92.
34. Yoneda, T., et al., *Regulatory mechanisms of TRAF2-mediated signal transduction by Bcl10, a MALT lymphoma-associated protein.* J Biol Chem, 2000. **275**(15): p. 11114-20.
35. Schaefer, B.C., et al., *Complex and dynamic redistribution of NF-{kappa}B signaling intermediates in response to T cell receptor stimulation.* Proc Natl Acad Sci U S A, 2004. **101**(4): p. 1004-9.
36. Lucas, P.C., et al., *Bcl10 and MALT1, independent targets of chromosomal translocation in malt lymphoma, cooperate in a novel NF-kappa B signaling pathway.* J Biol Chem, 2001. **276**(22): p. 19012-9.
37. Koseki, T., et al., *CIPER, a novel NF kappaB-activating protein containing a caspase recruitment domain with homology to Herpesvirus-2 protein E10.* J Biol Chem, 1999. **274**(15): p. 9955-61.
38. Srinivasula, S.M., et al., *CLAP, a novel caspase recruitment domain-containing protein in the tumor necrosis factor receptor pathway, regulates NF-kappaB activation and apoptosis.* J Biol Chem, 1999. **274**(25): p. 17946-54.

39. Sun, L., et al., *The TRAF6 ubiquitin ligase and TAK1 kinase mediate IKK activation by BCL10 and MALT1 in T lymphocytes.* Mol Cell, 2004. **14**(3): p. 289-301.
40. Che, T., et al., *MALT1/paracaspase is a signaling component downstream of CARMA1 and mediates T cell receptor-induced NF-kappaB activation.* J Biol Chem, 2004. **279**(16): p. 15870-6.
41. Yang, K., et al., *The coiled-coil domain of TRAF6 is essential for its auto-ubiquitination.* Biochem Biophys Res Commun, 2004. **324**(1): p. 432-9.
42. Wooff, J., et al., *The TRAF6 RING finger domain mediates physical interaction with Ubc13.* FEBS Lett, 2004. **566**(1-3): p. 229-33.
43. Kanayama, A., et al., *TAB2 and TAB3 activate the NF-kappaB pathway through binding to polyubiquitin chains.* Mol Cell, 2004. **15**(4): p. 535-48.
44. Zucca, E., E. Roggero, and S. Pileri, *B-cell lymphoma of MALT type: a review with special emphasis on diagnostic and management problems of low-grade gastric tumours.* Br J Haematol, 1998. **100**(1): p. 3-14.
45. Bertoni, F. and E. Zucca, *Delving deeper into MALT lymphoma biology.* J Clin Invest, 2006. **116**(1): p. 22-6.
46. Zhou, H., M.Q. Du, and V.M. Dixit, *Constitutive NF-kappaB activation by the t(11;18)(q21;q21) product in MALT lymphoma is linked to deregulated ubiquitin ligase activity.* Cancer Cell, 2005. **7**(5): p. 425-31.
47. Kuo, S.H., et al., *Nuclear expression of BCL10 or nuclear factor kappa B predicts Helicobacter pylori-independent status of early-stage, high-grade gastric mucosa-associated lymphoid tissue lymphomas.* J Clin Oncol, 2004. **22**(17): p. 3491-7.
48. Liu, Y., et al., *Characterization of Bcl10 as a potential transcriptional activator that interacts with general transcription factor TFIIB.* Biochem Biophys Res Commun, 2004. **320**(1): p. 1-6.
49. Franco, R., et al., *Nuclear bcl10 expression characterizes a group of ocular adnexa MALT lymphomas with shorter failure-free survival.* Mod Pathol, 2006.
50. Shen, L., et al., *BCL10 mutations are irrelevant to its aberrant nuclear localization in nasal NK/T-cell lymphoma.* Leukemia, 2003. **17**(11): p. 2240-2.
51. Ye, H., et al., *Strong BCL10 nuclear expression identifies gastric MALT lymphomas that do not respond to H pylori eradication.* Gut, 2006. **55**(1): p. 137-8.
52. Yeh, P.Y., et al., *A pathway for tumor necrosis factor-alpha-induced Bcl10 nuclear translocation. Bcl10 is up-regulated by NF-kappaB and phosphorylated by Akt1 and then complexes with Bcl3 to enter the nucleus.* J Biol Chem, 2006. **281**(1): p. 167-75.
53. Isakov, N. and A. Altman, *Protein kinase C(theta) in T cell activation.* Annu Rev Immunol, 2002. **20**: p. 761-94.
54. Deng, L., et al., *Activation of the IkappaB kinase complex by TRAF6 requires a dimeric ubiquitin-conjugating enzyme complex and a unique polyubiquitin chain.* Cell, 2000. **103**(2): p. 351-61.
55. Zhou, H., et al., *Bcl10 activates the NF-kappaB pathway through ubiquitination of NEMO.* Nature, 2004. **427**(6970): p. 167-71.
56. Karin, M. and Y. Ben-Neriah, *Phosphorylation meets ubiquitination: the control of NF-[kappa]B activity.* Annu Rev Immunol, 2000. **18**: p. 621-63.
57. Ghosh, S., M.J. May, and E.B. Kopp, *NF-kappa B and Rel proteins: evolutionarily conserved mediators of immune responses.* Annu Rev Immunol, 1998. **16**: p. 225-60.

58. Jacobelli, J., et al., *New views of the immunological synapse: variations in assembly and function.* Curr Opin Immunol, 2004. **16**(3): p. 345-52.
59. Gaide, O., et al., *CARMA1 is a critical lipid raft-associated regulator of TCR-induced NF-kappa B activation.* Nat Immunol, 2002. **3**(9): p. 836-43.
60. Hara, H., et al., *The molecular adapter Carma1 controls entry of IkappaB kinase into the central immune synapse.* J Exp Med, 2004. **200**(9): p. 1167-77.
61. Siegel, R.M., et al., *Death-effector filaments: novel cytoplasmic structures that recruit caspases and trigger apoptosis.* J Cell Biol, 1998. **141**(5): p. 1243-53.
62. Dittel, B.N. and C.A. Janeway, Jr., *Differential sensitivity to mutations in a single peptide by two TCRs having identical beta-chains and closely related alpha-chains.* J Immunol, 2000. **165**(11): p. 6334-40.
63. Rizzo, M.A., et al., *An improved cyan fluorescent protein variant useful for FRET.* Nat Biotechnol, 2004. **22**(4): p. 445-9.
64. Griesbeck, O., et al., *Reducing the environmental sensitivity of yellow fluorescent protein. Mechanism and applications.* J Biol Chem, 2001. **276**(31): p. 29188-94.
65. Patterson, G.H. and J. Lippincott-Schwartz, *A photoactivatable GFP for selective photolabeling of proteins and cells.* Science, 2002. **297**(5588): p. 1873-7.
66. Zacharias, D.A., et al., *Partitioning of lipid-modified monomeric GFPs into membrane microdomains of live cells.* Science, 2002. **296**(5569): p. 913-6.
67. Schaefer, B.C., et al., *A novel family of retroviral vectors for the rapid production of complex stable cell lines.* Anal Biochem, 2001. **297**(1): p. 86-93.
68. Uren, A.G., et al., *Identification of paracaspases and metacaspases: two ancient families of caspase-like proteins, one of which plays a key role in MALT lymphoma.* Mol Cell, 2000. **6**(4): p. 961-7.
69. Scharschmidt, E., et al., *Degradation of Bcl10 induced by T-cell activation negatively regulates NF-kappa B signaling.* Mol Cell Biol, 2004. **24**(9): p. 3860-73.
70. Karasawa, S., et al., *Cyan-emitting and orange-emitting fluorescent proteins as a donor/acceptor pair for fluorescence resonance energy transfer.* Biochem J, 2004. **381**(Pt 1): p. 307-12.
71. Bertin, J., et al., *CARD9 is a novel caspase recruitment domain-containing protein that interacts with BCL10/CLAP and activates NF-kappa B.* J Biol Chem, 2000. **275**(52): p. 41082-6.
72. Truong, K. and M. Ikura, *The use of FRET imaging microscopy to detect protein-protein interactions and protein conformational changes in vivo.* Curr Opin Struct Biol, 2001. **11**(5): p. 573-8.
73. Ruland, J., et al., *Bcl10 is a positive regulator of antigen receptor-induced activation of NF-kappaB and neural tube closure.* Cell, 2001. **104**(1): p. 33-42.
74. Bunnell, S.C., et al., *T cell receptor ligation induces the formation of dynamically regulated signaling assemblies.* J Cell Biol, 2002. **158**(7): p. 1263-75.
75. Douglass, A.D. and R.D. Vale, *Single-molecule microscopy reveals plasma membrane microdomains created by protein-protein networks that exclude or trap signaling molecules in T cells.* Cell, 2005. **121**(6): p. 937-50.
76. Brossard, C., et al., *Multifocal structure of the T cell - dendritic cell synapse.* Eur J Immunol, 2005. **35**(6): p. 1741-53.

77. Campi, G., R. Varma, and M.L. Dustin, *Actin and agonist MHC-peptide complex-dependent T cell receptor microclusters as scaffolds for signaling.* J Exp Med, 2005. **202**(8): p. 1031-6.
78. Yokosuka, T., et al., *Newly generated T cell receptor microclusters initiate and sustain T cell activation by recruitment of Zap70 and SLP-76.* Nat Immunol, 2005.
79. Sommer, K., et al., *Phosphorylation of the CARMA1 linker controls NF-kappaB activation.* Immunity, 2005. **23**(6): p. 561-74.
80. Shen, L., et al., *Aberrant BCL10 nuclear expression in nasal NK/T-cell lymphoma.* Blood, 2003. **102**(4): p. 1553-4.
81. Mitchell, T.C., et al., *A short domain within Bcl-3 is responsible for its lymphocyte survival activity.* Ann N Y Acad Sci, 2002. **975**: p. 132-47.
82. Bours, V., et al., *The oncoprotein Bcl-3 directly transactivates through kappa B motifs via association with DNA-binding p50B homodimers.* Cell, 1993. **72**(5): p. 729-39.
83. Narayan, P., et al., *CARMA1 is required for Akt-mediated NF-kappaB activation in T cells.* Mol Cell Biol, 2006. **26**(6): p. 2327-36.
84. Nakagawa, M., et al., *MALT1 contains nuclear export signals and regulates cytoplasmic localization of BCL10.* Blood, 2005: p. 2004-12-4785.
85. Chen, M., L.Y. Li, and Y.P. Qi, *Bcl10 protein can act as a transcription activator in yeast.* Mol Cell Biochem, 2003. **246**(1-2): p. 97-103.
86. Yeh, K.H., et al., *Nuclear expression of BCL10 or nuclear factor kappa B helps predict Helicobacter pylori-independent status of low-grade gastric mucosa-associated lymphoid tissue lymphomas with or without t(11;18)(q21;q21).* Blood, 2005. **106**(3): p. 1037-41.
87. Sagaert, X., et al., *MALT1 and BCL10 aberrations in MALT lymphomas and their effect on the expression of BCL10 in the tumour cells.* Mod Pathol, 2006. **19**(2): p. 225-32.
88. Rossman, J.S., et al., *POLKADOTS are foci of functional interactions in T-Cell receptor-mediated signaling to NF-kappaB.* Mol Biol Cell, 2006. **17**(5): p. 2166-76.
89. Harlow, E., Lane,D. and Harlow, E., *Using antibodies: a laboratory manual*. 1999, Cold Spring Harbor, N.Y.: Cold Spring Harbor Laboratory Press.
90. Inoue, T., et al., *Association of BCL10 germ line polymorphisms on chromosome 1p with advanced stage testicular germ cell tumor patients.* Cancer Lett, 2005.
91. Su, H., et al., *Requirement for caspase-8 in NF-kappaB activation by antigen receptor.* Science, 2005. **307**(5714): p. 1465-8.
92. Thome, M., et al., *Equine herpesvirus-2 E10 gene product, but not its cellular homologue, activates NF-kappaB transcription factor and c-Jun N-terminal kinase.* J Biol Chem, 1999. **274**(15): p. 9962-8.